CHAPTER THREE

Planar Cartesian Kinematics

The position and orientation of bodies in a plane are easily defined in terms of two position coordinates and one rotation coordinate. Both absolute constraints on the motion of a single body and relative constraints on the motion of pairs of bodies, due to joints between bodies, are formulated in terms of these Cartesian generalized coordinates. The constraint library developed includes absolute and relative point and orientation constraints, revolute and translational constraints, gear constraints, cam constraints, and composite constraints that are used to define the effect of special-purpose couplers that need not be represented as bodies in models of mechanical systems. In addition, kinematic drivers are introduced to control the motion of a system. Position, velocity, and acceleration equations are derived and their use in kinematic analysis is discussed. Elementary mechanism models are used to illustrate the formulation and solution of equations that determine position, velocity, and acceleration of all bodies in a system. Both well-behaved and singular configurations are studied to illustrate the pitfalls that will arise in kinematic analysis if mechanisms are poorly designed.

3.1. BASIC CONCEPTS IN PLANAR KINEMATICS

Kinematics, as the study of motion, is useful in two important ways. First, it is frequently necessary to generate, transmit, or control motion by the use of cams, gears, and linkages. Second, it is often necessary to determine the dynamic response of a system of interconnected bodies that results from applied forces. To formulate equations of motion, the kinematics of the system must be quantitatively defined.

A *rigid body* that is used to model a component of a mechanism is defined as a system of particles the distances between which remain unchanged. Each particle in a rigid body is located by its constant position vector in a reference frame that is attached to and moves with the body, called the *body-fixed reference frame.* In reality, all solids deform to some extent when forces are applied. Nevertheless, if movement associated with deformation is small, compared with the overall movement of a body, then the concept of a rigid body is acceptable.

For example, displacements due to the elastic vibration of the connecting rod in an engine may be of no consequence in the description of engine dynamics as a whole, so the rigid-body assumption is clearly in order. On the other hand, if stress in the connecting rod is to be evaluated, then deformation of the connecting rod is of primary importance and cannot be neglected. In this text, essentially all analysis is based on the assumption that bodies are rigid.

A *mechanism* is a collection of rigid bodies that are arranged to allow relative motion. This definition includes classical linkages, as well as interconnected bodies that make up a vehicle, vending machine, aircraft landing gear, engine, and so on. *Kinematics* is the study of the position, velocity, and acceleration of a system of interconnected bodies that make up a mechanism, independent of the forces that produce the motion.

Kinematic synthesis is the process of finding the geometry of a mechanism that will yield desired motion characteristics. *Kinematic analysis,* on the other hand, is the process of predicting position, velocity, and acceleration, once a design is specified. The processes of kinematic synthesis and analysis are intertwined. To do synthesis, the engineer needs an analysis capability to evaluate designs that are under consideration. This text is devoted to the kinematic and dynamic analysis of mechanical systems. For a treatment of kinematic synthesis and further literature on this subject, see Reference 23.

Any set of variables that uniquely specifies the position and orientation of all bodies in a mechanism, that is, the *configuration* of the mechanism, is called a set of *generalized coordinates.* Generalized coordinates may be *independent* (i.e., free to vary arbitrarily) or *dependent* (i.e., required to satisfy equations of constraint). For systems in motion, generalized coordinates vary with time. Generalized coordinates are designated in this text by a column vector $\mathbf{q} \equiv [q_1, q_2, \ldots, q_{nc}]^T$, where nc is the total number of generalized coordinates used to describe the configuration of the system.

To specify the configuration of a planar system, a *body-fixed x'-y' reference frame* is embedded in each body of the system, as shown in Fig. 3.1.1. Body i (i is an identifying number assigned to each body) can be located by specifying the global coordinates $\mathbf{r}_i = [x, y]_i^T$ of the origin of the body-fixed x_i'-y_i' frame and the angle ϕ_i of rotation of this frame relative to the global x-y frame. The column vector $\mathbf{q}_i \equiv [x, y, \phi]_i^T$ is the vector of planar *Cartesian generalized coordinates* for body i. Using Cartesian generalized coordinates for each body, a maximal set of coordinates is defined to specify the position and orientation of each body in the system.

If a planar mechanism is made up of nb rigid bodies, the number of planar Cartesian generalized coordinates is $nc = 3 \times nb$. The vector of generalized coordinates for the system is denoted by $\mathbf{q} = [\mathbf{q}_1^T, \mathbf{q}_2^T, \ldots, \mathbf{q}_{nb}^T]^T$. Since rigid bodies that make up a mechanism are interconnected by joints, there are equations of constraint that relate the generalized coordinates. Therefore, Cartesian generalized coordinates are generally dependent.

A kinematic constraint between two bodies imposes conditions on the

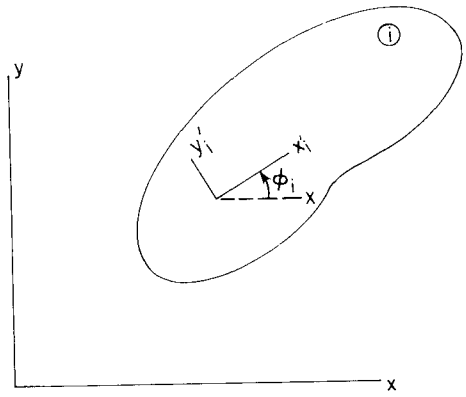

Figure 3.1.1 Planar Cartesian generalized coordinates.

relative motion between the pair of bodies. When these conditions are expressed as algebraic equations in terms of generalized coordinates, they are called *holonomic kinematic constraint equations.* A system of *nh* holonomic kinematic constraint equations that does not depend explicitly on time can be expressed as

$$\mathbf{\Phi}^K(\mathbf{q}) = [\Phi_1^K(\mathbf{q}), \ldots, \Phi_{nh}^K(\mathbf{q})]^T = \mathbf{0} \tag{3.1.1}$$

If time appears explicitly, as in the case of time-dependent kinematic couplings,

$$\mathbf{\Phi}^K(\mathbf{q}, t) = \mathbf{0} \tag{3.1.2}$$

where t is time. If t does not enter explicitly into the equation of constraint, as in Eq. 3.1.1, the constraint is called a *stationary constraint.* Constraints specified by equations in the form of Eq. 3.1.2 are called *time-dependent constraints.* More general constraint equations that contain inequalities or relations between velocity components are called *nonholonomic constraints.* In this text, the term *constraint* will mean holonomic constraint unless otherwise specified.

The analytical foundation of computer-aided kinematic analysis is a library of joints that restrict the motion of a body or relative motion of a pair of bodies. Algebraic equations of constraint must be derived that are equivalent to the physical joints. This equivalence is a critically important concept that is not generally given adequate attention. Constraint equations are often derived from the geometry of a joint; that is, they are implied by the geometry of the joint. This is not enough. *The equations of constraint must imply the geometry of the joint.* This is required in computer simulation, since it is the equations of constraint that are being satisfied. If they can be satisfied without yielding the geometrical relations due to the joints, then the mathematical model fails to define the motion of the system. This subtle but important point will be highlighted in the developments that follow.

If $nc > nh$, then the constraint equations of Eq. 3.1.1 or 3.1.2 are not

sufficient in number to determine $\mathbf{q}$. This is the usual case, since a mechanical system is usually designed to permit motion, distinguishing it from a *structure,* whose function is to transmit load and resist motion. If the constraints of Eq. 3.1.1 or 3.1.2 are consistent and independent (concepts to be defined precisely in Section 3.6), then the system is said to have $nc - nh$ *degrees of freedom,* abbreviated DOF $= nc - nh$. To determine the motion of a system, the engineer must define either (1) DOF additional driving conditions that uniquely determine $\mathbf{q}(t)$ algebraically (*kinematic analysis*), or (2) forces that act on the system, in which case $\mathbf{q}(t)$ is the solution of differential equations of motion (*dynamic analysis*). Kinematic analysis of planar systems is treated in Chapters 3 through 5 and dynamic analysis of planar systems is treated in Chapters 6 through 8.

If DOF independent *driving constraints* are specified for kinematic analysis, denoted

$$\mathbf{\Phi}^D(\mathbf{q}, t) = \mathbf{0} \tag{3.1.3}$$

then the configuration of the system as a function of time can be determined. That is, the combined constraints of Eqs. 3.1.2 and 3.1.3,

$$\mathbf{\Phi}(\mathbf{q}, t) = \begin{bmatrix} \mathbf{\Phi}^K(\mathbf{q}, t) \\ \mathbf{\Phi}^D(\mathbf{q}, t) \end{bmatrix} = \mathbf{0} \tag{3.1.4}$$

can be solved for $\mathbf{q}(t)$. Such a system is called *kinematically driven.*

Example 3.1.1: The simple pendulum of Fig. 3.1.2 is pivoted at point O, the origin of the x-y reference frame. This kinematic constraint is prescribed by the pair of equations

$$\mathbf{\Phi}^K(\mathbf{q}) \equiv \begin{bmatrix} x_1 - \sin \phi_1 \\ y_1 + \cos \phi_1 \end{bmatrix} = \mathbf{0} \tag{3.1.5}$$

where $\mathbf{q} = [x_1, y_1, \phi_1]^T$. Clearly, Eq. 3.1.5 can be solved for x_1 and y_1 as a function of ϕ_1, so one independent variable can specify the motion of the system. Thus, the system has one degree of freedom (DOF = 1).

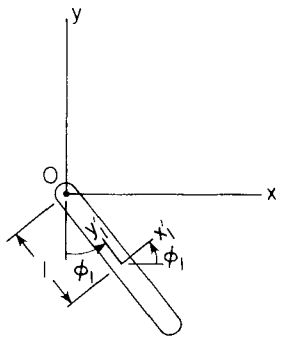

Figure 3.1.2 Simple pendulum.

Even though the elementary form of Eq. 3.1.5 permits easy solution for some variables as functions of others, this is not possible for most mechanisms and machines that are of practical interest. To set the stage for generally applicable methods that are developed in the following sections of this chapter, the conceptually trivial simple pendulum is analyzed here. To specify the motion of the simple pendulum, a driving constraint must be introduced; for example, specifying the time history of ϕ_1,

$$\Phi^D(\mathbf{q}, t) \equiv \phi_1 - f(t) = 0 \tag{3.1.6}$$

Combining Eqs. 3.1.5 and 3.1.6 yields the system kinematic constraint equation

$$\boldsymbol{\Phi}(\mathbf{q}, t) = \begin{bmatrix} \boldsymbol{\Phi}^K(\mathbf{q}) \\ \Phi^D(\mathbf{q}, t) \end{bmatrix} = \begin{bmatrix} x_1 - \sin\phi_1 \\ y_1 + \cos\phi_1 \\ \phi_1 - f(t) \end{bmatrix} = 0 \tag{3.1.7}$$

It is shown in Section 3.6 that if $\boldsymbol{\Phi}_\mathbf{q}$ is nonsingular, that is, $|\boldsymbol{\Phi}_\mathbf{q}| \neq 0$ at some value of $\mathbf{q}$ that satisfies Eq. 3.1.7, then Eq. 3.1.7 can be solved for $\mathbf{q}$ as a function of time. To test this condition, note that

$$|\boldsymbol{\Phi}_\mathbf{q}| = \begin{vmatrix} 1 & 0 & -\cos\phi_1 \\ 0 & 1 & -\sin\phi_1 \\ 0 & 0 & 1 \end{vmatrix} = 1 \tag{3.1.8}$$

Under this condition, the numerical methods presented in Chapter 4 permit effective computation of the solution of Eq. 3.1.7 for $\mathbf{q}$ at discrete instants in time, even for complicated nonlinear equations for which a closed-form solution is extremely messy, if not impossible to obtain.

Assume that numerical methods have been used to solve Eq. 3.1.4 for $\mathbf{q}$ at discrete instants in time. Since $\mathbf{q}$ is not known as an explicit function of time, it cannot be differentiated to obtain $\dot{\mathbf{q}}$ or $\ddot{\mathbf{q}}$. An alternative that is well suited for numerical computation is to use the chain rule of differentiation to evaluate derivatives of both sides of Eq. 3.1.4 with respect to time to obtain the *velocity equation*

$$\dot{\boldsymbol{\Phi}} = \boldsymbol{\Phi}_\mathbf{q}\dot{\mathbf{q}} + \boldsymbol{\Phi}_t = 0$$

or

$$\boldsymbol{\Phi}_\mathbf{q}\dot{\mathbf{q}} = -\boldsymbol{\Phi}_t \equiv \boldsymbol{\nu} \tag{3.1.9}$$

If $\boldsymbol{\Phi}_\mathbf{q}$ is nonsingular, Eq. 3.1.9 can be solved for $\dot{\mathbf{q}}$ at discrete instants in time. Similarly, both sides of Eq. 3.1.9 can be differentiated with respect to time, using

the chain rule of differentiation, to obtain

$$\boldsymbol{\Phi}_{\mathbf{q}}\ddot{\mathbf{q}} + (\boldsymbol{\Phi}_{\mathbf{q}}\dot{\mathbf{q}})_{\mathbf{q}}\dot{\mathbf{q}} + \boldsymbol{\Phi}_{\mathbf{q}t}\dot{\mathbf{q}} = -\boldsymbol{\Phi}_{t\mathbf{q}}\dot{\mathbf{q}} - \boldsymbol{\Phi}_{tt}$$

where for purposes of applying the chain rule of differentiation all variables are treated as independent; in particular, $\dot{\mathbf{q}}_{\mathbf{q}} = \mathbf{0}$. Since $\boldsymbol{\Phi}_{t\mathbf{q}} = \boldsymbol{\Phi}_{\mathbf{q}t}$, this result can be rearranged to obtain the *acceleration equation*

$$\boldsymbol{\Phi}_{\mathbf{q}}\ddot{\mathbf{q}} = -(\boldsymbol{\Phi}_{\mathbf{q}}\dot{\mathbf{q}})_{\mathbf{q}}\dot{\mathbf{q}} - 2\boldsymbol{\Phi}_{\mathbf{q}t}\dot{\mathbf{q}} - \boldsymbol{\Phi}_{tt} \equiv \boldsymbol{\gamma} \tag{3.1.10}$$

Since $\boldsymbol{\Phi}_{\mathbf{q}}$ is nonsingular, Eq. 3.1.10 can be solved for $\ddot{\mathbf{q}}$ at discrete instants in time (Prob. 3.1.1).

In Example 3.1.1, $\boldsymbol{\Phi}_{\mathbf{q}t} = \mathbf{0}$, $\boldsymbol{\Phi}_{tt} = [0, 0, -\ddot{f}(t)]^T$, and

$$(\boldsymbol{\Phi}_{\mathbf{q}}\dot{\mathbf{q}})_{\mathbf{q}}\dot{\mathbf{q}} = \begin{bmatrix} \dot{x} - \dot{\phi}_1 \cos\phi_1 \\ \dot{y}_1 - \dot{\phi}_1 \sin\phi_1 \\ \dot{\phi}_1 \end{bmatrix}_{\mathbf{q}} \dot{\mathbf{q}} = \begin{bmatrix} \dot{\phi}_1^2 \sin\phi_1 \\ -\dot{\phi}_1^2 \cos\phi_1 \\ 0 \end{bmatrix}$$

so Eq. 3.1.10 is

$$\boldsymbol{\Phi}_{\mathbf{q}}\ddot{\mathbf{q}} = \begin{bmatrix} -\dot{\phi}_1^2 \sin\phi_1 \\ \dot{\phi}_1^2 \cos\phi_1 \\ \ddot{f}(t) \end{bmatrix}$$

The matrix $\boldsymbol{\Phi}_{\mathbf{q}}$ that arises in the velocity and accelerations, Eqs. 3.1.9 and 3.1.10, plays a central role in the theory and numerical methods of kinematics and dynamics. It is called the *Jacobian matrix,* or simply the *Jacobian.* While it may be assembled in an ad hoc way using the definitions of matrix calculus of Chapter 2, it is assembled in a systematic way for each of the contraints considered later in this chapter. The importance of the Jacobian will become clear as the reader proceeds through the remainder of the text. Without question, it is the most important matrix that is used in the kinematics and dynamics of constrained mechanical systems.

Evaluation of the right side of Eq. 3.1.10 involves calculation of second derivatives, as outlined in Example 3.1.1. To be more specific,

$$\boldsymbol{\Phi}_{tt} = \left[\frac{\partial^2 \Phi_i}{\partial t^2}\right]_{nh\times 1}$$

$$\boldsymbol{\Phi}_{\mathbf{q}t} = \left[\frac{\partial^2 \Phi_i}{\partial q_j \, \partial t}\right]_{nh\times nc}$$

and

$$(\boldsymbol{\Phi}_{\mathbf{q}}\dot{\mathbf{q}})_{\mathbf{q}} = \left[\frac{\partial}{\partial q_j}\left(\sum_{k=1}^{nc} \frac{\partial \Phi_i}{\partial q_k}\dot{q}_k\right)\right]_{nc\times nc}$$

$$= \left[\sum_{k=1}^{nc} \frac{\partial^2 \Phi_i}{\partial q_j \, \partial q_k}\dot{q}_k\right]_{nc\times nc}$$

where nh is the number of holonomic constraints and nc is the number of generalized coordinates.

Example 3.1.2: Consider next an elementary two-body model of the slider–crank mechanism of Example 2.4.3. Rather than using the relative angle generalized coordinates that were used there, consider the Cartesian coordinates shown in Fig. 3.1.3.

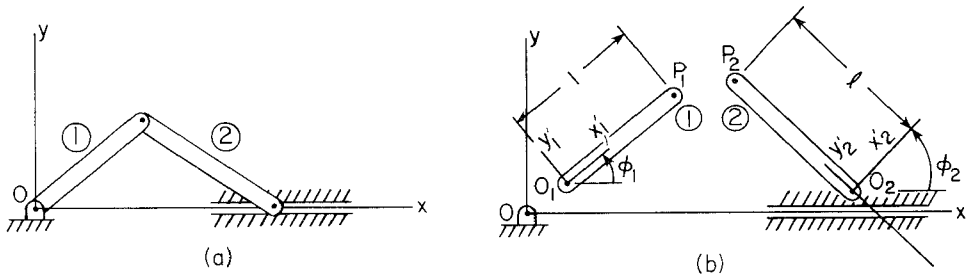

Figure 3.1.3 Cartesian coordinates for two-body slider–crank model. (a) Assembled. (b) Dissected.

To assemble the mechanism, three geometric constraint conditions must be imposed, as follows:

1. Point O_1 on the crank (body 1) must coincide with the origin O of the x-y frame; that is, $x_1 = y_1 = 0$.
2. Point O_2 on the coupler (body 2) must lie on the x axis; that is, $y_2 = 0$.
3. Points P_1 and P_2 on the crank and coupler, respectively, must coincide; that is,

$$\mathbf{r}^{P_1} \equiv \begin{bmatrix} x_1 + \cos\phi_1 \\ y_1 + \sin\phi_1 \end{bmatrix} = \begin{bmatrix} x_2 - \ell\sin\phi_2 \\ y_2 + \ell\cos\phi_2 \end{bmatrix} \equiv \mathbf{r}^{P_2}$$

In terms of $\mathbf{q} = [x_1, y_1, \phi_1, x_2, y_2, \phi_2]^T$, the combined system of kinematic constraint equations is thus

$$\mathbf{\Phi}^K(\mathbf{q}) = \begin{bmatrix} x_1 \\ y_1 \\ y_2 \\ x_1 - x_2 + \cos\phi_1 + \ell\sin\phi_2 \\ y_1 - y_2 + \sin\phi_1 - \ell\cos\phi_2 \end{bmatrix} \tag{3.1.11}$$

Presuming the constraint equations of Eq. 3.1.11 are independent (to be verified in Section 3.6), DOF $= nc - nh = 6 - 5 = 1$. Thus, one driving constraint is required; for example, the crank is to be rotated with constant angular velocity ω, so

$$\Phi^D(\mathbf{q}, t) = \phi_1 - \omega t \tag{3.1.12}$$

The kinematic equations that determine the motion of this system are thus

$$\mathbf{\Phi}(\mathbf{q}, t) = \begin{bmatrix} \mathbf{\Phi}^K(\mathbf{q}) \\ \mathbf{\Phi}^D(\mathbf{q}) \end{bmatrix} = \mathbf{0} \tag{3.1.13}$$

At any instant t_i in time, Eq. 3.1.13 may be solved by numerical methods (see Chapter 4) for $\mathbf{q}(t_i)$. Differentiating both sides of Eq. 3.1.13 with respect to time yields the velocity equation

$$\mathbf{\Phi}_\mathbf{q}(\mathbf{q}(t_i), t_i)\dot{\mathbf{q}}(t_i)$$

$$= \begin{bmatrix} 1 & 0 & 0 & 0 & 0 & 0 \\ 0 & 1 & 0 & 0 & 0 & 0 \\ 0 & 0 & 0 & 0 & 1 & 0 \\ 1 & 0 & -\sin\phi_1(t_1) & -1 & 0 & \ell\cos\phi_2(t_i) \\ 0 & 1 & \cos\phi_1(t_1) & 0 & -1 & \ell\sin\phi_2(t_i) \\ 0 & 0 & 1 & 0 & 0 & 0 \end{bmatrix} \begin{bmatrix} \dot{x}_1(t_i) \\ \dot{y}_1(t_i) \\ \dot{\phi}_1(t_i) \\ \dot{x}_2(t_i) \\ \dot{y}_2(t_i) \\ \dot{\phi}_2(t_i) \end{bmatrix} = \begin{bmatrix} 0 \\ 0 \\ 0 \\ 0 \\ 0 \\ \omega \end{bmatrix} = -\mathbf{\Phi}_t$$

(3.1.14)

Since $|\mathbf{\Phi}_\mathbf{q}| = -\ell\sin\phi_2$ and, with $\ell > 1$, $|\phi_2 - \pi/2| \leq \text{Arcsin}(1/\ell)$, $|\mathbf{\Phi}_\mathbf{q}| \neq 0$ and Eq. 3.1.14 may be solved for $\dot{\mathbf{q}}(t_i)$ (Prob. 3.1.3). Similarly, both sides of Eq. 3.1.14 may be differentiated, to obtain the acceleration equation

$$\mathbf{\Phi}_\mathbf{q}(\mathbf{q}(t_i), t_i)\ddot{\mathbf{q}}(t_i) = \begin{bmatrix} 0 \\ 0 \\ 0 \\ \dot{\phi}_1^2(t_i)\cos\phi_1(t_i) + \ell\dot{\phi}_2^2(t_i)\sin\phi_2(t_i) \\ \dot{\phi}_1^2(t_i)\sin\phi_1(t_i) - \ell\dot{\phi}_2^2(t_i)\cos\phi_2(t_i) \\ 0 \end{bmatrix} \tag{3.1.15}$$

where the coefficient matrix on the left is the same as in Eq. 3.1.14. Since $\mathbf{q}(t_i)$ is found from Eq. 3.1.13 and $\dot{\mathbf{q}}(t_i)$ is found from Eq. 3.1.14, Eq. 3.1.15 may be solved for $\ddot{\mathbf{q}}(t_i)$ (Prob. 3.1.4).

Examples 3.1.1 and 3.1.2, while addressing elementary mechanisms, illustrate an approach that is used throughout this text for the formulation and solution of kinematic equations of general mechanical systems. The remainder of Chapter 3 is devoted to deriving a library of kinematic constraints between pairs of bodies that can be used to assemble kinematic equations for broad classes of mechanisms and machines. The resulting kinematic constraint equations are coupled with driving constraints that uniquely determine the motion of the system. Nonlinear equations of constraint are solved for position and orientation and linear equations in velocity and acceleration are solved, using the methods employed in Examples 3.1.1 and 3.1.2. To place the detailed developments of subsequent sections into the context of system kinematic analysis, the reader may wish to refer to Examples 3.1.1 and 3.1.2.

As an additional aid in interpreting the detailed developments that follow, the reader should keep in mind the basic objective of computer-aided kinematic analysis, which is to create a systematic method for both formulating and solving kinematic equations that can be implemented on a digital computer. Only if such a systematic approach is adopted can the burden of extensive analytical derivation be taken from the shoulders of the engineer and delegated to the computer. It is this objective that leads to what might appear to be excessively large matrices, such as those encountered in Example 3.1.2. The reader might be interested to note that the constraint Jacobian $\mathbf{\Phi}_{\mathbf{q}}$ of Eq. 3.1.14 for the slider–crank mechanism contains many zeros and ones. This elementary structure is exploited in Chapter 4 to efficiently solve position, velocity, and acceleration equations of kinematic analysis.

Example 3.1.3: To illustrate a potential problem that must be avoided in computer-aided kinematics, consider the sliding body shown in Fig. 3.1.4,

Constraint equations that are consistent with constraints on body 1 may be written as the condition that P_1 remain on the slide axis $y = x$, that is,

$$\Phi_1 \equiv y_1 - x_1 = 0 \tag{3.1.16}$$

and the condition that the y' axis remain orthogonal to the slide axis, or $\mathbf{r}_1$ since it is along the slide, that is,

$$\Phi_2 \equiv \mathbf{r}_1^T \mathbf{j}_1 = \mathbf{r}_1^T \mathbf{A}(\phi_1) \begin{bmatrix} 0 \\ 1 \end{bmatrix}$$

$$= y_1 \cos \phi_1 - x_1 \sin \phi_1 \tag{3.1.17}$$

To illustrate the use of these constraint equations, consider the driver

$$\Phi^D \equiv x_1 - vt = 0 \tag{3.1.18}$$

where v is the horizontal component of velocity of P_1. To check for the solvability of Eqs. 3.1.16 through 3.1.18, the determinant of the Jacobian is

$$|\mathbf{\Phi}_{\mathbf{q}_1}| = -(y_1 \sin \phi_1 + x_1 \cos \phi_1)$$

Thus, all is well if $\mathbf{r}_1 \neq \mathbf{0}$. However, $\mathbf{\Phi}_{\mathbf{q}_1}$ is singular when the center of the block is at the origin of the x-y frame, and the kinematic and driving constraints fail to

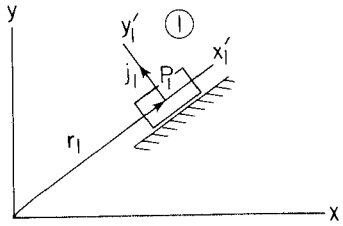

Figure 3.1.4 Inclined slider.

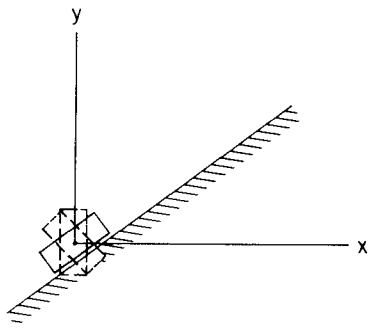

Figure 3.1.5 Inclined slider at singular point.

uniquely define motion at this point. In fact, computer solution methods will fail due to the singular Jacobian.

This mathematical breakdown is puzzling, since there is no physical difficulty when $\mathbf{r}_1 = \mathbf{0}$ (Prob. 3.2.3). The problem has been created by choosing constraint equations that are implied by the geometry of the system, but which fail to imply its geometry when $\mathbf{r}_1 = \mathbf{0}$. To see this more clearly, note that Eq. 3.1.17 is satisfied by arbitrary ϕ_1 when $\mathbf{r}_1 = \mathbf{0}$, as shown in Fig. 3.1.5.

Even in this trivial example, it is possible to make a fatal formulation error by deriving constraint equations that fail to uniquely define the kinematics of a system. The danger of making such errors is greater in more complex kinematic joints, particularly for the spatial systems in Part II of this text. The engineer must, therefore, be careful to assure that the equations used in computer-aided analysis in fact reliably describe the behavior of the system. If they fail at even one point, as in this example, the entire system simulation will break down.

3.2. CONSTRAINTS BETWEEN A BODY AND GROUND (ABSOLUTE CONSTRAINTS)

In many mechanisms, the motion of a body is constrained relative to ground, that is, relative to the stationary x-y reference frame. Constraint equations may be expressed as relationships among the generalized coordinates of a single body, since no other body is involved. Consider for example the case in which point P_i on body i, shown in Fig. 3.2.1, can only move on a circular path. This may be due to a link of fixed length with revolute joints in body i and the x-y plane, as shown in Fig. 3.2.1. The *absolute distance constraint* that defines this physical limitation on motion, using Eq. 2.4.8, is

$$\begin{aligned}\Phi^{ad(i)} &\equiv (\mathbf{r}_i^P - \mathbf{C})^T(\mathbf{r}_i^P - \mathbf{C}) - C_3^2 \\ &= (x_i + x_i'^P \cos\phi_i - y_i'^P \sin\phi_i - C_1)^2 \\ &\quad + (y_i + x_i'^P \sin\phi_i + y_i'^P \cos\phi_i - C_2)^2 - C_3^2 = 0 \end{aligned} \tag{3.2.1}$$

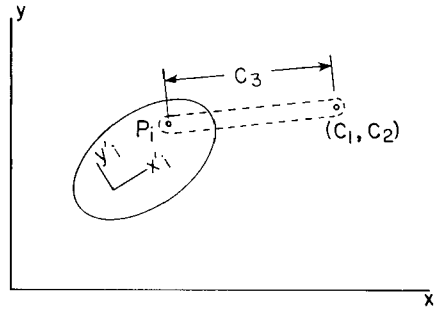

Figure 3.2.1 Constraint that distance from point P to (C_1, C_2) equals C_3.

where $\mathbf{C} = [C_1, C_2]^T$ is the given point at the center of the circle in the x-y plane and $C_3 > 0$ is its given radius. Here, x_i^P and y_i^P are the coordinates of point P_i in the x-y frame and $x_i'^P$ and $y_i'^P$ are the constant coordinates of P_i in the x_i'-y_i' frame, since P_i is fixed to body i. Using Eq. 2.4.8, x_i^P and y_i^P are written as functions of $\mathbf{q}_i = [x_i, y_i, \phi_i]^T$, as in the right side of Eq. 3.2.1.

The Jacobian of $\Phi^{ad(i)}$ with respect to $\mathbf{q}_i$ is

$$\begin{aligned}\mathbf{\Phi}_{\mathbf{q}_i}^{ad(i)} &= 2[(\mathbf{r}_i^P - \mathbf{C})^T, \mathbf{s}_i'^{PT}\mathbf{B}_i^T(\mathbf{r}_i^P - \mathbf{C})] \\ &= 2[(x_i^P - C_1), (y_i^P - C_2), -(x_i^P - C_1)(x_i'^P \sin\phi_i - y_i'^P \cos\phi_i) \\ &\quad + (y_i^P - C_2)(x_i'^P \cos\phi_i - y_i'^P \sin\phi_i)] \end{aligned} \tag{3.2.2}$$

where the chain rule of differentiation and $d\mathbf{A}/d\phi = \mathbf{B}$ have been used.

Since $\Phi^{ad(i)}$ does not depend explicitly on time, the right side of the velocity equation of Eq. 3.1.9 is

$$\nu^{ad(i)} = 0$$

With a somewhat more intricate calculation, the right side of the acceleration equation of Eq. 3.1.10 is obtained, using the Jacobian of Eq. 3.2.2, as

$$\begin{aligned}\gamma^{ad(i,j)} &= -\frac{\partial}{\partial \mathbf{q}_i}\{2(\mathbf{r}_i^P - \mathbf{C})^T\dot{\mathbf{r}}_i + 2\mathbf{s}_i'^{PT}\mathbf{B}_i^T(\mathbf{r}_i^P - \mathbf{C})\dot{\phi}_i\}\dot{\mathbf{q}}_i \\ &= -2[\dot{\mathbf{r}}_i^T\dot{\mathbf{r}}_i + 2\mathbf{s}_i'^{PT}\mathbf{B}_i^T\dot{\mathbf{r}}_i\dot{\phi}_i + \mathbf{s}_i'^{PT}\mathbf{B}_i^T\mathbf{B}_i\mathbf{s}_i'^P\dot{\phi}_i^2 - \mathbf{s}_i'^{PT}\mathbf{A}_i^T(\mathbf{r}_i^P - \mathbf{C})\dot{\phi}_i^2] \\ &= -2[\dot{\mathbf{r}}_i^{PT}\dot{\mathbf{r}}_i^P - \mathbf{s}_i'^{PT}\mathbf{A}_i^T(\mathbf{r}_i^P - \mathbf{C})\dot{\phi}_i^2]\end{aligned}$$

where Eqs. 2.6.3 and 2.6.8 have been used.

The restriction $C_3 > 0$ is required so that Eq. 3.2.1 represents a single constraint. If $C_3 = 0$, Eq. 3.2.1 requires that both $x_i^P = C_1$ and $y_i^P = C_2$, which is a pair of constraint equations. Furthermore, if $C_3 = 0$, the Jacobian $\Phi_{\mathbf{q}}^{ad(i)}$ of Eq. 3.2.2 is zero, leading to later computational trouble.

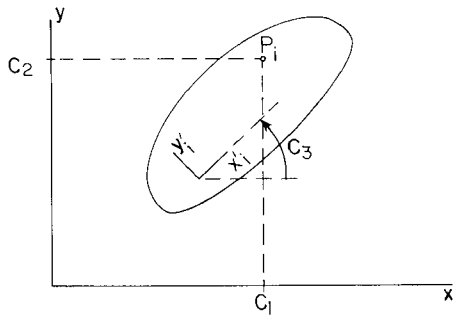

Figure 3.2.2 Constraints on absolute coordinates of point P_i and on angular orientation.

An *absolute position constraint* on point P_i of body i in the x or y direction might be imagined as the condition that a pin on body i at point P_i slide in a slot in the x-y plane that is parallel to the x or y axis, respctively. As shown in Fig. 3.2.2, the following constraint equations define this condition, using Eq. 2.4.8:

$$\begin{aligned}\Phi^{ax(i)} &\equiv x_i^P - C_1 \\ &= x_i + x_i'^P \cos\phi_i - y_i'^P \sin\phi_i - C_1 = 0 \end{aligned} \tag{3.2.3}$$

$$\begin{aligned}\Phi^{ay(i)} &\equiv y_i^P - C_2 \\ &= y_i + x_i'^P \sin\phi_i + y_i'^P \cos\phi_i - C_2 = 0 \end{aligned} \tag{3.2.4}$$

where C_1 and C_2 are given constants and $x_i'^P$ and $y_i'^P$ are the constant body-fixed coordinates of point P_i on body i. The Jacobians of these constraint functions with respect to $\mathbf{q}_i$ are

$$\begin{aligned}\Phi_{\mathbf{q}_i}^{ax(i)} &= [1,\ 0,\ -x_i'^P \sin\phi_i - y_i'^P \cos\phi_i] \\ \Phi_{\mathbf{q}_i}^{ay(i)} &= [0,\ 1,\ x_i'^P \cos\phi_i - y_i'^P \sin\phi_i] \end{aligned} \tag{3.2.5}$$

An *absolute angular constraint* on a body is defined by the following equation:

$$\Phi^{a\phi(i)} \equiv \phi_i - C_3 = 0 \tag{3.2.6}$$

where C_3 is a given constant. Figure 3.2.2 illustrates the constraint of Eq. 3.2.6. The Jacobian of this constraint function with respect to $\mathbf{q}_i$ is simply

$$\Phi_{\mathbf{q}_i}^{a\phi(i)} = [0,\ 0,\ 1] \tag{3.2.7}$$

Since these constraints are not explicitly time dependent, from Eq. 3.1.9,

$$\gamma^{ax(i)} = \gamma^{ay(i)} = \gamma^{a\phi(i)} = 0$$

Expanding terms in Eq. 3.1.10, using the Jacobians of Eqs. 3.2.5 and 3.2.6,

$$\gamma^{ax(i)} = (x_i'^P \cos\phi_i - y_i'^P \sin\phi_i)\dot{\phi}_i^2$$
$$\gamma^{ay(i)} = (x_i'^P \sin\phi_i + y_i'^P \cos\phi_i)\dot{\phi}_i^2$$
$$\gamma^{a\phi(i)} = 0$$

Example 3.2.1: Figure 3.2.3 shows a simple pendulum with its pivot pin P_1 located at $(C_1, C_2) = (1, 1)$ in the x-y plane. With the origin of the x_1'-y_1' frame at the center of the pendulum, whose length is two units, $x_1'^P = 1$ and $y_1'^P = 0$. Equations 3.2.3 and 3.2.4 thus describe the kinematics of the pendulum. Note that the constraint equations for the simple pendulum of Example 3.1.1 could have been written in this way.

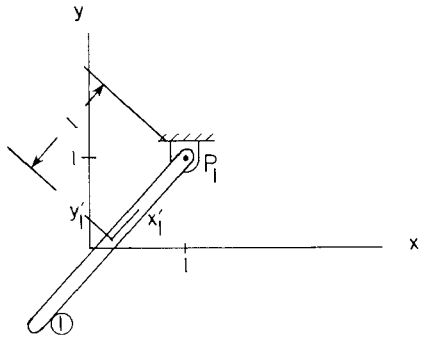

Figure 3.2.3 Simple pendulum with absolute constraints.

Example 3.2.2: As an example of an absolute angular constraint, Fig. 3.2.4 shows a joint that allows body 1 to slide along the x axis, with the body-fixed x_1' axis and the x axis coinciding. The kinematic constraint between this slider and ground is defined by Eq. 3.2.4, with $x_1'^P = y_1'^P = 0$ and $C_2 = 0$, and by Eq. 3.2.6 with $C_3 = 0$.

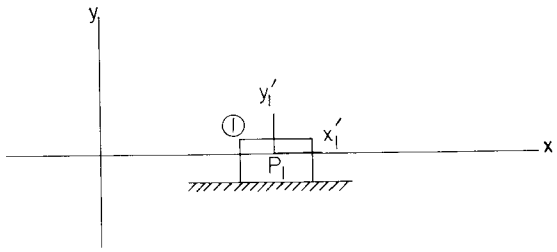

Figure 3.2.4 Slider along x axis.

3.3 CONSTRAINTS BETWEEN PAIRS OF BODIES (RELATIVE CONSTRAINTS)

The constraints described in Section 3.2 impose restrictions on the motion of a single body relative to the global reference frame. In most kinematic systems, constraints are imposed on the relative position and orientation of pairs of bodies that are connected by joints. In this section, commonly used kinematic pairs are formulated. The technique employed to formulate kinematic constraint equations for these joints may be applied to most other commonly used or special-purpose joints.

The objective for each joint treated is to define a set of algebraic constraint equations that are "equivalent to the physical joint." Since the physical joint is to be represented by constraint equations, it is important that the equations employed imply the relative position and orientation restrictions imposed by the physical joint. It is easy to write down equations that are implied by the geometry of the joint, as in Example 3.1.3, but that do not imply the geometry of the joint. If this is done, the computer model will fail to represent the real physical kinematics and numerical difficulties will arise.

3.3.1 Relative Coordinate Constraints

Simple equations can be derived to define the following constraints:

(1) A *relative x constraint* requires that the difference between the x coordinates of point P_j on body j and point P_i on body i equal a given constant C_1 (see Fig. 3.3.1); that is, using Eq. 2.4.8,

$$\Phi^{rx(i,j)} \equiv x_j^P - x_i^P - C_1$$
$$= x_j + x_j'^P \cos\phi_j - y_j'^P \sin\phi_j - x_i - x_i'^P \cos\phi_i + y_i'^P \sin\phi_i - C_1 = 0 \qquad \textbf{(3.3.1)}$$

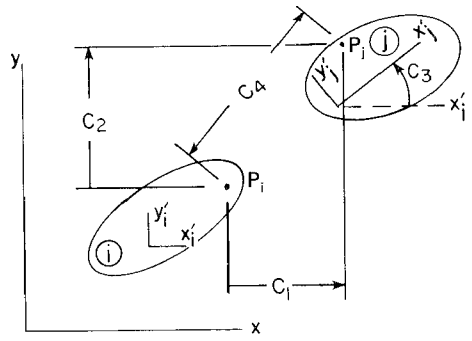

Figure 3.3.1 Simple constraints.

The Jacobians of this constraint with respect to $\mathbf{q}_i$ and $\mathbf{q}_j$ are

$$\begin{aligned}\Phi_{\mathbf{q}_i}^{rx(i,j)} &= [-1,\ 0,\ x_i'^P \sin\phi_i + y_i'^P \cos\phi_i] \\ \Phi_{\mathbf{q}_j}^{rx(i,j)} &= [1,\ 0,\ -x_j'^P \sin\phi_j - y_j'^P \cos\phi_j]\end{aligned} \tag{3.3.2}$$

From Eqs. 3.1.9 and 3.1.10, using the Jacobians of Eq. 3.3.2,

$$\begin{aligned}\nu^{rx(i,j)} &= 0 \\ \gamma^{rx(i,j)} &= -(x_i'^P \cos\phi_i - y_i'^P \sin\phi_i)\dot{\phi}_i^2 + (x_j'^P \cos\phi_j - y_j'^P \sin\phi_j)\dot{\phi}_j^2\end{aligned}$$

(2) A *relative y constraint* requires that the difference between the y coordinates of point P_j on body j and point P_i on body i equal a given constant C_2 (see Fig. 3.3.1); that is, using Eq. 2.4.8,

$$\begin{aligned}\Phi^{ry(i,j)} &= y_j^P - y_i^P - C_2 \\ &= y_j + x_j'^P \sin\phi_j + y_j'^P \cos\phi_j - y_i - x_i'^P \sin\phi_i - y_i'^P \cos\phi_i - C_2 = 0\end{aligned} \tag{3.3.3}$$

The Jacobians of this constraint with respect to $\mathbf{q}_i$ and $\mathbf{q}_j$ are

$$\begin{aligned}\Phi_{\mathbf{q}_i}^{ry(i,j)} &= [0,\ -1,\ -x_i'^P \cos\phi_i + y_i'^P \sin\phi_i] \\ \Phi_{\mathbf{q}_j}^{ry(i,j)} &= [0,\ 1,\ x_j'^P \cos\phi_j - y_j'^P \sin\phi_j]\end{aligned} \tag{3.3.4}$$

Again, from Eqs. 3.1.9 and 3.1.10,

$$\begin{aligned}\nu^{ry(i,j)} &= 0 \\ \gamma^{ry(i,j)} &= -(x_i'^P \sin\phi_i + y_i'^P \cos\phi_i)\dot{\phi}_i^2 + (x_j'^P \sin\phi_j + y_j'^P \cos\phi_j)\dot{\phi}_j^2\end{aligned}$$

(3) A *relative ϕ constraint* requires that the difference between the rotation angles of bodies i and j equal a given constant C_3 (see Fig. 3.3.1); that is,

$$\Phi^{r\phi(i,j)} \equiv \phi_j - \phi_i - C_3 = 0 \tag{3.3.5}$$

The Jacobians of this constraint with respect to $\mathbf{q}_i$ and $\mathbf{q}_j$ are simply

$$\begin{aligned}\Phi_{\mathbf{q}_i}^{r\phi(i,j)} &= [0,\ 0,\ -1] \\ \Phi_{\mathbf{q}_j}^{r\phi(i,j)} &= [0,\ 0,\ 1]\end{aligned} \tag{3.3.6}$$

Finally, from Eqs. 3.1.9 and 3.1.10,

$$\begin{aligned}\nu^{r\phi(i,j)} &= 0 \\ \gamma^{r\phi(i,j)} &= 0\end{aligned}$$

(4) A *relative distance constraint* between point P_i on body i and point P_j on body j requires that the distance between these points equal a given constant

$C_4 > 0$ (see Fig. 3.3.1); that is, using Eq. 2.4.8,

$$\begin{aligned}\Phi^{rd(i,j)} &\equiv (\mathbf{r}_i^P - \mathbf{r}_j^P)^T(\mathbf{r}_i^P - \mathbf{r}_j^P) - C_4^2 \\ &= (x_i + x_i'^P \cos\phi_i - y_i'^P \sin\phi_i - x_j - x_j'^P \cos\phi_j + y_j'^P \sin\phi_j)^2 \\ &\quad + (y_i + x_i'^P \sin\phi_i + y_i'^P \cos\phi_i - y_j - x_j'^P \sin\phi_j - y_j'^P \cos\phi_j)^2 \\ &\quad - C_4^2 = 0\end{aligned} \tag{3.3.7}$$

The Jacobians of this constraint with respect to $\mathbf{q}_i$ and $\mathbf{q}_j$ are

$$\begin{aligned}\Phi_{\mathbf{q}_i}^{rd(i,j)} &= 2[(\mathbf{r}_i^P - \mathbf{r}_j^P)^T,\ \mathbf{s}_i'^{P^T}\mathbf{B}_i^T(\mathbf{r}_i^P - \mathbf{r}_j^P)] \\ \Phi_{\mathbf{q}_j}^{rd(i,j)} &= 2[-(\mathbf{r}_i^P - \mathbf{r}_j^P)^T,\ -\mathbf{s}_j'^{P^T}\mathbf{B}_j^T(\mathbf{r}_i^P - \mathbf{r}_j^P)]\end{aligned} \tag{3.3.8}$$

Since there is no explicit time dependence in Eq. 3.3.7, from Eq. 3.1.9,

$$\nu^{rd(i,j)} = 0$$

Expanding terms in Eq. 3.1.10, using the Jacobians of Eq. 3.3.8, leads to calculations similar to those encountered in expanding $\gamma^{ad(i)}$; that is,

$$\begin{aligned}\gamma^{rd(i,j)} &= -2\{(\dot{\mathbf{r}}_i - \dot{\mathbf{r}}_j)^T(\dot{\mathbf{r}}_i - \dot{\mathbf{r}}_j) \\ &\quad + (\dot{\mathbf{r}}_i - \dot{\mathbf{r}}_j)^T(\mathbf{B}_i\mathbf{s}_i'^P\dot{\phi}_i - \mathbf{B}_j\mathbf{s}_j'^P\dot{\phi}_j) \\ &\quad - (\mathbf{s}_i'^{P^T}\mathbf{A}_i^T\dot{\phi}_i^2 - \mathbf{s}_j'^P\mathbf{A}_j^T\dot{\phi}_j^2)(\mathbf{r}_i^P - \mathbf{r}_j^P) \\ &\quad + (\mathbf{s}_i'^{P^T}\mathbf{B}_i^T\dot{\phi}_i - \mathbf{s}_j'^{P^T}\mathbf{B}_j^T\dot{\phi}_j)(\dot{\mathbf{r}}_i - \dot{\mathbf{r}}_j + \mathbf{B}_i\mathbf{s}_i'^P\dot{\phi}_i - \mathbf{B}_j\mathbf{s}_j'^P\dot{\phi}_j)\} \\ &= -2\{(\dot{\mathbf{r}}_i^P - \dot{\mathbf{r}}_j^P)^T(\dot{\mathbf{r}}_i^P - \dot{\mathbf{r}}_j^P) \\ &\quad - (\mathbf{s}_i'^{P^T}\mathbf{A}_i^T\dot{\phi}_i^2 - \mathbf{s}_j'^{P^T}\mathbf{A}_j^T\dot{\phi}_j^2)(\mathbf{r}_i^P - \mathbf{r}_j^P)\}\end{aligned}$$

As noted following Eq. 3.2.1, $C_4 > 0$ is required to rule out both physical and mathematical singularities.

Example 3.3.1: The two-body slider-crank mechanism of Examples 2.4.3 and 3.1.2 (Fig. 3.1.3) can be modeled using an absolute x position constraint on point O_1 (Eq. 3.2.3) with $C_1 = 0$, absolute y position constraints on points O_1 and O_2 (Eq. 3.2.4) with $C_2 = 0$, and relative x and y constraints between P_1 and P_2 (Eqs. 3.3.1 and 3.3.3) with $C_1 = C_2 = 0$ (Prob. 3.3.1). Many other combinations of bodies and relative and absolute constraints can be used to model the slider-crank mechanism (Prob. 3.3.2).

Example 3.3.2: The four-bar mechanism (three moving bodies and ground) of Fig. 3.3.2(a) may be modeled in many ways. Using the points defined in Fig. 3.3.2(b), the following are kinematically equivalent models (Prob. 3.3.3):

1. Bodies 1, 2, and 3
   Constraints: (i) Absolute x and y constraints on points P_1 and Q_3

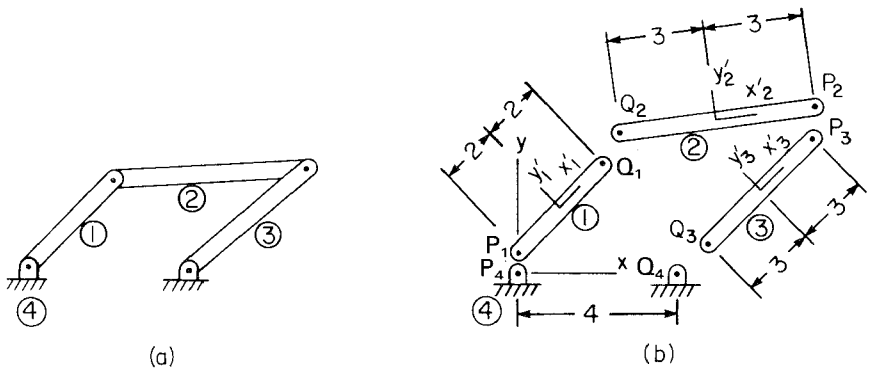

Figure 3.3.2 Four-bar mechanism. (a) Assembled. (b) Dissected.

(ii) Relative x and y constraints between points Q_1 and Q_2 and between points P_2 and P_3

$$\text{DOF} = 3nb - nh = 9 - 8 = 1$$

2. Bodies 1 and 3
Constraints: (i) Absolute x and y constraints on points P_1 and Q_3
(ii) Relative distance constraint between points Q_1 and P_3

$$\text{DOF} = 3nb - nh = 6 - 5 = 1$$

3. Bodies 1 and 2
Constraints: (i) Absolute x and y constraints on point P_1
(ii) Absolute distance constraint on points P_2 from point Q_4
(iii) Relative x and y constraints between points Q_1 and Q_2

$$\text{DOF} = 3nb - nc = 6 - 5 = 1$$

4. Bodies 2
Constraints: (i) Absolute distance constraint on point Q_2 from point P_4 and on point P_2 from point Q_4

$$\text{DOF} = 3nb - nh = 3 - 2 = 1$$

While these models are kinematically equivalent, if the angular orientation of body 1 is to be driven, model 4 cannot be used, and if the angular orientation of body 3 is to be driven, models 3 and 4 cannot be used.

3.3.2 Revolute and Translational Joints

In more complex constraints between bodies, it is helpful to draw figures to aid in developing vector equations that define the constraints. The vector equations may then be manipulated into more useful algebraic forms for numerical

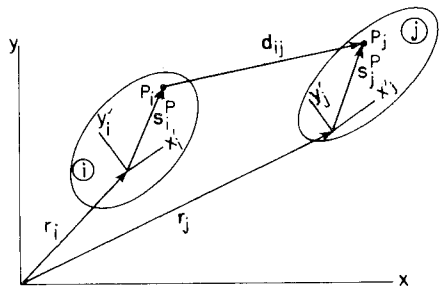

Figure 3.3.3 Relative position of two bodies.

computation and analysis. For example, Fig. 3.3.3 illustrates adjacent bodies i and j. The origins of their corresponding body-fixed reference frames are located by vectors $\mathbf{r}_i$ and $\mathbf{r}_j$ with respect to the global x-y frame. Points P_i and P_j on bodies i and j are located by vectors $\mathbf{s}_i^P$ and $\mathbf{s}_j^P$ (constant vectors $\mathbf{s}_i'^P$ and $\mathbf{s}_j'^P$ in the x_i'-y_i' and x_j'-y_j' frames), respectively. Points P_i and P_j are connected by a vector $\mathbf{d}_{ij}$:

$$\mathbf{d}_{ij} = \mathbf{r}_j + \mathbf{s}_j^P - \mathbf{r}_i - \mathbf{s}_i^P \tag{3.3.9}$$

A *revolute joint* allows relative rotation about a point P that is common to bodies i and j, as shown in Fig. 3.3.4. Physically, such a joint is a rotational bearing between the bodies. If one body is held fixed, the other body has only a single rotational degree of freedom. Thus, a revolute joint eliminates two degrees of freedom from the pair. This joint is defined by locating point P_i on body i by $\mathbf{s}_i'^P$ in the x_i'-y_i' frame and P_j on body j by $\mathbf{s}_j'^P$ in the $x_j' - y_j'$ frame.

Constraint equations that define a revolute joint are obtained by requiring that points P_i and P_j coincide. Employing Eq. 3.3.9 and setting $\mathbf{d}_{ij} = \mathbf{0}$, the constraint equations can be written as

$$\begin{aligned}\mathbf{\Phi}^{r(i,j)} &= \mathbf{r}_i + \mathbf{s}_i^P - \mathbf{r}_j - \mathbf{s}_j^P \\ &= \mathbf{r}_i + \mathbf{A}_i\mathbf{s}_i'^P - \mathbf{r}_j - \mathbf{A}_j\mathbf{s}_j'^P = \mathbf{0}\end{aligned} \tag{3.3.10}$$

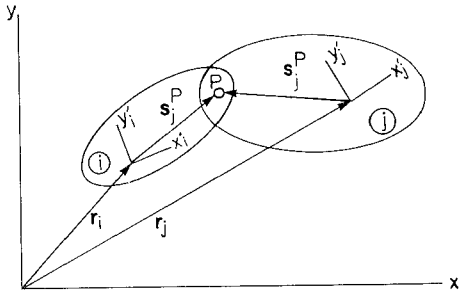

Figure 3.3.4 Revolute joint.

More explicitly,

$$\mathbf{\Phi}^{r(i,j)} \equiv \begin{bmatrix} x_i + x_i'^P \cos\phi_i - y_i'^P \sin\phi_i - x_j - x_j'^P \cos\phi_j + y_j'^P \sin\phi_j \\ y_i + x_i'^P \sin\phi_i + y_i'^P \cos\phi_i - y_j - x_j'^P \sin\phi_j - y_j'^P \cos\phi_j \end{bmatrix} = \mathbf{0} \quad \textbf{(3.3.11)}$$

To confirm that Eq. 3.3.11 is equivalent to the physical revolute joint, it must be shown that it implies the geometry of the joint. Since Eq. 3.3.11 implies $\mathbf{d}_{ij} = \mathbf{0}$, points P_i and P_j coincide (see Fig. 3.3.4), which is the definition of the physical joint.

The Jacobians of this constraint with respect to $\mathbf{q}_i$ and $\mathbf{q}_j$ are, from Eqs. 3.3.10 and 2.6.3,

$$\begin{aligned} \mathbf{\Phi}_{\mathbf{q}_i}^{r(i,j)} &= [\mathbf{I}, \mathbf{B}_i \mathbf{s}_i'^P] \\ \mathbf{\Phi}_{\mathbf{q}_j}^{r(i,j)} &= [-\mathbf{I}, -\mathbf{B}_j \mathbf{s}_j'^P] \end{aligned} \quad \textbf{(3.3.12)}$$

Since Eq. 3.3.11 does not depend explicitly on time, from Eq. 3.1.9,

$$\boldsymbol{\nu}^{r(i,j)} = \mathbf{0}$$

Using matrix algebra and the Jacobians of Eq. 3.3.12, Eq. 3.1.10 yields

$$\boldsymbol{\gamma}^{r(i,j)} = \mathbf{A}_i \mathbf{s}_i'^P \dot{\phi}_i^2 - \mathbf{A}_j \mathbf{s}_j'^P \dot{\phi}_j^2$$

where Eq. 2.6.8 has been used.

Example 3.3.3: The four-bar mechanism of Fig. 3.3.2 can be modeled by designating body 4 as ground and using the absolute x, y, and ϕ constraints of Eqs. 3.2.3, 3.2.4, and 3.2.6, with $\mathbf{s}'^P = \mathbf{0}$ and $C_k = 0$, $k = 1, 2, 3$, to cause the $x_4' - y_4'$ frame to coincide with the x-y frame. With ground modeled as a body, the four rotational couplings in the mechanism can be modeled as four revolute joints defined by Eq. 3.3.11, as follows:

(i) Between bodies 1 and 4 (ground), with $\mathbf{s}_1'^P = [-2, 0]^T$ and $\mathbf{s}_4'^P = \mathbf{0}$.
(ii) Between bodies 1 and 2, with $\mathbf{s}_1'^Q = [2, 0]^T$ and $\mathbf{s}_2'^Q = [-3, 0]^T$.
(iii) Between bodies 2 and 3, with $\mathbf{s}_2'^P = [3, 0]^T$ and $\mathbf{s}_3'^P = [3, 0]^T$.
(iv) Between bodies 3 and 4, with $\mathbf{s}_3'^Q = [-3, 0]^T$ and $\mathbf{s}_4'^Q = [4, 0]^T$.

Including the three constraints on body 4 and four revolute joints, providing all constraints are independent,

$$\text{DOF} = 3nb - nh = 3 \times 4 - 3 - 4 \times 2 = 12 - 11 = 1$$

A *translational joint* allows relative translation of a pair of bodies along a common axis, but no relative rotation of the bodies. Physically, such a joint may be defined as a straight block (or key) on one body that fits precisely in a straight slot (or keyway) on the second body and allows relative translation along their common center lines. If one body were held fixed, the other body has only a single translational degree of freedom. Thus, a translational joint eliminates two degrees of freedom from the pair.

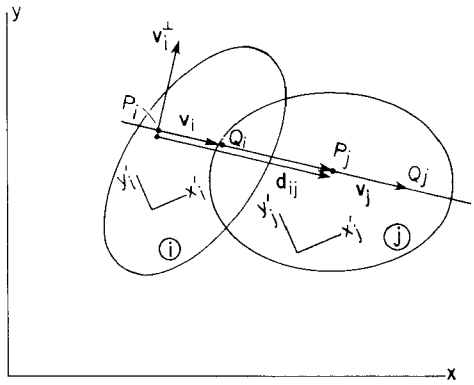

Figure 3.3.5 Translational joint.

For the translational joint shown in Fig. 3.3.5, let points P_i, Q_i, P_j, and Q_j be specified on a line that is parallel to or on the path of relative translation between bodies i and j. Noncoincident points P_i and Q_i are located on body i, and P_j and Q_j are located on body j. Vector $\mathbf{v}_i$ in body i connects points P_i and Q_i, and vector $\mathbf{v}_j$ in body j connects points P_j and Q_j; that is, $\mathbf{v}_i = \mathbf{A}_i \mathbf{v}'_i$, where $\mathbf{v}'_i = [x_i^P - x_i^Q, y_i^P - y_i^Q]^T$ and, similarly, $\mathbf{v}_j$ is defined by data that locate P_j and Q_j on body j. The vector $\mathbf{d}_{ij}$ that connects points P_i and P_j has variable length. Vectors $\mathbf{v}_i$ and $\mathbf{v}_j$ must remain collinear at all times. To have these three vectors collinear, it is necessary that $\mathbf{d}_{ij}$ and $\mathbf{v}_j$ be perpendicular to $\mathbf{v}_i^\perp$, which is perpendicular to $\mathbf{v}_i$. Using Eqs. 2.3.5 and 2.6.6, this is (Prob. 3.3.4)

$$\begin{aligned}\boldsymbol{\Phi}^{t(i,j)} &= \begin{bmatrix} (\mathbf{v}_i^\perp)^T \mathbf{d}_{ij} \\ (\mathbf{v}_i^\perp)^T \mathbf{v}_j \end{bmatrix} \\ &= \begin{bmatrix} \mathbf{v}_i'^T \mathbf{R}^T \mathbf{A}_i^T (\mathbf{r}_j + \mathbf{A}_j \mathbf{s}_j'^P - \mathbf{r}_i - \mathbf{A}_i \mathbf{s}_i'^P) \\ \mathbf{v}_i'^T \mathbf{R}^T \mathbf{A}_i^T \mathbf{A}_j \mathbf{v}'_j \end{bmatrix} \\ &= \begin{bmatrix} \mathbf{v}_i'^T \mathbf{B}_i^T (\mathbf{r}_j - \mathbf{r}_i) - \mathbf{v}_i'^T \mathbf{B}_{ij} \mathbf{s}_j'^P - \mathbf{v}_i'^T \mathbf{R}^T \mathbf{s}_i'^P \\ -\mathbf{v}_i'^T \mathbf{B}_{ij} \mathbf{v}'_j \end{bmatrix} = \mathbf{0} \end{aligned} \tag{3.3.13}$$

As long as $\mathbf{d}_{ij} \neq \mathbf{0}$, Eq. 3.3.13 implies that the three vectors are parallel. Since they have points in common, they are collinear. If $\mathbf{d}_{ij} = \mathbf{0}$, which is possible, then $\mathbf{v}_i$ and $\mathbf{v}_j$ emanate from the same point and, by the second of Eqs. 3.3.13, they are parallel. Thus they are collinear and Eq. 3.3.13 is equivalent to the geometry of the translational joint.

Using Eq. 2.6.8, the Jacobians of $\boldsymbol{\Phi}^{t(i,j)}$ with respect to $\mathbf{q}_i$ and $\mathbf{q}_j$ are (Prob. 3.3.5)

$$\begin{aligned} \boldsymbol{\Phi}_{\mathbf{q}_i}^{t(i,j)} &= \begin{bmatrix} -\mathbf{v}_i'^T \mathbf{B}_i^T, & -\mathbf{v}_i'^T \mathbf{A}_i^T (\mathbf{r}_j - \mathbf{r}_i) - \mathbf{v}_i'^T \mathbf{A}_{ij} \mathbf{s}_j'^P \\ \mathbf{0}, & -\mathbf{v}_i'^T \mathbf{A}_{ij} \mathbf{v}'_j \end{bmatrix} \\ \boldsymbol{\Phi}_{\mathbf{q}_j}^{t(i,j)} &= \begin{bmatrix} \mathbf{v}_i'^T \mathbf{B}_i^T, & \mathbf{v}_i'^T \mathbf{A}_{ij} \mathbf{s}_j'^P \\ \mathbf{0}, & \mathbf{v}_i'^T \mathbf{A}_{ij} \mathbf{v}'_j \end{bmatrix} \end{aligned} \tag{3.3.14}$$

Since Eq. 3.3.13 does not depend explicitly on time,

$$\boldsymbol{\nu}^{t(i,j)} = \mathbf{0}$$

Using matrix algebra and the Jacobians of Eq. 3.3.14, Eq. 3.1.10 may be expanded as

$$\boldsymbol{\gamma}^{t(i,j)} = -[\mathbf{G}^t_{\mathbf{r}_i}\dot{\mathbf{r}}_i + \mathbf{G}^t_{\phi_i}\dot{\phi}_i + \mathbf{G}^t_{\mathbf{r}_j}\dot{\mathbf{r}}_j + \mathbf{G}^t_{\phi_j}\dot{\phi}_j]$$

where

$$\mathbf{G}^t \equiv \boldsymbol{\Phi}^{t(i,j)}_{\mathbf{q}}\dot{\mathbf{q}}$$
$$= \begin{bmatrix} \mathbf{v}_i'^T\mathbf{B}_i^T(\dot{\mathbf{r}}_j - \dot{\mathbf{r}}_i) + \mathbf{v}_i'^T\mathbf{A}_{ij}\mathbf{s}_j'^P(\dot{\phi}_j - \dot{\phi}_i) - \mathbf{v}_i'^T\mathbf{A}_i^T(\mathbf{r}_j - \mathbf{r}_i)\dot{\phi}_i \\ \mathbf{v}_i'^T\mathbf{A}_{ij}\mathbf{v}_j'(\dot{\phi}_j - \dot{\phi}_i) \end{bmatrix}$$

Using Eqs. 2.4.12 and 2.6.8,

$$\boldsymbol{\gamma}^{t(i,j)} = -\begin{bmatrix} \mathbf{v}_i'^T[\mathbf{B}_{ij}\mathbf{s}_j'^P(\dot{\phi}_j - \dot{\phi}_i)^2 - \mathbf{B}_i^T(\mathbf{r}_j - \mathbf{r}_i)\dot{\phi}_i^2 - 2\mathbf{A}_i^T(\dot{\mathbf{r}}_j - \dot{\mathbf{r}}_i)\dot{\phi}_i \\ 0 \end{bmatrix}$$

where the second term on the right is zero, because of Eq. 3.3.13.

Example 3.3.4: Rather than the simplified two-body model of the slider–crank mechanism in Examples 2.4.3 and 3.1.2, the full four-body model of Fig. 3.3.6 can be employed.

To cause the x'_4-y'_4 frame to coincide with the x-y frame, Eqs. 3.2.3, 3.2.4, and 3.2.6 can be used with $\mathbf{s}'^P = \mathbf{0}$ and $C_k = 0$, $k = 1, 2, 3$. Three revolute joints are defined by Eq. 3.3.11, as follows:

(i) Between bodies 1 and 4, with $\mathbf{s}_1'^Q = [-2, 0]^T$ and $\mathbf{s}_4'^Q = \mathbf{0}$.
(ii) Between bodies 1 and 2, with $\mathbf{s}_1'^P = [2, 0]^T$ and $\mathbf{s}_2'^Q = [-3, 0]^T$.
(iii) Between bodies 2 and 3, with $\mathbf{s}_2'^P = [3, 0]^T$ and $\mathbf{s}_3'^P = \mathbf{0}$.

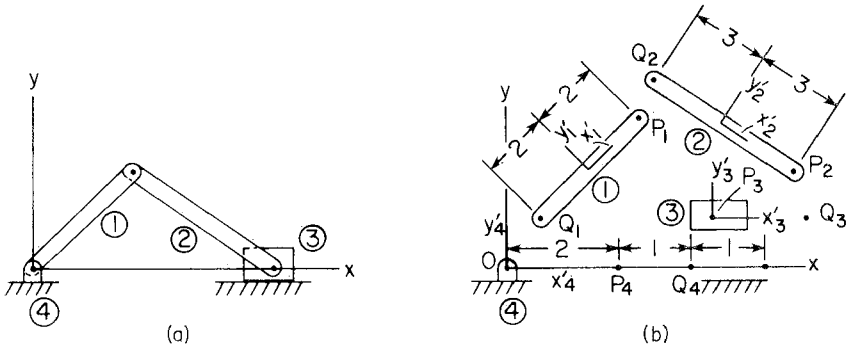

Figure 3.3.6 Four-body slider–crank. (a) Assembled. (b) Dissected.

The final constraint is a translational joint between bodies 3 and 4, which is defined by Eq. 3.3.13 with

$$\mathbf{s}_3'^P = \mathbf{0}, \qquad \mathbf{v}_3' = [1, 0]^T, \qquad \mathbf{s}_4'^P = [2, 0]^T, \qquad \mathbf{v}_4' = [1, 0]^T$$

Accounting for four bodies and all constraints, providing all constraints are independent,

$$\text{DOF} = 3nb - nh = 3 \times 4 - 3 - 3 \times 2 - 2 = 1$$

3.3.3 Composite Joints

In many kinematics applications, the only function of a body is to connect two other bodies, using a combination of revolute and translational joints. Such a connection is called a *coupler,* which need not be treated as a body. The resulting combination may be viewed as a *composite joint,* yielding elementary constraint equations and avoiding the need to introduce generalized coordinates for the coupler. In dynamics, such a body is called a *massless link,* since it is used to represent the kinematic effects of parts that may have insignificant mass. In kinematics, of course, the concept of mass need not arise.

Figure 3.3.7 illustrates a pair of rigid bodies that are connected by a coupler with two revolute joints, called a *revolute–revolute composite joint.* If this special joint were modeled using an additional rigid body and two revolute joints, three additional generalized coordinates and four constraint equations would be required. As shown next, only one constraint equation is required for this composite joint, which simply requires that the length of vector $\mathbf{d}_{ij}$ remain constant and equal to $C > 0$. The constraint equation is thus

$$\Phi^{rr(i,j)} \equiv (x_i^P - x_j^P)^2 + (y_i^P - y_j^P)^2 - C^2 = 0 \tag{3.3.15}$$

The revolute–revolute composite constraint is just a special case of Eq. 3.3.7, with $C_4 = C$. Its Jacobians are given by Eq. 3.3.8: $\nu^{rr(i,j)} = 0$ and $\gamma^{rr(i,j)} = \gamma^{rd(i,j)}$.

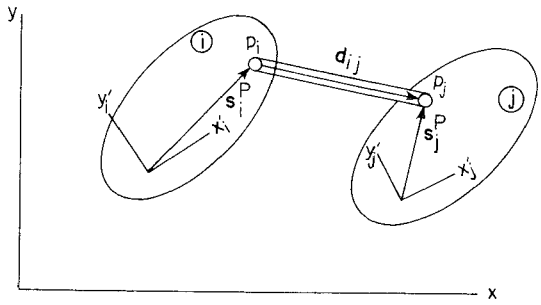

Figure 3.3.7 Revolute–revolute composite joint.

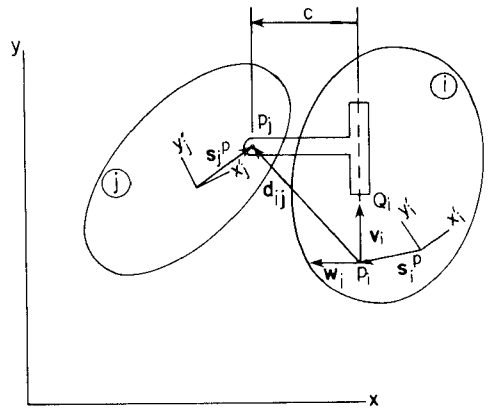

Figure 3.3.8 Revolute–translational composite joint.

Figure 3.3.8 illustrates a *revolute–translational composite joint.* Bodies i and j are connected by a coupler, with a revolute joint on body j and a translational joint on body i. Two noncoincident points P_i and Q_i are chosen on the line of translation in body i. The revolute joint has a given constant directed distance C from the line of translation, with C positive if the revolute joint is to the left of the line of translation, viewed from P_i to Q_i, and negative otherwise.

Note that if body j is fixed, then the coupler, and hence body i, can rotate. Furthermore, body i can translate in the direction $\mathbf{v}_i$. Thus, it has two remaining degrees of freedom. Since the revolute–translational joint eliminates only one degree of freedom, it should be defined by a single scalar constraint equation; that is, the directed distance from the line of translation to the revolute joint should be C.

To formulate this condition, a unit vector $\mathbf{w}_i$, directed to the left of the line of translation, is formed:

$$\mathbf{w}_i = \frac{1}{v_i}\mathbf{v}_i^{\perp} = \frac{1}{v_i}\mathbf{A}_i\mathbf{R}\mathbf{v}_i' \tag{3.3.16}$$

where v_i is the constant distance between P_i and Q_i. The directed distance C must thus be equal to the scalar product of $\mathbf{w}_i$ and $\mathbf{d}_{ij}$, yielding the desired constraint equation:

$$\begin{aligned}\Phi^{rt(i,j)} &= \frac{1}{v_i}\mathbf{v}_i'^T\mathbf{R}^T\mathbf{A}_i^T(\mathbf{r}_j + \mathbf{A}_j\mathbf{s}_j'^P - \mathbf{r}_i - \mathbf{A}_i\mathbf{s}_i'^P) - C \\ &= \frac{1}{v_i}[\mathbf{v}_i'^T\mathbf{B}_i^T(\mathbf{r}_j - \mathbf{r}_i) - \mathbf{v}_i'^T\mathbf{B}_{ij}\mathbf{s}_j'^P - \mathbf{v}_i'^T\mathbf{R}^T\mathbf{s}_i'^P] - C = 0\end{aligned} \tag{3.3.17}$$

The Jacobian matrices for this constraint with respect to $\mathbf{q}_i$ and $\mathbf{q}_j$ are

$$\begin{aligned}\Phi_{\mathbf{q}_i}^{rt(i,j)} &= \frac{1}{v_i}[-\mathbf{v}_i'^T\mathbf{B}_i^T,\ -\mathbf{v}_i'^T\mathbf{A}_i^T(\mathbf{r}_j-\mathbf{r}_i)-\mathbf{v}_i'^T\mathbf{A}_{ij}\mathbf{s}_j'^P] \\ \Phi_{\mathbf{q}_j}^{rt(i,j)} &= \frac{1}{v_i}[\mathbf{v}_i'^T\mathbf{B}_i^T,\ \mathbf{v}_i'^T\mathbf{A}_{ij}\mathbf{s}_j'^P]\end{aligned} \tag{3.3.18}$$

Since there is no explicit time dependence in Eq. 3.3.17,

$$\nu^{rt(i,j)} = 0$$

Using matrix algebra and the Jacobians of Eq. 3.3.18,

$$\gamma^{rt(i,j)} = -[G_{\mathbf{r}_i}^{rt}\dot{\mathbf{r}}_i + G_{\phi_i}^{rt}\dot{\phi}_i + G_{\mathbf{r}_j}^{rt}\dot{\mathbf{r}}_j + G_{\phi_i}^{rt}\dot{\phi}_i]$$

where

$$\begin{aligned}G^{rt} &\equiv \Phi_{\mathbf{q}}^{rt(i,j)}\dot{\mathbf{q}} \\ &= \frac{1}{v_i}[\mathbf{v}_i'^T\mathbf{B}_i^T(\dot{\mathbf{r}}_j-\dot{\mathbf{r}}_i)-\mathbf{v}_i'^T\mathbf{A}_i^T(\mathbf{r}_j-\mathbf{r}_i)\dot{\phi}_i \\ &\quad + \mathbf{v}_i'^T\mathbf{A}_{ij}\mathbf{s}_j'^P(\dot{\phi}_j-\dot{\phi}_i)]\end{aligned}$$

Using Eqs. 2.4.12 and 2.6.8,

$$\begin{aligned}\gamma^{rt(i,j)} = \frac{1}{v_i}\mathbf{v}_i'^T[&2\mathbf{A}_i^T(\dot{\mathbf{r}}_j-\dot{\mathbf{r}}_i)\dot{\phi}_i \\ &+ \mathbf{B}_i^T(\mathbf{r}_j-\mathbf{r}_i)\dot{\phi}_i^2 - \mathbf{B}_{ij}\mathbf{s}_j'^P(\dot{\phi}_j-\dot{\phi}_i)^2]\end{aligned}$$

Example 3.3.5: The slider–crank mechanism of Example 3.3.4, shown in Fig. 3.3.6, can be modeled by replacing body 3 and its associated revolute joint with body 2 and translational joint with body 4 by a revolute–translational composite joint between bodies 4 and 2. The constraint is defined by Eq. 3.3.17, with

$$\mathbf{s}_4'^P = [2,\ 0]^T, \qquad \mathbf{v}_4' = [1,\ 0]^T, \qquad \mathbf{s}_2'^P = [3,\ 0]^T, \qquad C = 0$$

Since only bodies 1, 2, and 4 remain, with three absolute constraints on body 4, revolute joints (i) and (ii) from Example 3.3.4, and the single constraint of Eq. 3.3.17,

$$\text{DOF} = 3nb - nh = 3\times 3 - 3 - 2\times 2 - 1 = 1$$

3.4 GEARS AND CAM–FOLLOWERS

3.4.1 Gears

A *convex–convex gear set* or simply *gear set* consists of a pair of gears on two bodies that are constrained so that the distance $R_i + R_j$ between their centers is

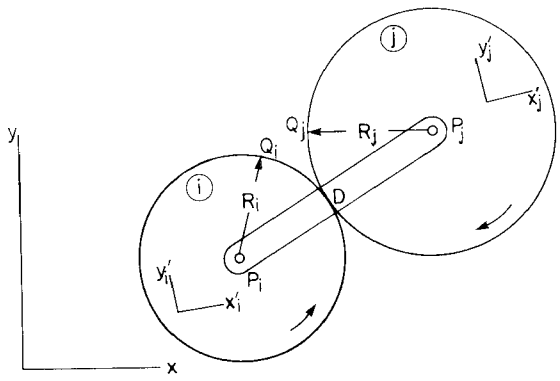

Figure 3.4.1 Gear set.

fixed, as shown in Fig. 3.4.1. Gear teeth on the periphery of the gears cause the pitch circles shown to roll relative to each other, without slip. Thus, the arc lengths DQ_i and DQ_j of contact on the gears must be equal, where points Q_i and Q_j are defined so that they coincide at the initial assembly of the gear set.

Based on the geometry of the gear set shown in Fig. 3.4.2,

$$\begin{aligned} \alpha_i &= \phi_i + \theta_i - \theta \\ \alpha_j &= -(\phi_j + \theta_j - \theta - \pi) \\ \alpha_i R_i &= \alpha_j R_j \end{aligned} \tag{3.4.1}$$

where θ_i and θ_j are data that define the assembly of the gear set, and the third equation is obtained by equating lengths of arcs DQ_i and DQ_j. These are the defining equations for the gear set.

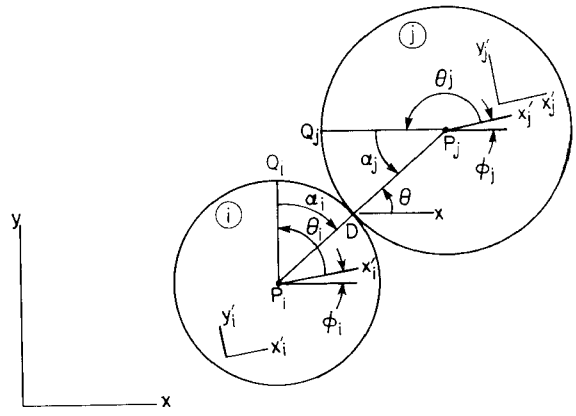

Figure 3.4.2 Geometry of gear set.

Solving Eqs. 3.4.1 for θ,

$$\theta = \frac{R_i(\phi_i + \theta_i) + R_j(\phi_j + \theta_j) - R_j\pi}{R_i + R_j} \tag{3.4.2}$$

Since the distance between gear centers is established by other constraints, the *gear constraint* is just

$$\begin{aligned}\Phi^{g(i,j)} &= (\mathbf{r}_j^P - \mathbf{r}_i^P)\mathbf{u}^\perp \\ &= (x_j^P - x_i^P)\sin\theta - (y_j^P - y_i^P)\cos\theta = 0\end{aligned} \tag{3.4.3}$$

where θ is given by Eq. 3.4.2 and $\mathbf{u}^\perp \equiv [-\sin\theta, \cos\theta]^T$; that is, $\mathbf{u} = [\cos\theta, \sin\theta]^T$ is a unit vector along the line from P_i to P_j in Fig. 3.4.2.

It is important to confirm that Eq. 3.4.3, with additional constraints that assure the distance between points P_i and P_j is $R_i + R_j$, imply that the gear set geometric relations of Eq. 3.4.1 hold. Since the distance between P_i and P_j is $R_i + R_j$ and at initial assembly Q_i and Q_j coincide, then, for $|t - t_0|$ small, Eq. 3.4.3 implies that θ of Eq. 3.4.2 is the angle shown in Fig. 3.4.2. Thus α_i and α_j are related to θ as defined in the first two of Eqs. 3.4.1. Substituting θ of Eq. 3.4.2 into these relations and expanding,

$$\begin{aligned}R_i\alpha_i - R_j\alpha_j &= R_i(\phi_i + \theta_i - \theta) + R_j(\phi_j + \theta_j - \theta - \pi) \\ &= R_i(\phi_i + \theta_i) + R_j(\phi_j + \theta_j - \pi) - (R_i + R_j)\theta \\ &= 0\end{aligned}$$

Thus, providing $\mathbf{q}_i$ and $\mathbf{q}_j$ are continuous functions of time, Eqs. 3.4.1 hold for all time, and Eq. 3.4.3 plus the distance constraint between P_i and P_j implies the geometry of the convex–convex gear set.

The Jacobians of the constraint of Eq. 3.4.3, with respect to $\mathbf{q}_i$ and $\mathbf{q}_j$, are

$$\begin{aligned}\Phi_{\mathbf{q}_i}^{g(i,j)} &= \left[-\mathbf{u}^T,\ -\mathbf{s}_i'^{P^T}\mathbf{B}_i^T\mathbf{u} + (\mathbf{r}_j^P - \mathbf{r}_i^P)^T\mathbf{u}^\perp\left(\frac{R_i}{R_i + R_j}\right)\right] \\ \Phi_{\mathbf{q}_j}^{g(i,j)} &= \left[\mathbf{u}^T,\ \mathbf{s}_j'^{P^T}\mathbf{B}_j^T\mathbf{u} + (\mathbf{r}_j^P - \mathbf{r}_i^P)^T\mathbf{u}^\perp\left(\frac{R_j}{R_i + R_j}\right)\right]\end{aligned} \tag{3.4.4}$$

where $d\mathbf{u}/d\theta = [-\sin\theta, \cos\theta]^T = \mathbf{u}^\perp$ (see Eq. 2.3.5) has been used.

As in all previous constraints, there is no explicit time dependence in Eq. 3.4.3, so

$$\nu^g = 0$$

Using the Jacobians of Eq. 3.4.4 and Eqs. 3.4.2 and 3.4.3, Eq. 3.1.10 yields

$$\gamma^g = \left[2(\dot{\mathbf{r}}_j^P - \dot{\mathbf{r}}_i^P)^T\mathbf{u}\left(\frac{R_i\dot{\phi}_i + R_j\dot{\phi}_j}{R_i + R_j}\right) + (\mathbf{A}_j\mathbf{s}_j'^P\dot{\phi}_j^2 - \mathbf{A}_i\mathbf{s}_i'^P\dot{\phi}_i^2)^T\mathbf{u}^\perp\right]$$

Example 3.4.1: Consider the pair of gears shown in Fig. 3.4.3, with gear 1 fixed to ground. Let $\phi_1 = 0$, $\theta_1 = \pi/6$, $\theta_2 = 7\pi/6$, $R_1 = 1$, and $R_2 = 2$. A revolute–revolute composite joint of length 3 connects the centers of the gears. Find angle ϕ_2 as gear 2 falls to the position shown, in which P_2 is on the vertical line through P_1.

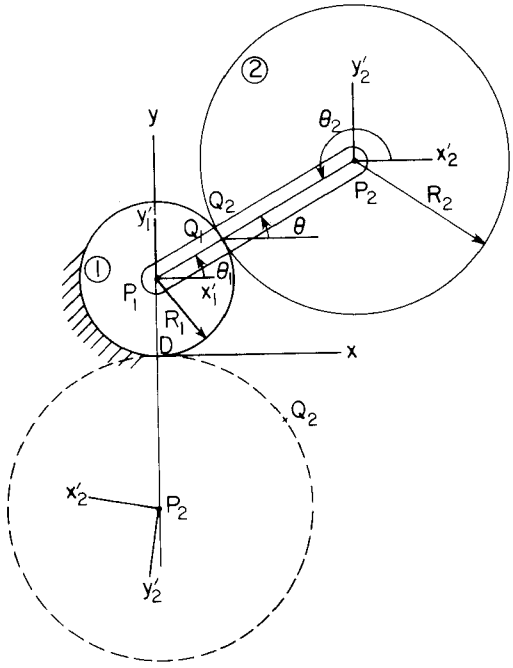

Figure 3.4.3 Gear joint with distance constraint.

From Eq. 3.4.3,

$$-(-2-1)\cos\theta = 0$$

Thus,

$$\theta = -\frac{\pi}{2}$$

Substituting into Eq. 3.4.2,

$$-\frac{\pi}{2} = \frac{1(0+\pi/6) + 2(\phi_2 + 7\pi/6) - 2\pi}{1+2}$$

Thus, $\phi_2 = -\pi$.

Consider next the *concave–convex gear set* shown in Fig. 3.4.4, in which the smaller gear on body j with center at P_j makes rolling contact inside the larger

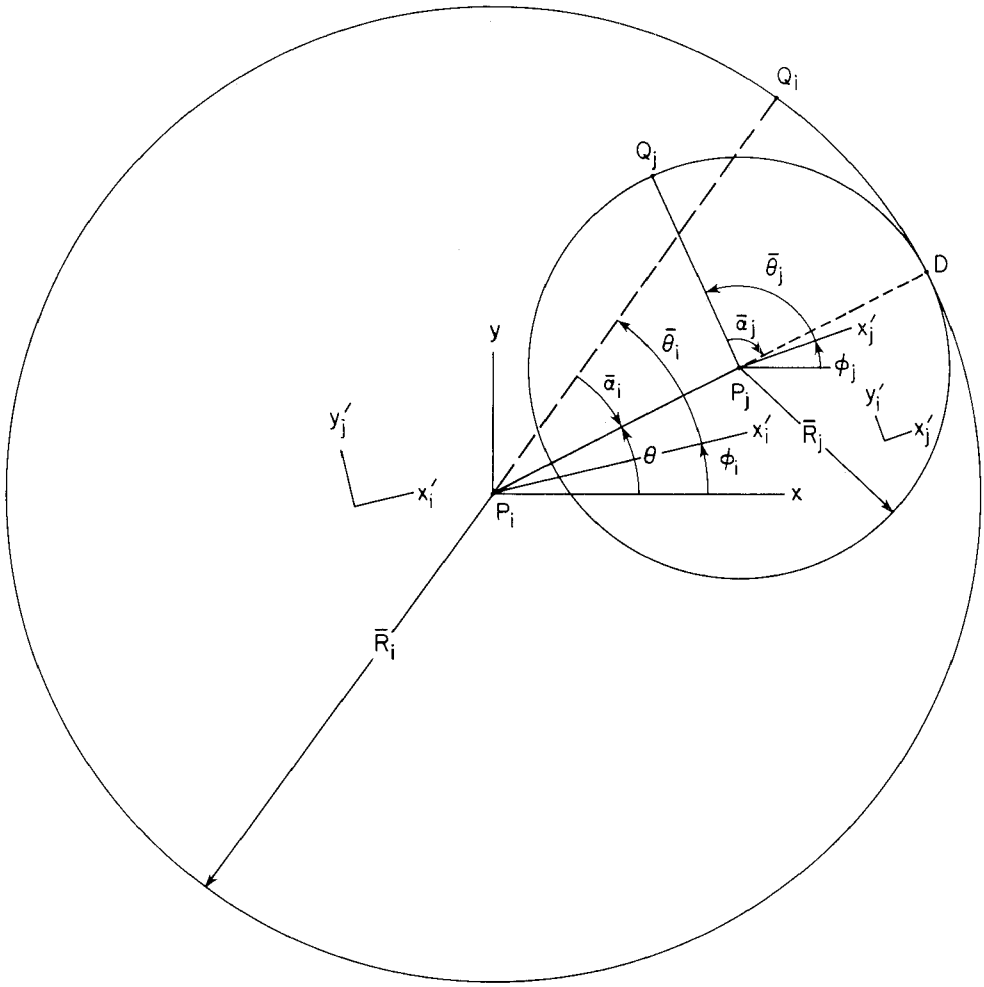

Figure 3.4.4 Concave–convex gear set.

interior gear with center at point P_i on body i. A bar (or distance constraint) of length $\bar{R}_i - \bar{R}_j > 0$ separates the centers of the gears.

Based on the geometry of Fig. 3.4.4,

$$\begin{aligned} \bar{\alpha}_i &= \phi_i + \bar{\theta}_i - \theta \\ \bar{\alpha}_j &= \phi_j + \bar{\theta}_j - \theta \\ \bar{\alpha}_i \bar{R}_i &= \bar{\alpha}_j \bar{R}_j \end{aligned} \tag{3.4.5}$$

where $\bar{\theta}_i$ and $\bar{\theta}_j$ define the assembly of the gear set. Solving Eq. 3.4.5 for θ,

$$\theta = \frac{-\bar{R}_i(\phi_i + \bar{\theta}_i) + \bar{R}_j(\phi_j + \bar{\theta}_j)}{-\bar{R}_i + \bar{R}_j} \tag{3.4.6}$$

From the geometry of the gear set, with the distance between P_i and P_j fixed by other constraints, Eq. 3.4.3 remains valid as an equation of constraint for the concave–convex gear set, but with θ defined by Eq. 3.4.6. A repetition of the argument that follows Eq. 3.4.3 shows that Eqs. 3.4.3 and 3.4.6, taken with additional constraints that define the distance between P_i and P_j, imply the geometry of the gear set.

Note that, if the following conventions are adopted,

$$\begin{aligned} R_i &= -\bar{R}_i < 0 \\ R_j &= \bar{R}_j > 0 \\ \theta_i &= \bar{\theta}_i \\ \theta_j &= \bar{\theta}_j - \pi \end{aligned} \tag{3.4.7}$$

then Eq. 3.4.6 takes exactly the form of Eq. 3.4.2. With this notation, Eq. 3.4.3 is unchanged, and Eq. 3.4.4 gives the constraint Jacobian for the concave–convex gear set.

If the radius of the gear on body i becomes infinite, a straight gear profile called a *rack* results. The gear on body j is then called a *pinion,* and the gear pair is called a *rack and pinion,* as shown in Fig. 3.4.5. If the pinion is on the left of the rack, as viewed from point P_i to point Q_i, then the radius of the pinion is taken as positive. If the pinion is on the right, its radius is negative.

This pair may be interpreted as a special case of the revolute–translational composite joint in which the advance s of the pinion, that is, the distance between points Q_i and D in Fig. 3.4.5, is dictated by the condition that lengths DQ_i and DQ_j in Fig. 3.4.5 be equal. Thus, the revolute–translational equation of Eq. 3.3.17, with i and j interchanged and $C = R_j$, must hold. The equal arc length

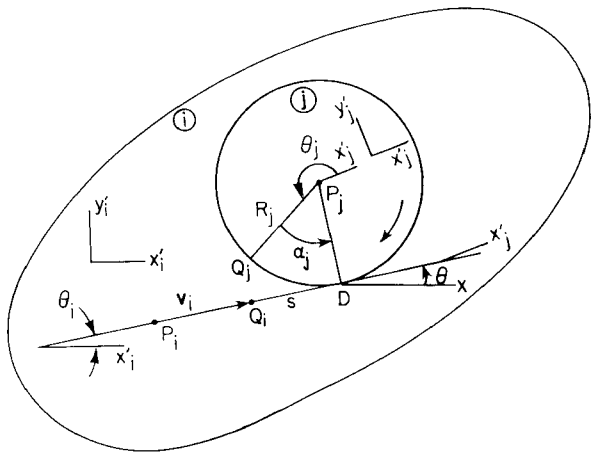

Figure 3.4.5 Rack and pinion.

condition is

$$s - R_j\alpha_j = 0 \tag{3.4.8}$$

To write Eq. 3.4.8 in terms of generalized coordinates, note from Fig. 3.4.5 that

$$s = \frac{1}{v_i}\mathbf{v}_i^T(\mathbf{r}_j^P - \mathbf{r}_i^Q) \tag{3.4.9}$$

$$\theta = \phi_i + \theta_i \tag{3.4.10}$$

and

$$\phi_j + \theta_j + \alpha_j + \frac{\pi}{2} = \theta + 2\pi \tag{3.4.11}$$

From Eqs. 3.4.10 and 3.4.11,

$$\alpha_j = \phi_i + \theta_i - \phi_j - \theta_j + \frac{3\pi}{2} \tag{3.4.12}$$

Substituting Eqs. 3.4.9 and 3.4.12 into Eq. 3.4.8 and writing the revolute–translational constraint of Eq. 3.3.17 in vector form, the constraint equations for this pair are

$$\mathbf{\Phi}^{rp(i,j)} = \begin{bmatrix} (\mathbf{r}_j^P - \mathbf{r}_i^Q)^T\mathbf{v}_i - v_iR_j\alpha_j \\ (\mathbf{r}_j^P - \mathbf{r}_i^P)^T\mathbf{v}_i^\perp - v_iR_j \end{bmatrix} = \mathbf{0} \tag{3.4.13}$$

Derivation of the Jacobians, $\mathbf{v}^{rp(i,j)}$, and $\boldsymbol{\gamma}^{rp(i,j)}$ for this constraint are left as an exercise (Prob. 3.4.4).

Example 3.4.2: Rotation of the gear in Fig. 3.4.6 is controlled by the horizontal motion of point P_1 of the rack. For analytical simplicity, let $\mathbf{q} = [x_1, \phi_1, \phi_2]^T$ be a reduced set of generalized coordinates. Let the distance from

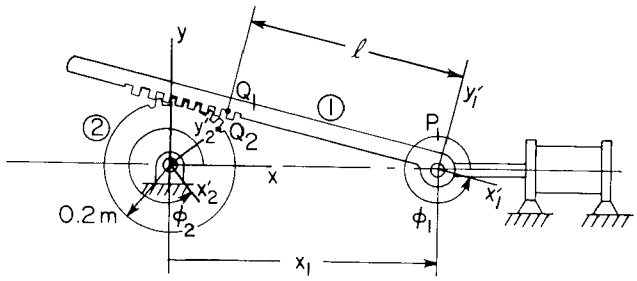

Figure 3.4.6 Slider–crank with a rack and pinion.

point P_1 to point Q_1 be ℓ. Then the vector $\mathbf{v}_1$ in Fig. 3.4.5 is

$$\mathbf{v}_1 = \begin{bmatrix} \cos\phi_1 & -\sin\phi_1 \\ \sin\phi_1 & \cos\phi_1 \end{bmatrix} \begin{bmatrix} -\ell \\ 0 \end{bmatrix} = \begin{bmatrix} -\ell\cos\phi_1 \\ -\ell\sin\phi_1 \end{bmatrix}$$

From Eq. 3.4.12,

$$\alpha_2 = \phi_1 + 0 - \phi_2 - \frac{3\pi}{2} + \frac{3\pi}{2} = \phi_1 - \phi_2$$

With this result and from the first of Eqs. 3.4.13,

$$-\left\{ \begin{bmatrix} x_1 \\ 0 \end{bmatrix} + \begin{bmatrix} \cos\phi_1 & -\sin\phi_1 \\ \sin\phi_1 & \cos\phi_1 \end{bmatrix} \begin{bmatrix} -\ell \\ 0 \end{bmatrix} \right\}^T \begin{bmatrix} -\ell\cos\phi_1 \\ -\ell\sin\phi_1 \end{bmatrix} - \ell(0.2)(\phi_1 - \phi_2) = 0$$

By simplifying,

$$x_1\cos\phi_1 - \ell = 0.2(\phi_1 - \phi_2) = 0$$

From the second of Eqs. 3.4.13,

$$-[x_1, 0] \begin{bmatrix} 0 & -1 \\ 1 & 0 \end{bmatrix} \begin{bmatrix} -\ell\cos\phi_1 \\ -\ell\sin\phi_1 \end{bmatrix} - 0.2\ell = -x_1\ell\sin\phi_1 - 0.2\ell = 0$$

Thus the constraint equation of the rack and pinion joint, Eq. 3.4.13, is

$$\mathbf{\Phi}(\mathbf{q}) = \begin{bmatrix} x_1\cos\phi_1 - \ell - 0.2(\phi_1 - \phi_2) \\ x_1\sin\phi_1 + 0.2 \end{bmatrix} = \mathbf{0}$$

Differentiating both sides,

$$\begin{bmatrix} \cos\phi_1 & -(x_1\sin\phi_1 + 0.2) & 0.2 \\ \sin\phi_1 & x_1\cos\phi_1 & 0 \end{bmatrix} \begin{bmatrix} \dot{x}_1 \\ \dot{\phi}_1 \\ \dot{\phi}_2 \end{bmatrix} = \mathbf{0} \qquad \textbf{(3.4.14)}$$

If the piston has velocity $\dot{x}_1 = 0.3$ m/s when $x_1 = 0.8$ m, then $\dot{\phi}_1$ and $\dot{\phi}_2$ can be found by partitioning Eq. 3.4.14:

$$\begin{bmatrix} -x_1\sin\phi_1 - 0.2 & 0.2 \\ x_1\cos\phi_1 & 0 \end{bmatrix} \begin{bmatrix} \dot{\phi}_1 \\ \dot{\phi}_2 \end{bmatrix} = \begin{bmatrix} -\cos\phi_1 \\ -\sin\phi_1 \end{bmatrix} \dot{x}_1$$

The angular velocities are thus

$$[\dot{\phi}_1, \dot{\phi}_2]^T = [0.0968, -1.4524]^T$$

3.4.2 Cam–Followers

A *cam–follower* pair is shown in its most general form in Fig. 3.4.7, where body i is the cam and body j is the follower. The two bodies are in contact at point P, but sliding is permitted, unlike the case of a gear set. It is assumed that the cam and its follower always remain in contact with each other; that is, no chattering is allowed. In addition, it is assumed that the contact surfaces (outlines) are either

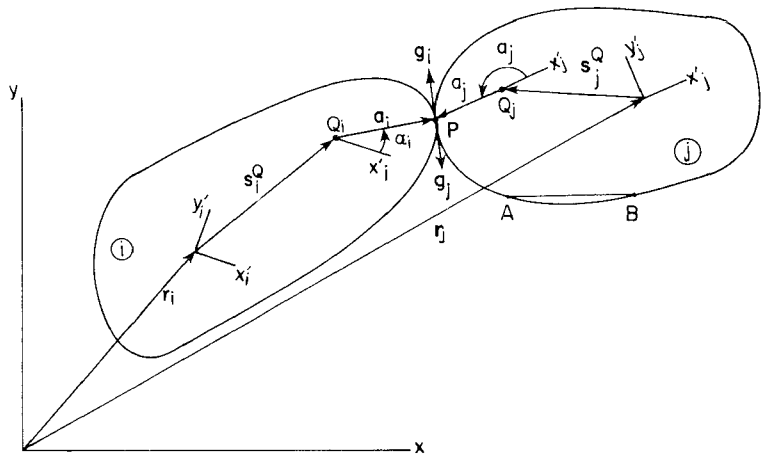

Figure 3.4.7 Cam–follower pair.

convex shapes or flat. An outline is *convex* if the straight line between any pair of points on the outline lies inside the body (e.g., points A and B on body j in Fig. 3.4.7).

A curve that defines the boundary of a body may have a general convex outline, as shown in Fig. 3.4.8. A point P on the boundary can be located in a polar coordinate system that is fixed in the body, with origin at point Q. The angle α is measured relative to the body-fixed x' axis, as shown in Fig. 3.4.8.

The location of point P in the x'-y' frame is given by

$$\mathbf{r}'^{P} = \mathbf{s}'^{Q} + \mathbf{a}' \tag{3.4.15}$$

In terms of the angle α,

$$\mathbf{a}' = \rho(\alpha)\mathbf{u}'(\alpha) \tag{3.4.16}$$

where $\rho(\alpha)$ is the length of $\mathbf{a}(\alpha)$ and $\mathbf{u}'(\alpha) = [\cos\alpha, \sin\alpha]^T$.

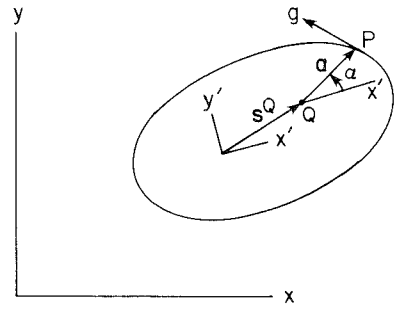

Figure 3.4.8 Body outline representation.

The tangent to the outline curve at point P in Fig. 3.4.8 is expressed in the x'-y' frame as

$$\mathbf{g}' = \frac{d\mathbf{a}'}{d\alpha} = \rho_\alpha \mathbf{u}' + \rho \mathbf{u}'_\alpha$$
$$= \rho_\alpha \mathbf{u}' + \rho \mathbf{u}'^{\perp} \tag{3.4.17}$$

A cam outline $\rho(\alpha)$ is often described by a table of data points. A numerical method of curve fitting and interpolation must then be applied. Cubic spline interpolation is suggested for this purpose, since it provides continuous first and second derivatives [24].

Since the two bodies must remain in contact, from Fig. 3.4.7, a loop equation yields

$$\mathbf{r}_i + \mathbf{s}_i^Q + \mathbf{a}_i - \mathbf{a}_j - \mathbf{s}_j^Q - \mathbf{r}_j = \mathbf{0} \tag{3.4.18}$$

Equation 3.4.18 provides two algebraic constraint equations that involve the outline curve parameters α_i and α_j and the Cartesian coordinates of the bodies. Since the cam and follower are in contact at only one point, the tangents to both outlines at point P, that is, $\mathbf{g}_i$ and $\mathbf{g}_j$, must be collinear; so

$$\mathbf{g}_i^{\perp T}\mathbf{g}_j = (\mathbf{R}\mathbf{g}_i)^T\mathbf{g}_j = \mathbf{g}_i^T\mathbf{R}^T\mathbf{g}_j = -\mathbf{g}_i'^T\mathbf{B}_{ij}\mathbf{g}_j' = 0 \tag{3.4.19}$$

where Eqs. 2.6.5 and 2.6.6 have been used. The expanded form of Eqs. 3.4.18 and 3.4.19 yield three constraint equations:

$$\mathbf{\Phi}^{cf(i,j)} \equiv \begin{bmatrix} \mathbf{r}_i + \mathbf{A}_i(\mathbf{s}_i'^Q + \rho_i\mathbf{u}_i') - \mathbf{A}_j(\rho_j\mathbf{u}_j' + \mathbf{s}_j'^Q) - \mathbf{r}_j \\ -\mathbf{g}_i'^T\mathbf{B}_{ij}\mathbf{g}_j' \end{bmatrix} = \mathbf{0} \tag{3.4.20}$$

The outline parameters α_i and α_j appear in Eq. 3.4.20. They are treated as additional unknown generalized coordinates that locate the point P of contact. Hence, the vector of generalized coordinates for a mechanism with nb rigid bodies and one cam–follower joint has $nc = 3nb + 2$ components; that is,

$$\mathbf{q} \equiv [x_1, y_1, \phi_1, \ldots, x_{nb}, y_{nb}, \phi_{nb}, \alpha_i, \alpha_j]^T$$

Since it is defined by three constraint equations and two excess variables, each cam–follower pair eliminates only one relative degree of freedom between the bodies it connects.

The Jacobians of the constraint of Eq. 3.4.20, with respect to $\mathbf{q}_i$, α_i, $\mathbf{q}_j$, and α_j, using Eqs. 2.4.11, 2.4.12, and 2.6.8, are

$$\mathbf{\Phi}_{\mathbf{q}_i}^{cf(i,j)} = \begin{bmatrix} \mathbf{I} & \mathbf{B}_i(\mathbf{s}_i'^Q + \rho_i\mathbf{u}_i') \\ \mathbf{0} & -\mathbf{g}_i'^T\mathbf{A}_{ij}\mathbf{g}_j' \end{bmatrix} \qquad \mathbf{\Phi}_{\alpha_i}^{cf(i,j)} = \begin{bmatrix} \mathbf{A}_i\mathbf{g}_i' \\ -(\mathbf{g}_i')_{\alpha_i}^T\mathbf{B}_{ij}\mathbf{g}_j' \end{bmatrix} \tag{3.4.21}$$

$$\mathbf{\Phi}_{\mathbf{q}_j}^{cf(i,j)} = \begin{bmatrix} -\mathbf{I} & -\mathbf{B}_j(\mathbf{s}_j'^Q + \rho_j\mathbf{u}_j') \\ \mathbf{0} & \mathbf{g}_i'^T\mathbf{A}_{ij}\mathbf{g}_i' \end{bmatrix} \qquad \mathbf{\Phi}_{\alpha_j}^{cf(i,j)} = \begin{bmatrix} -\mathbf{A}_j\mathbf{g}_j' \\ -\mathbf{g}_i'^T\mathbf{B}_{ij}(\mathbf{g}_j')_{\alpha_j} \end{bmatrix}$$

Since there is no explicit dependence on time in Eq. 3.4.20,

$$\boldsymbol{\nu}^{cf(i,j)} = \mathbf{0}$$

Carrying out the expansion of Eq. 3.1.10, using the Jacobians of Eqs. 3.4.21 and 3.4.19 and recalling that α_i and α_j are generalized coordinates,

$$\boldsymbol{\gamma}^{cf(i,j)} = \begin{bmatrix} \mathbf{A}_i(\mathbf{s}_i'^{Q} + \rho_i \mathbf{u}_i')\dot{\phi}_i^2 - \mathbf{A}_j(\mathbf{s}_j'^{Q} + \rho_j \mathbf{u}_j')\dot{\phi}_j^2 - \mathbf{A}_i(\mathbf{g}_i')_{\alpha_i}\dot{\alpha}_i^2 \\ + \mathbf{A}_j(\mathbf{g}_j')_{\alpha_j}\dot{\alpha}_j^2 - 2\mathbf{B}_i\mathbf{g}_i'\dot{\phi}_i\dot{\alpha}_i + 2\mathbf{B}_j\mathbf{g}_j'\dot{\phi}_j\dot{\alpha}_j \\ (\mathbf{g}_i')^T_{\alpha_i\alpha_i}\mathbf{B}_{ij}\mathbf{g}_j'\dot{\alpha}_i^2 + \mathbf{g}_i'^T\mathbf{B}_{ij}(\mathbf{g}_j')_{\alpha_j\alpha_j}\dot{\alpha}_j^2 - 2[(\mathbf{g}_i')^T_{\alpha_i}\mathbf{A}_{ij}\mathbf{g}_j'\dot{\alpha}_i \\ + \mathbf{g}_i'^T\mathbf{A}_{ij}(\mathbf{g}_j')_{\alpha_j}\dot{\alpha}_j](\dot{\phi}_j - \dot{\phi}_i) + 2(\mathbf{g}_i')^T_{\alpha_i}\mathbf{B}_{ij}(\mathbf{g}_j')_{\alpha_j}\dot{\alpha}_i\dot{\alpha}_j \end{bmatrix} \tag{3.4.22}$$

Example 3.4.3: A cam–follower joint that is used in a valve operating system of an internal combustion engine is shown in Fig. 3.4.9. Let the outline of the cam consist of a cosine curve and part of a circle:

$$\rho_1(\alpha_1) = \begin{cases} -\frac{1}{4}\cos 3\alpha_1 + \frac{5}{4}, & \text{if } 0 \leq \alpha_1 \leq \dfrac{2\pi}{3} \\ 1, & \text{if } \dfrac{2\pi}{3} \leq \alpha_1 < 2\pi \end{cases}$$

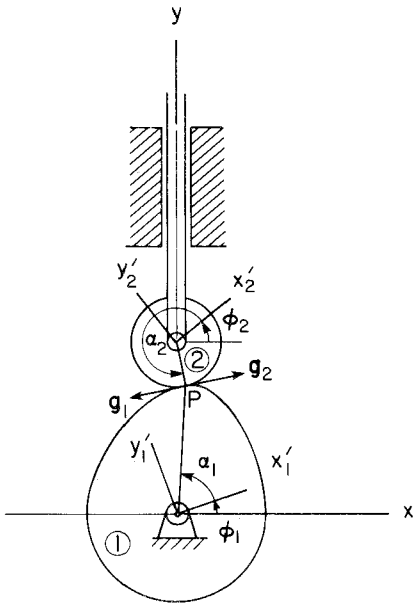

Figure 3.4.9 Cam–follower joint in an internal combustion engine.

Let the radius of the roller be $\frac{1}{4}$, so the outline of the follower is simply

$$\rho_2(\alpha_2) = \tfrac{1}{4}$$

In the configuration shown in Fig. 3.4.9, $0 \leq \alpha_1 \leq (2\pi/3)$. Hence, from Eqs. 3.4.16 and 3.4.17, the tangent vectors to the outlines are

$$\begin{aligned} \mathbf{g}_1' &= \begin{bmatrix} (\frac{3}{4}\sin 3\alpha_1)\cos\alpha_1 - (-\frac{1}{4}\cos 3\alpha_1 + \frac{5}{4})\sin\alpha_1 \\ (\frac{3}{4}\sin 3\alpha_1)\sin\alpha_1 + (-\frac{1}{4}\cos 3\alpha_1 + \frac{5}{4})\cos\alpha_1 \end{bmatrix} \\ \mathbf{g}_2' &= [-\tfrac{1}{4}\sin\alpha_2,\ \tfrac{1}{4}\cos\alpha_2]^T \end{aligned} \tag{3.4.23}$$

Thus, the explicit form of the third constraint equation of Eq. 3.4.20 is

$$\begin{aligned} &\{[\tfrac{3}{4}\sin 3\alpha_1\cos\alpha_1 + (\tfrac{1}{4}\cos 3\alpha_1 - \tfrac{5}{4})\sin\alpha_1]\cos\phi_1 \\ &\quad - [\tfrac{3}{4}\sin 3\alpha_1\sin\alpha_1 - (\tfrac{1}{4}\cos 3\alpha_1 - \tfrac{5}{4})\cos\alpha_1]\sin\phi_1\} \\ &\quad \times \{-\tfrac{1}{4}\sin\alpha_2\sin\phi_2 + \tfrac{1}{4}\cos\alpha_2\cos\phi_2\} \\ &\quad - \{[\tfrac{3}{4}\sin 3\alpha_1\cos\alpha_1 + (\tfrac{1}{4}\cos 3\alpha_1 - \tfrac{5}{4})\sin\alpha_1]\sin\phi_1 \\ &\quad + [\tfrac{3}{4}\sin 3\alpha_1\sin\alpha_1 - (\tfrac{1}{4}\cos 3\alpha_1 - \tfrac{5}{4})\cos\alpha_1]\cos\phi_1\} \\ &\quad \times \{-\tfrac{1}{4}\sin\alpha_2\cos\phi_2 - \tfrac{1}{4}\cos\alpha_2\sin\phi_2\} = 0 \end{aligned}$$

A *cam–flat-faced follower pair* is shown in Fig. 3.4.10. The cam, which is shown as body i, may have a convex outline that is parameterized by α_i, as in Eq. 3.4.16. The contacting surface of the follower on body j is flat. The unit vector $\mathbf{u}_j$ defines the line of contact. Since the point P is the point of contact,

$$\mathbf{r}_i^P - \mathbf{a}_j - \mathbf{r}_j^Q = \mathbf{0} \tag{3.4.24}$$

The x_j'-y_j' component form of vector $\mathbf{u}_j$ is

$$\mathbf{u}_j' \equiv \frac{1}{|\mathbf{r}_j'^Q - \mathbf{r}_j'^C|}(\mathbf{r}_j'^Q - \mathbf{r}_j'^C) \tag{3.4.25}$$

Then $\mathbf{u}_j = \mathbf{A}_j\mathbf{u}_j'$.

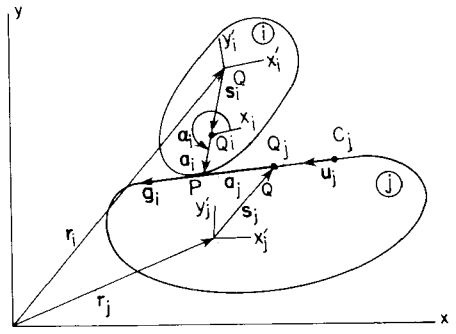

Figure 3.4.10 Cam–flat-faced follower pair.

Since $\mathbf{a}_j$ must be parallel to $\mathbf{u}_j$,

$$\mathbf{a}_j = \rho_j \mathbf{u}_j = \rho_j \mathbf{A}_j \mathbf{u}'_j \tag{3.4.26}$$

where ρ_j is the length of $\mathbf{a}_j$. Taking the scalar product of both sides of Eq. 3.4.24 with

$$\mathbf{u}_j^{\perp} = \mathbf{R}\mathbf{u}_j = \mathbf{R}\mathbf{A}_j\mathbf{u}'_j = \mathbf{B}_j\mathbf{u}'_j$$

yields

$$(\mathbf{r}_i^P - \mathbf{r}_j^Q)^T \mathbf{u}_j^{\perp} = (\mathbf{r}_i^P - \mathbf{r}_j^Q)^T \mathbf{B}_j \mathbf{u}'_j \tag{3.4.27}$$

where $\mathbf{u}'_j$ is constant.

A second constraint equation follows from the condition that the tangent $\mathbf{g}_i$ at point P to body i must be parallel to $\mathbf{u}_j$. Hence

$$\mathbf{g}_i^{\perp T}\mathbf{u}_j = (\mathbf{R}\mathbf{g}_i)^T\mathbf{u}_j = \mathbf{g}_i^T\mathbf{R}^T\mathbf{u}_j = \mathbf{g}_i'^T\mathbf{B}_{ij}\mathbf{u}'_j = 0 \tag{3.4.28}$$

where $\mathbf{g}'_i$ is given by Eq. 3.4.17.

To show that Eqs. 3.4.27 and 3.4.28 imply the geometry of the joint, note first that Eq. 3.4.27 requires that $\mathbf{r}_i^P - \mathbf{r}_j^Q$ be parallel to $\mathbf{u}_j$. Since they have point Q in common, they are collinear. Thus, point P on the cam surface of body i lies on the flat face on body j. Since Eq. 3.4.28 requires that the cam surface of body i be tangent to the flat face on body j at point P, these equations imply the geometry of the joint. For convenience, they are summarized as

$$\mathbf{\Phi}^{cff(i,j)} \equiv \begin{bmatrix} (\mathbf{r}_i^P - \mathbf{r}_j^Q)^T \mathbf{B}_j \mathbf{u}'_j \\ \mathbf{g}_i'^T \mathbf{B}_{ij} \mathbf{u}'_j \end{bmatrix} = \mathbf{0} \tag{3.4.29}$$

This formulation eliminates one relative degree of freedom between the two bodies, since α_i appears in $\mathbf{r}_i^P$, through Eqs. 3.4.15, and is retained as an additonal generalized coordinate. For a system with nb rigid bodies and one cam–flat-faced follower pair, the vector of generalized coordinates will have $nc = 3nb + 1$ components:

$$\mathbf{q} = [x_1, y_1, \phi_1, \ldots, x_{nb}, y_{nb}, \phi_{nb}, \alpha_i]^T$$

The Jacobians of the constraint of Eq. 3.4.29, with respect to $\mathbf{q}_i$, α_i, and $\mathbf{q}_j$, are calculated using the vector and matrix relations of Chapter 2 as

$$\begin{aligned}
\mathbf{\Phi}_{\mathbf{q}_i}^{cff(i,j)} &= \begin{bmatrix} \mathbf{u}_j'^T\mathbf{B}_j^T & (\mathbf{s}_i'^P + \rho_i\mathbf{u}_i')^T\mathbf{A}_{ij}\mathbf{u}'_j \\ \mathbf{0} & \mathbf{g}_i'^T\mathbf{A}_{ij}\mathbf{u}'_j \end{bmatrix} \\
\mathbf{\Phi}_{\alpha_i}^{cff(i,j)} &= \begin{bmatrix} \mathbf{g}_i'^T\mathbf{B}_{ij}\mathbf{u}'_j \\ (\mathbf{g}'_i)_{\alpha_i}^T\mathbf{B}_{ij}\mathbf{u}'_j \end{bmatrix} \\
\mathbf{\Phi}_{\mathbf{q}_j}^{cff(i,j)} &= \begin{bmatrix} -\mathbf{u}_j'^T\mathbf{B}_j^T & -(\mathbf{r}_i^P - \mathbf{r}_j)^T\mathbf{A}_j\mathbf{u}'_j \\ \mathbf{0} & -\mathbf{g}_i'^T\mathbf{A}_{ij}\mathbf{u}'_j \end{bmatrix}
\end{aligned} \tag{3.4.30}$$

Since there is no explicit time dependence in Eq. 3.4.29, from Eq. 3.1.9,

$$\boldsymbol{\gamma}^{cff(i,j)} = \mathbf{0}$$

Carrying out the expansion for $\boldsymbol{\gamma}$ in Eq. 3.1.10, using the Jacobians of Eq. 3.4.30,

$$\boldsymbol{\gamma}^{cff(i,j)} = \begin{bmatrix} 2(\dot{\mathbf{r}}_i^P - \dot{\mathbf{r}}_j)^T \mathbf{A}_j \mathbf{u}_j' \dot{\phi}_j + (\mathbf{s}_i'^P + \rho_i \mathbf{u}_i')^T \mathbf{B}_{ij} \mathbf{u}_j' \dot{\phi}_i^2 + (\mathbf{r}_i^P - \mathbf{r}_j)^T \mathbf{B}_j \mathbf{u}_j' \dot{\phi}_j^2 \\ \quad - (\mathbf{g}_i')_{\alpha_i}^T \mathbf{B}_{ij} \mathbf{u}_j' \dot{\alpha}_i^2 - 2\mathbf{g}_i'^T \mathbf{A}_{ij} \mathbf{u}_j' \dot{\alpha}_i \dot{\phi}_i \\ \mathbf{g}_i'^T \mathbf{B}_{ij} \mathbf{u}_j' (\dot{\phi}_j - \dot{\phi}_i)^2 - (\mathbf{g}_i')_{\alpha_i \alpha_i}^T \mathbf{B}_{ij} \mathbf{u}_j' \dot{\alpha}_i^2 \\ \quad + 2(\mathbf{g}_i')_{\alpha_i}^T \mathbf{A}_{ij} \mathbf{u}_j' (\dot{\phi}_j - \dot{\phi}_i) \dot{\alpha}_i \end{bmatrix}$$

Example 3.4.4: The roller follower of the cam–follower joint in Example 3.4.3 is replaced by the cam–flat-faced follower joint shown in Fig. 3.4.11. The outline of the cam is the same as in Example 3.4.2, that is, Eq. 3.4.21.

The vector $\mathbf{u}_2$ that is parallel to the flat face is simply

$$\mathbf{u}_2 = [-1, 0]^T$$

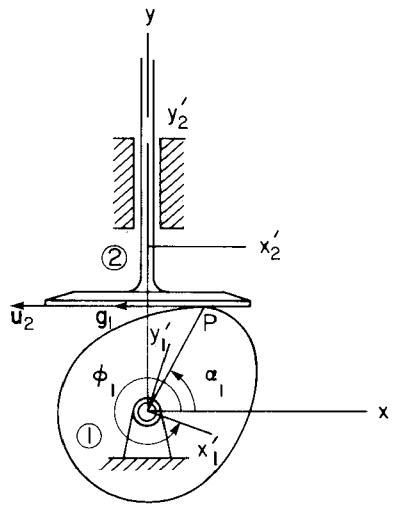

Figure 3.4.11 Cam–flat-faced follower in an internal combustion engine.

When $0 \leq \alpha_1 \leq (2\pi/3)$, as shown in Fig. 3.4.11, the second constraint equation of Eq. 3.4.29 is, from Eq. 3.4.23,

$$-\{\tfrac{3}{4}\sin 3\alpha_1 \cos \alpha_1 - (\tfrac{1}{4}\cos 3\alpha_1 - \tfrac{5}{4})\sin \alpha_1\}\cos \phi_1 + \{\tfrac{3}{4}\sin 3\alpha_1 \sin \alpha_1 - (\tfrac{1}{4}\cos 3\alpha_1 - \tfrac{5}{4})\cos \alpha_1\}\sin \phi_1 = 0$$

3.4.3 Point–Follower

A *point–follower* joint between bodies i and j is shown schematically in Fig. 3.4.12. Pin P is attached to body i and can slide and rotate in a slot on body j.

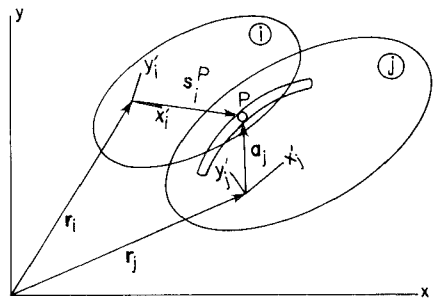

Figure 3.4.12 Point–follower pair.

The coordinates of any point on the slot, relative to the body-fixed reference frame on body j, can be described by $\mathbf{a}_j = \mathbf{A}_j\rho_j(\alpha_j)\mathbf{u}_j'(\alpha_j)$, as in Eq. 3.4.16.

Constraint equations for this joint are similar to the constraint equations of a revolute joint. Note that the position of point P on body j is not constant, but varies as a function of the variable α_j. Hence the constraint equations are

$$\mathbf{\Phi}^{pf(i,j)} \equiv \mathbf{r}_i + \mathbf{A}_i\mathbf{s}_i'^P - \mathbf{A}_j\rho_j\mathbf{u}_j' - \mathbf{r}_j = \mathbf{0} \tag{3.4.31}$$

In this case, α_j is added to the vector of generalized coordinates, and the constraint equations of Eq. 3.4.31 are employed to describe the point–follower joint. Thus, a point–follower joint eliminates only one degree of freedom.

The Jacobians of this constraint with respect to $\mathbf{q}_i$, $\mathbf{q}_j$, and α_j are

$$\begin{aligned}
\mathbf{\Phi}_{\mathbf{q}_i}^{pf(i,j)} &= [\mathbf{I}, \mathbf{B}_i\mathbf{s}_i'^P] \\
\mathbf{\Phi}_{\mathbf{q}_j}^{pf(i,j)} &= [-\mathbf{I}, -\mathbf{B}_j\rho_j\mathbf{u}_j'] \\
\mathbf{\Phi}_{\alpha_j}^{pf(i,j)} &= -\mathbf{A}_j\mathbf{g}_j'
\end{aligned} \tag{3.4.32}$$

Since the constraint of Eq. 3.4.31 does not depend explicitly on time, from Eq. 3.1.9,

$$\boldsymbol{\nu}^{pf(i,j)} = \mathbf{0}$$

Using the Jacobians of Eq. 3.4.32 in Eq. 3.1.10,

$$\boldsymbol{\gamma}^{pf(i,j)} = \mathbf{A}_i\mathbf{s}_i'^P\dot{\phi}_i^2 - \mathbf{A}_j\rho_j\mathbf{u}_j'\dot{\phi}_j^2 + \mathbf{A}_j(\mathbf{g}_j')_{\alpha_j}\dot{\alpha}_j^2 + 2\mathbf{B}_j\mathbf{g}_j'\dot{\phi}_j\dot{\alpha}_j$$

Example 3.4.5: The cam-follower joint in Example 3.4.3 may be modeled as a point–follower joint, as shown in Fig. 3.4.13. The equation of the slot is the same as given in Example 3.4.3.

For a minimal set of generalized coordinates in this example, $\mathbf{q} = [\phi_1, y_2, \alpha_1]^T$, and the constraint equation of Eq. 3.4.31 is simply

$$y_2 - \ell - \rho_1(\alpha_1) = y_2 - \ell + \tfrac{1}{4}\cos 3\alpha_1 - \tfrac{5}{4} = 0$$

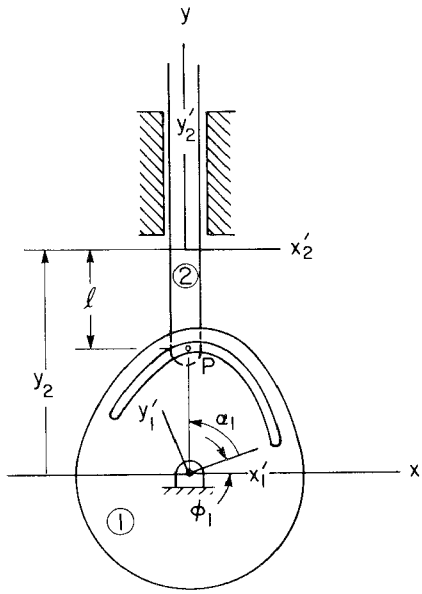

Figure 3.4.13 Point–follower model of valve lifter.

Substituting $\phi_1 + \alpha_1 = \pi/2$ into this equation,

$$y_2 - \ell + \tfrac{1}{4}\cos\left(\frac{3\pi}{2} - 3\phi_1\right) - \tfrac{5}{4} = y_2 - \ell - \tfrac{1}{4}\sin 3\phi_1 - \tfrac{5}{4} = 0$$

Differentiating with respect to time,

$$\dot{y}_2 = \tfrac{3}{4}\cos 3\phi_1$$

3.5 DRIVING CONSTRAINTS

The kinematic constraints presented in Sections 3.2 through 3.4 represent physical connections between bodies; hence they impose limitations on the relative motion of connected bodies. These kinematic constraints are functions of the system generalized coordinates, but they do not depend explicitly on time. Such constraints describe the physical structure of a machine and normally provide one or more degrees of freedom that allow movement of the system.

In addition to kinematic structure, the motion of many mechanical systems is described by actuator input that specifies the time history of some position coordinates or the relative position of pairs of bodies. Robot and numerically controlled machine tool applications are typical of this mode of operation. To uniquely determine the time history of motion of a mechanism, a number of

inputs must be specified, equal in number to the number of degrees of freedom of the system. As will be shown in Section 3.6, it is important that these additional input conditions be independent of the kinematic constraint equations. While it is not sufficient to simply count the number of variables and constraint equations to determine the number of degrees of freedom, this is a useful initial computation to guide the engineer in specifying an appropriate number of time-dependent driving conditions.

A family of standard drivers, called *driving constraints,* is presented in this section for use in kinematic analysis.

3.5.1 Absolute Drivers

Analogous to absolute constraints that may be imposed on the coordinates of a point on body i or on rotation of body i, time-dependent absolute coordinate constraints, called *drivers,* may be imposed. Allowing the parameters C_1, C_2, and C_3 in the constraints of Eqs. 3.2.3 through 3.2.6 to be time dependent, the following *absolute coordinate drivers* are obtained:

$$\Phi^{axd(i)} = x_i^P - C_1(t) = 0 \tag{3.5.1}$$

$$\Phi^{ayd(i)} = y_i^P - C_2(t) = 0 \tag{3.5.2}$$

$$\Phi^{a\phi d(i)} = \phi_i - C_3(t) = 0 \tag{3.5.3}$$

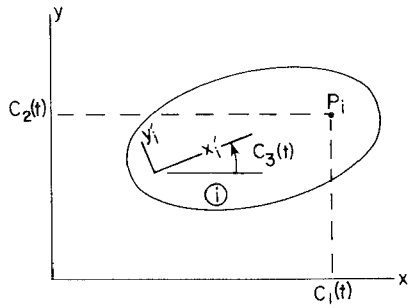

Figure 3.5.1 Absolute coordinate drivers.

The geometry of these drivers is shown in Fig. 3.5.1. The engineer must describe the time-dependent functions $C_k(t)$ and the location of point P on body i in order to complete definition of these driving constraints. Note that the Jacobians of these driving constraints are the same as in Eqs. 3.2.5 and 3.2.7.

Example 3.5.1: The two-body slider–crank shown in Fig. 3.5.2 models a rocker mechanism in which motion of the piston is controlled by hydraulic flow,

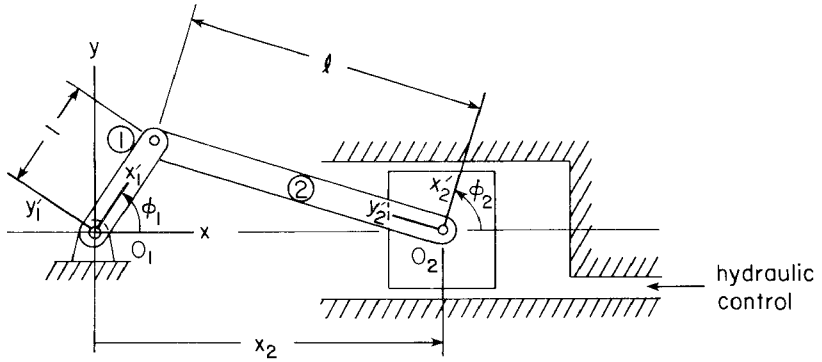

Figure 3.5.2 Two-body slider–crank model with an absolute driver.

specified as

$$x_2 = \sqrt{\ell^2 - 1} + \tfrac{1}{2}\sin \omega t = C(t) \tag{3.5.4}$$

where $\ell > 1$ and ω are constants.

For analytical simplicity, let a reduced set of generalized coordinates be $\mathbf{q} = [x_2, \phi_1, \phi_2]^T$. Equation 3.5.4 represents an absolute driver of the form of Eq. 3.5.1. The composite constraint equation is, from Example 3.1.2 and Eq. 3.5.4,

$$\mathbf{\Phi}(\mathbf{q}) \equiv \begin{bmatrix} -x_2 + \cos\phi_1 + \ell \sin\phi_2 \\ \sin\phi_1 - \ell\cos\phi_2 \\ x_2 - \sqrt{\ell^2 - 1} - \tfrac{1}{2}\sin\omega t \end{bmatrix} = \mathbf{0}$$

Taking the time derivative of both sides yields the velocity equation

$$\begin{bmatrix} -1 & -\sin\phi_1 & \ell\cos\phi_2 \\ 0 & \cos\phi_1 & \ell\sin\phi_2 \\ 1 & 0 & 0 \end{bmatrix} \begin{bmatrix} \dot{x}_2 \\ \dot{\phi}_1 \\ \dot{\phi}_2 \end{bmatrix} = \begin{bmatrix} 0 \\ 0 \\ \tfrac{1}{2}\omega\cos\omega t \end{bmatrix}$$

The solution for $\dot{\phi}_1$ is

$$\dot{\phi}_1 = -\frac{\omega \sin\phi_2 \cos\omega t}{2\cos(\phi_1 - \phi_2)}$$

Note that if the numerator is not zero, $\dot{\phi}_1$ approaches infinity as $\cos(\phi_1 - \phi_2)$ approaches zero. This singular configuration occurs when $\phi_1 = \phi_2 + (\frac{1}{2} + k)\pi$, where k is an integer. Singular behavior of mechanisms is discussed in Section 3.7.

Example 3.5.2: The four-bar mechanism of Fig. 3.3.2 has one degree of freedom, as shown in Examples 3.3.2 and 3.3.3. Hence a rotational driver $\phi_1 = \omega t$ determines the complete motion. Note that when ground is not modeled as a body [Example 3.3.2(1)], the driver is an absolute rotational driver. A reduced set of generalized coordinates is chosen as $\mathbf{q} = [\phi_1, x_2, y_2, \phi_2, \phi_3]^T$. Dimensions of the mechanism are shown in Fig. 3.5.3.

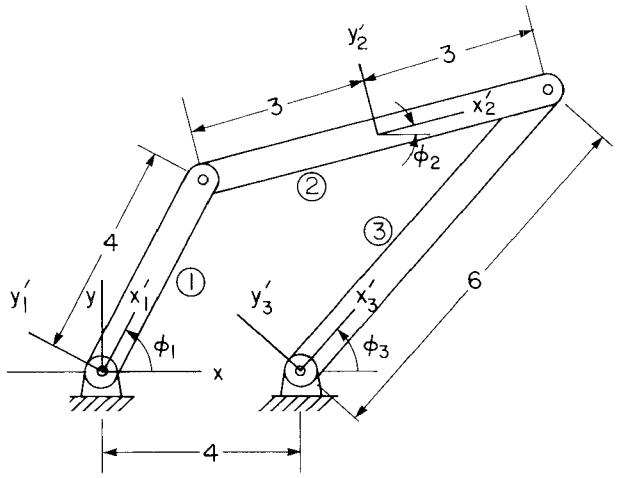

Figure 3.5.3 Four-bar mechanism with an absolute rotational driver.

Composite constraint equations, derived directly in terms of the reduced generalized coordinates, are

$$\mathbf{\Phi}(\mathbf{q}) \equiv \begin{bmatrix} x_2 - 4\cos\phi_1 - 3\cos\phi_2 \\ y_2 - 4\sin\phi_1 - 3\sin\phi_2 \\ 4 - 4\cos\phi_1 - 6\cos\phi_2 + 6\cos\phi_3 \\ 4\sin\phi_1 + 6\sin\phi_2 - 6\sin\phi_3 \\ \phi_1 - \omega t \end{bmatrix} = \mathbf{0}$$

Differentiating with respect to time yields the velocity equation

$$\begin{bmatrix} 4\sin\phi_1 & 1 & 0 & 3\sin\phi_2 & 0 \\ -4\cos\phi_1 & 0 & 1 & -3\cos\phi_2 & 0 \\ 4\sin\phi_1 & 0 & 0 & 6\sin\phi_2 & -6\sin\phi_3 \\ 4\cos\phi_1 & 0 & 0 & 6\cos\phi_2 & -6\cos\phi_3 \\ 1 & 0 & 0 & 0 & 0 \end{bmatrix} \begin{bmatrix} \dot\phi_1 \\ \dot x_2 \\ \dot y_2 \\ \dot\phi_2 \\ \dot\phi_3 \end{bmatrix} = \begin{bmatrix} 0 \\ 0 \\ 0 \\ 0 \\ \omega \end{bmatrix}$$

whose solution is

$$\dot\phi_1 = \omega$$

$$\dot x_2 = -4\omega\sin\phi_1 - 2\omega\sin\phi_2 \frac{\sin(\phi_3 - \phi_1)}{\sin(\phi_2 - \phi_3)}$$

$$\dot y_2 = 4\omega\cos\phi_1 + 2\omega\cos\phi_2 \frac{\sin(\phi_3 - \phi_1)}{\sin(\phi_2 - \phi_3)}$$

$$\dot\phi_2 = \frac{2\omega\sin(\phi_3 - \phi_1)}{3\sin(\phi_2 - \phi_3)}$$

$$\dot\phi_3 = -\frac{2\omega\sin(\phi_1 - \phi_2)}{\sin(\phi_2 - \phi_3)}$$

3.5.2 Relative Drivers

Just as in Section 3.3.1, constraints between coordinates of points on pairs of bodies, or between the orientation of bodies in Eqs. 3.3.1, 3.3.3, and 3.3.5 can be specified as functions of time, in the form of *relative coordinate drivers,*

$$\Phi^{rxd(i,j)} = x_j^P - x_i^P - C_1(t) = 0 \tag{3.5.5}$$

$$\Phi^{ryd(i,j)} = y_j^P - y_i^P - C_2(t) = 0 \tag{3.5.6}$$

$$\Phi^{r\phi d(i,j)} = \phi_j - \phi_i - C_3(t) = 0 \tag{3.5.7}$$

The geometry of these driving constraints is shown in Fig. 3.5.4. The Jacobians of these driving constraints are the same as in Eqs. 3.3.2, 3.3.4, and 3.3.6.

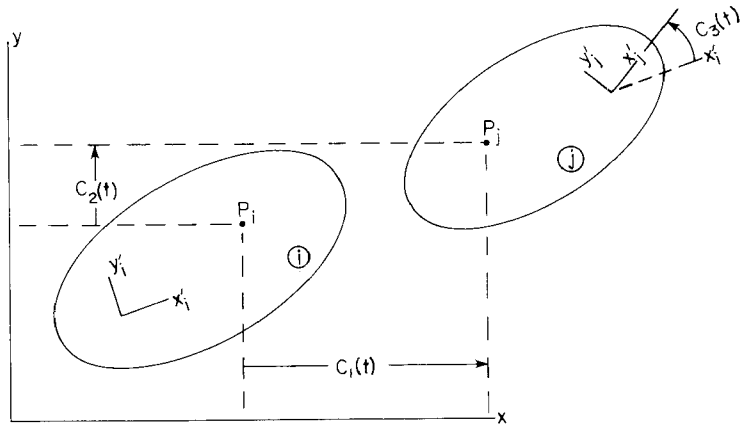

Figure 3.5.4 Relative coordinate drivers.

Analogous to the distance constraint of Eq. 3.3.7 in Section 3.3.1, the length $C_4(t) > 0$ of the actuator can be specified as a function of time, to obtain the *relative distance driver*

$$\Phi^{rdd(i,j)} = (x_j^P - x_i^P)^2 + (y_j^P - y_i^P)^2 - (C_4(t))^2 = 0 \tag{3.5.8}$$

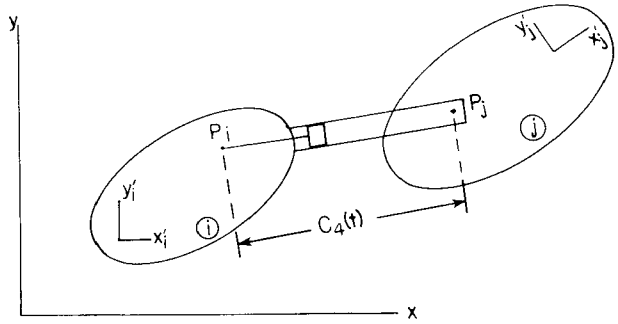

Figure 3.5.5 Relative distance driver.

between a pair of points on two bodies, as shown in Fig. 3.5.5. As in the case of the distance constraint, it is important that $C_4(t) > 0$, since, if $C_4(t) = 0$, Eq. 3.5.8 is equivalent to a pair of scalar constraint equations that describes a revolute joint. The Jacobian of this driver is given in Eq. 3.3.8.

As suggested by Fig. 3.5.5, the distance driver may be defined physically by the action of a hydraulic actuator, in which the volume of fluid inserted in a chamber is controlled to specify the time history of length of the strut.

Example 3.5.3: An excavator boom assembly with two hydraulic actuators (for simplicity the shovel actuator is not included) is shown in Fig. 3.5.6. Let a reduced set of generalized coordinates be $\mathbf{q} = [\phi_1, x_2, y_2, \phi_2]^T$ and let the distance driver inputs be

$$C_{41}(t) = \tfrac{1}{5}t + 1.8$$
$$C_{12}(t) = \tfrac{1}{10}t + 1.9$$

The relative distance driver constraint equations of Eq. 3.5.8, with the revolute constraint equations, yield the composite constraint equations

$$\mathbf{\Phi}(\mathbf{q}) \equiv \begin{bmatrix} x_2 - 2\sqrt{3}\cos\phi_1 \\ y_2 - 2\sqrt{3}\sin\phi_1 \\ (\sqrt{3}\cos\phi_1 - 0.5)^2 + (\sqrt{3}\sin\phi_1 + 0.5)^2 - (C_{41}(t))^2 \\ u^2 + v^2 - (C_{12}(t))^2 \end{bmatrix} = \mathbf{0} \qquad (3.5.9)$$

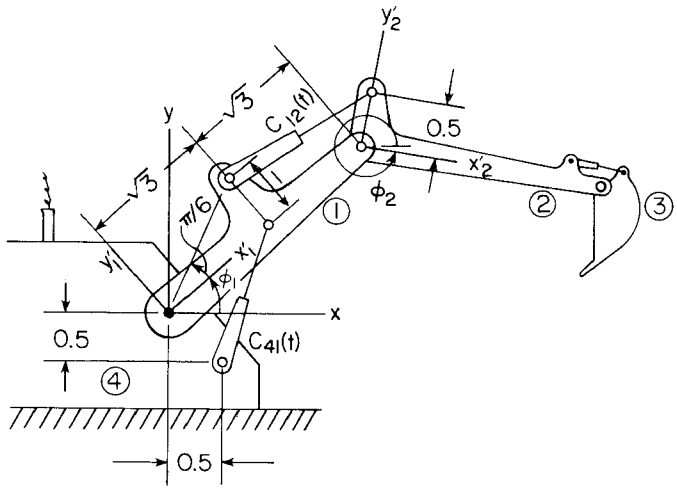

Figure 3.5.6 Excavator boom assembly with two distance drivers.

where

$$u = \left\{2\cos\left(\phi_1 + \frac{\pi}{6}\right) - (x_2 - 0.5\sin\phi_2)\right\}$$

$$v = \left\{2\sin\left(\phi_1 + \frac{\pi}{6}\right) - (y_2 + 0.5\cos\phi_2)\right\}$$

Differentiating with respect to time, the velocity equation is

$$\begin{bmatrix} 2\sqrt{3}\sin\phi_1 & 1 & 0 & 0 \\ -2\sqrt{3}\cos\phi_1 & 0 & 1 & 0 \\ -2\sqrt{3}(\sqrt{3}\cos\phi_1 - 0.5)\sin\phi_1 + 2\sqrt{3}(\sqrt{3}\sin\phi_1 + 0.5)\cos\phi_1 & 0 & 0 & 0 \\ -4u\sin\left(\phi_1 + \frac{\pi}{6}\right) + 4v\cos\left(\phi_1 + \frac{\pi}{6}\right) & -2u & -2v & u\cos\phi_2 + v\sin\phi_2 \end{bmatrix} \begin{bmatrix} \dot{\phi}_1 \\ \dot{x}_2 \\ \dot{y}_2 \\ \dot{\phi}_2 \end{bmatrix}$$

$$= \begin{bmatrix} 0 \\ 0 \\ \frac{2(\frac{1}{5}t + 1.8)}{5} \\ \frac{(\frac{1}{10}t + 1.9)}{5} \end{bmatrix} \qquad \textbf{(3.5.10)}$$

The solution for $\dot{\phi}_1$ and $\dot{\phi}_2$ is

$$\dot{\phi}_1 = \frac{t + 9}{-25\sqrt{3}\{(\sqrt{3}\cos\phi_1 - 0.5)\sin\phi_1 - (\sqrt{3}\sin\phi_1 + 0.5)\cos\phi_1\}}$$

$$\dot{\phi}_2 = \frac{1}{B}\{C - A + 4\sqrt{3}\,u\sin\phi_1 - 4\sqrt{3}\,v\cos\phi_1)\,\dot{\phi}_1\}$$

where

$$A = -4\left\{2\cos\left(\phi_1 + \frac{\pi}{6}\right) - x_2 + 0.5\sin\phi_2\right\}\sin\left(\phi_1 + \frac{\pi}{6}\right) + 4\left\{2\sin\left(\phi_1 + \frac{\pi}{6}\right) - y_2 - 0.5\cos\phi_2\right\}\cos\left(\phi_1 + \frac{\pi}{6}\right)$$

$$B = \left\{2\cos\left(\phi_1 + \frac{\pi}{6}\right) - x_2 + 0.5\sin\phi_2\right\}\cos\phi_2 + \left\{2\sin\left(\phi_1 + \frac{\pi}{6}\right) - y_2 - 0.5\cos\phi_2\right\}\sin\phi_2$$

$$C = \frac{t + 19}{50}$$

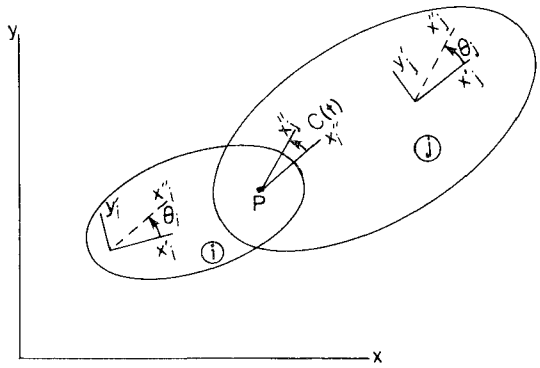

Figure 3.5.7 Revolute–rotational driver.

A common form of driver that is encountered in mechanical systems is an electrical or hydraulic actuator that controls the relative angular orientation of a pair of bodies at a revolute joint. The geometry of a *revolute–rotational driver* is shown in Fig. 3.5.7, where the attachment angles θ_i and θ_j of the actuator on bodies i and j, respectively, are defined by the physical mounting of the actuator on the two bodies. The analytical form of this driving constraint is simply

$$\Phi^{rrd(i,j)} = (\phi_j + \theta_j) - (\phi_i + \theta_i) - C(t) = 0 \qquad \textbf{(3.5.11)}$$

where $C(t)$ is the driving angle of the body-fixed x_j'' axis on body j, relative to the body-fixed x_i'' axis on body i, with counterclockwise positive. The Jacobian of this driver is given in Eq. 3.3.6.

Example 3.5.4: One of the distance drivers in Example 3.5.3 is replaced by a revolute–rotational driver

$$C(t) = \tfrac{1}{10}t$$

as shown in Fig. 3.5.8.

Let the generalized coordinate vector again be $\mathbf{q} = [\phi_1, x_2, y_2, \phi_2]^T$. Then the composite constraint equation is Eq. 3.5.9, with the fourth equation replaced by

$$\phi_2 - \phi_1 - \tfrac{1}{10}t = 0$$

Similarly, the fourth equation of Eq. 3.5.10 is replaced by

$$[-1, 0, 0, 1][\dot{\phi}_1, \dot{x}_2, \dot{y}_2, \dot{\phi}_2]^T = \tfrac{1}{10}t$$

The solution for $\dot{\phi}_2$ is

$$\dot{\phi}_2 = \frac{t+9}{-25\sqrt{3}\,\{(\sqrt{3}\cos\phi_1 - 0.5)\sin\phi_1 - (\sqrt{3}\sin\phi_1 + 0.5)\cos\phi_1\}} + \frac{1}{10}$$

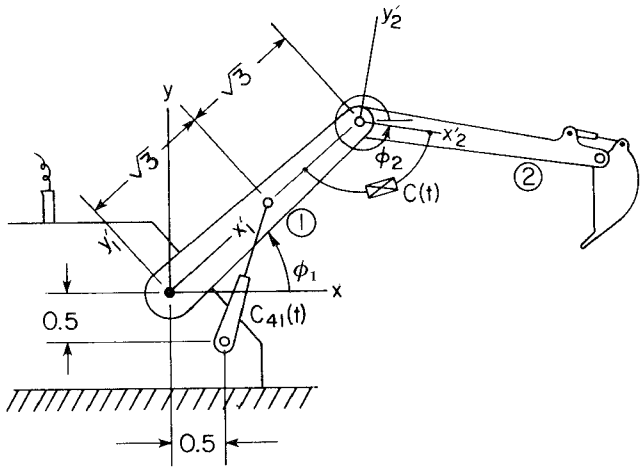

Figure 3.5.8 Excavator boom assembly with a distance driver and a revolute–rotational driver.

A common form of relative position driver that is encountered in robots and numerically controlled machine tools, as well as in other machine applications, is the relative translation of a pair of bodies along a translational joint, as shown in Fig. 3.5.9. Electrical and hydraulic actuators may act directly or through a gearing system that controls translation of body j relative to body i.

The mathematical form of the *translational–distance driver* is, using the notation of Fig. 3.5.9,

$$\frac{\mathbf{v}_i^T \mathbf{d}_{ij}}{v_i} - C(t) = 0$$

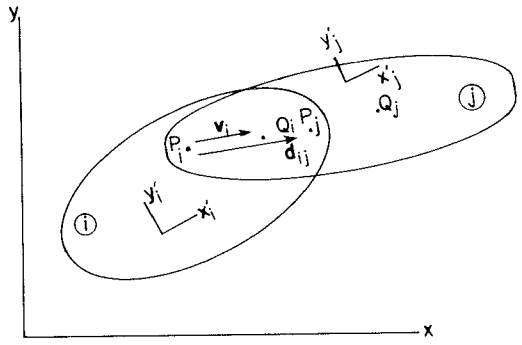

Figure 3.5.9 Translational–distance driver.

where $C(t)$, which can be zero, is the time history of the directed distance from P_i and P_j, and v_i is the constant distance on body i between points P_i and Q_i. This equation can be expanded as

$$\Phi^{tdd(i,j)} = \mathbf{v}_i'^T\mathbf{A}_i^T(\mathbf{r}_j - \mathbf{r}_i) + \mathbf{v}_i'^T\mathbf{A}_{ij}\mathbf{s}_j'^P - \mathbf{v}_i'^T\mathbf{s}_i'^P - v_iC(t) = 0 \tag{3.5.12}$$

The Jacobians of this driver are

$$\begin{aligned}\Phi_{\mathbf{q}_i}^{tdd(i,j)} &= [-\mathbf{v}_i'^T\mathbf{A}_i^T,\ \mathbf{v}_i'^T\mathbf{B}_i^T(\mathbf{r}_j - \mathbf{r}_i)] \\ \Phi_{\mathbf{q}_j}^{tdd(i,j)} &= [\mathbf{v}_i'^T\mathbf{A}_i^T,\ \mathbf{0}]\end{aligned} \tag{3.5.13}$$

where the fact that $\mathbf{A}_{ij}$ is constant, due to the translational joint between bodies i and j, is used.

Example 3.5.5: The boom of a crane is shown in Fig. 3.5.10. Body 1 is hinged to ground at point O and is driven by the rotational driver

$$\phi_1 = 0.025t \tag{3.5.14}$$

The relative distance between bodies 1 and 2 is driven by the translational–distance driver

$$\frac{\mathbf{v}_1^T\mathbf{d}_{12}}{v_1} = C(t) = 0.1t \tag{3.5.15}$$

where $\mathbf{v}_1$ and $\mathbf{d}_{12}$ are shown in Fig. 3.5.10. Let $\mathbf{q} = [\phi_1, x_2, y_2, \phi_2]^T$ be a reduced set of generalized coordinates. With Eq. 3.5.15, Eq. 3.5.12 is

$$[v_1\cos\phi_1,\ v_1\sin\phi_1]\begin{bmatrix}x_2\\ y_2\end{bmatrix} - v_1(0.1t) = 0 \tag{3.5.16}$$

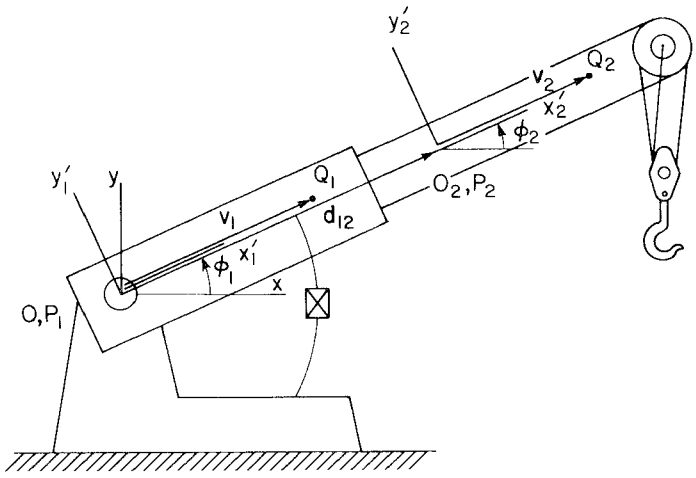

Figure 3.5.10 Wrecker boom with a translational-distance driver.

The translational joint constraint of Eq. 3.3.13 is

$$\begin{bmatrix} \left(\begin{bmatrix} 0 & -1 \\ 1 & 0 \end{bmatrix}\begin{bmatrix} v_1 \cos\phi_1 \\ v_1 \sin\phi_1 \end{bmatrix}\right)^T \begin{bmatrix} x_2 \\ y_2 \end{bmatrix} \\ \left(\begin{bmatrix} 0 & -1 \\ 1 & 0 \end{bmatrix}\begin{bmatrix} v_1 \cos\phi_1 \\ v_1 \sin\phi_1 \end{bmatrix}\right)^T \begin{bmatrix} v_2 \cos\phi_2 \\ v_2 \sin\phi_2 \end{bmatrix} \end{bmatrix} = \mathbf{0}$$

or, in simplified form,

$$\begin{bmatrix} -v_1(\sin\phi_1)x_2 + v_1(\cos\phi_1)y_2 \\ -v_1 v_2 \sin\phi_1 \cos\phi_2 + v_1 v_2 \cos\phi_1 \sin\phi_2 \end{bmatrix} = \mathbf{0} \qquad \textbf{(3.5.17)}$$

From Eqs. 3.5.14, 3.5.16, and 3.5.17, the composite constraint equation is

$$\mathbf{\Phi(q)} \equiv \begin{bmatrix} -x_2 \sin\phi_1 + y_2 \cos\phi_1 \\ \sin(\phi_1 - \phi_2) \\ \phi_1 - 0.025t \\ x_2 \cos\phi_1 + y_2 \sin\phi_1 - 0.1t \end{bmatrix} = \mathbf{0}$$

Differentiating with respect to time, the velocity equation is

$$\begin{bmatrix} -x_2 \cos\phi_1 - y_2 \sin\phi_1 & -\sin\phi_1 & \cos\phi_1 & 0 \\ \cos(\phi_1 - \phi_2) & 0 & 0 & -\cos(\phi_1 - \phi_2) \\ 1 & 0 & 0 & 0 \\ -x_2 \sin\phi_1 + y_2 \cos\phi_1 & \cos\phi_1 & \sin\phi_1 & 0 \end{bmatrix} \begin{bmatrix} \dot{\phi}_1 \\ \dot{x}_2 \\ \dot{y}_2 \\ \dot{\phi}_2 \end{bmatrix} = \begin{bmatrix} 0 \\ 0 \\ 0.025 \\ 0.1 \end{bmatrix}$$

The solution is

$$\dot{\phi}_1 = 0.025$$
$$\dot{x}_2 = -y_2\dot{\phi}_1 = -0.025y_2 + 0.1\cos\phi_1$$
$$\dot{y}_2 = x_2\dot{\phi}_1 = 0.025x_2 + 0.1\sin\phi_1$$
$$\dot{\phi}_2 = \dot{\phi}_1 = 0.025$$

3.5.3 Right Sides of Velocity and Acceleration Equations

With the exception of the translational–distance driver, the equations for driving constraints derived in this section are of the form of constraint equations of Sections 3.2 and 3.3, but with isolated time-dependent terms; that is, for a kinematic constraint

$$\mathbf{\Phi(q)} = \mathbf{0} \qquad \textbf{(3.5.18)}$$

the associated driver is of the form

$$\mathbf{\Phi}^d(\mathbf{q}, t) = \mathbf{\Phi(q)} - \mathbf{C}(t) = \mathbf{0} \qquad \textbf{(3.5.19)}$$

Thus, the right sides of velocity and acceleration equations for Eqs. 3.1.9 and

TABLE 3.5.1 Right Sides of Velocity and Acceleration Equations

Φ	Eq.	$\nu = -\Phi_t$	$\gamma = -(\Phi_{\mathbf{q}}\dot{\mathbf{q}})_{\mathbf{q}}\dot{\mathbf{q}} - \Phi_{tt}$
$\Phi^{axd(i)}$	3.5.1	$\dot{C}_1(t)$	$\gamma^{ax(i)} + \ddot{C}_1(t)$
$\Phi^{ayd(i)}$	3.5.2	$\dot{C}_2(t)$	$\gamma^{ay(i)} + \ddot{C}_2(t)$
$\Phi^{a\phi d(i)}$	3.5.3	$\dot{C}_3(t)$	$\ddot{C}_3(t)$
$\Phi^{rxd(i,j)}$	3.5.5	$\dot{C}_1(t)$	$\gamma^{rx(i,j)} + \ddot{C}_1(t)$
$\Phi^{ryd(i,j)}$	3.5.6	$\dot{C}_2(t)$	$\gamma^{ry(i,j)} + \ddot{C}_2(t)$
$\Phi^{r\phi d(i,j)}$	3.5.7	$\dot{C}_3(t)$	$\ddot{C}_3(t)$
$\Phi^{rdd(i,j)}$	3.5.8	$2C_4(t)\dot{C}_4(t)$	$\gamma^{rd(i,j)} + 2C_4(t)\ddot{C}_4(t) + 2(\dot{C}_4(t))^2$
$\Phi^{rrd(i,j)}$	3.5.11	$\dot{C}(t)$	$\ddot{C}(t)$
$\Phi^{tdd(i,j)}$	3.5.12	$v_i\dot{C}(t)$	$\mathbf{v}_i^T[\mathbf{A}_i^T(\mathbf{r}_j - \mathbf{r}_i)\dot{\phi}_i^2 - 2\mathbf{B}_i(\dot{\mathbf{r}}_j - \dot{\mathbf{r}}_i)\dot{\phi}_i] + v_i\ddot{C}(t)$

3.1.10, respectively, are

$$\boldsymbol{\nu}^d = \dot{\mathbf{C}}(t) \tag{3.5.20}$$

$$\boldsymbol{\gamma}^d = \boldsymbol{\gamma} + \ddot{\mathbf{C}}(t) \tag{3.5.21}$$

where $\boldsymbol{\gamma}$ is the right side of the acceleration equation for the kinematic constraint of Eq. 3.5.18.

Using the form of $\boldsymbol{\nu}^d$ and $\boldsymbol{\gamma}^d$ of Eqs. 3.5.20 and 3.5.21, with the right sides of velocity and acceleration equations derived for the kinematic constraints of Sections 3.2 and 3.3, the right sides of driving constraint velocity and acceleration equations can be obtained. The results of these calculations are summarized in Table 3.5.1.

3.6 POSITION, VELOCITY, AND ACCELERATION ANALYSIS

The kinematic constraints presented in Sections 3.2 through 3.4 and the driving constraints presented in Section 3.5 provide the analytical foundation for the analysis of position, velocity, and acceleration of planar mechanical systems. The forms of position, velocity, and acceleration equations are presented in this section, and the computational approach that is developed in detail in Chapter 4 is outlined.

3.6.1 Position Analysis

The kinematic constraints formulated in Sections 3.2 through 3.4 provide the geometric definition of the permissible motion of a system. For a particular system, they may be written in matrix form as

$$\boldsymbol{\Phi}^K(\mathbf{q}) \equiv [\Phi_1^K(\mathbf{q}), \ldots, \Phi_{nh}^K(\mathbf{q})]^T = \mathbf{0} \tag{3.6.1}$$

where $\mathbf{q}$ is the vector of nc generalized coordinates for the complete system and nh is the number of holonomic constraint equations.

In addition to the kinematic constraints, the driving constraints of Section 3.5 may be assembled in matrix form as

$$\mathbf{\Phi}^D(\mathbf{q}, t) \equiv [\Phi_1^D(\mathbf{q}, t), \ldots, \Phi_{\text{DOF}}^D(\mathbf{q}, t)]^T = \mathbf{0} \tag{3.6.2}$$

These equations are time dependent and provide impetus for motion of the system. It is presumed that the number of driving constraints in Eq. 3.6.2 is equal to the number of degrees of freedom of the physical system and that $nh + \text{DOF} = nc$. Therefore, Eqs. 3.6.1 and 3.6.2 comprise nc equations in nc generalized coordinates.

Assembling the kinematic and driving constraints of Eqs. 3.6.1 and 3.6.2 in matrix form, the system of constraint equations is

$$\mathbf{\Phi}(\mathbf{q}, t) = \begin{bmatrix} \mathbf{\Phi}^K(\mathbf{q}) \\ \mathbf{\Phi}^D(\mathbf{q}, t) \end{bmatrix}_{nc \times 1} = \mathbf{0} \tag{3.6.3}$$

The objective of *position analysis* is to solve this system of equations for the vector $\mathbf{q}$ of system generalized coordinates as a function of time. Since these equations are highly nonlinear, finding an analytical solution is generally impossible. Furthermore, it is easy to formulate a set of system kinematic constraints and drivers that cannot be physically satisfied, and hence for which no solution exists. Position analysis must therefore seriously consider questions of the existence of solutions of Eq. 3.6.3, as well as the numerical methods of solving the equations when a solution exists.

Example 3.6.1: Body 1, shown in Fig. 3.6.1, is to slide along the x axis of the x-y frame without rotation. A pair of constraint equations that accomplishes this objective is

$$\mathbf{\Phi}^1 = \begin{bmatrix} y_1 + \sin \phi_1 \\ y_1 - \sin \phi_1 \end{bmatrix} = \mathbf{0}$$

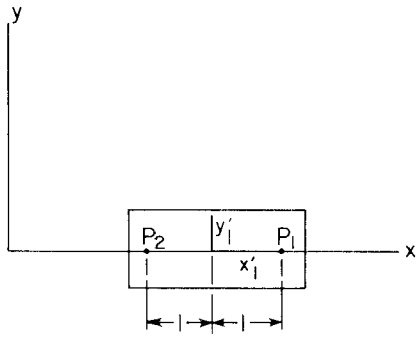

Figure 3.6.1 Block sliding along x axis.

Since this requires $\sin \phi_1 = 0$, $\phi_1 = 0$. The Jacobian of this constraint is

$$\mathbf{\Phi}_{\mathbf{q}}^{1} = \begin{bmatrix} 0 & 1 & \cos \phi_1 \\ 0 & 1 & -\cos \phi_1 \end{bmatrix}$$

Since $\cos \phi_1 = 1$, this matrix has full row rank.

If the additional constraint $\phi_1 = 0$ is inadvertently imposed, the constraint equations become

$$\mathbf{\Phi}^{2} \equiv \begin{bmatrix} y_1 + \sin \phi_1 \\ y_1 - \sin \phi_1 \\ \phi_1 \end{bmatrix} = \mathbf{0}$$

with Jacobian

$$\mathbf{\Phi}_{\mathbf{q}}^{2} = \begin{bmatrix} 0 & 1 & \cos \phi_1 \\ 0 & 1 & -\cos \phi_1 \\ 0 & 0 & 1 \end{bmatrix}$$

Since $|\mathbf{\Phi}_{\mathbf{q}}^{2}| = 0$, $\mathbf{\Phi}_{\mathbf{q}}^{2}$ is now rank deficient and constraints $\mathbf{\Phi}^{2} = \mathbf{0}$ are not independent. In this simple case, it is clear that the third constraint equation is a *redundant constraint* and is automatically satisfied if the first two constraint equations are satisfied. It thus represents a *consistent redundancy*.

Finally, let the constraint $\phi_1 = 0.1$ be added to the original pair of constraint equations, in which case the constraint equations are

$$\mathbf{\Phi}^{3} = \begin{bmatrix} y_1 + \sin \phi_1 \\ y_1 - \sin \phi_1 \\ \phi_1 - 0.1 \end{bmatrix} = \mathbf{0}$$

Since $\mathbf{\Phi}_{\mathbf{q}}^{3} = \mathbf{\Phi}_{\mathbf{q}}^{2}$, $\mathbf{\Phi}_{\mathbf{q}}^{3}$ is row rank deficient and it appears that the last constraint equation is again redundant. In this case, however, the last constraint equation represents an *inconsistent redundancy*; that is, $\mathbf{\Phi}^{3} = \mathbf{0}$ cannot be satisfied for any value of $\mathbf{q}$.

While Example 3.6.1 is trivial, it illustrates difficulties that can arise in complex mechanism models. It is surprisingly easy to inadvertently include redundant constraints in a model, especially for the spatial systems treated in Part II of the text. Computational checks are required to assure that the mechanism defined by constraints that are imposed can in fact be assembled, that is, to assume the constraints are consistent. If the constraints cannot be satisfied, they are said to be inconsistent. If constraints are consistent, the row rank of the constraint Jacobian $\mathbf{\Phi}_{\mathbf{q}}$ must be confirmed to be equal to the number of constraint equations. If not, one or more constraint equations are redundant.

A crucial ingredient in solving Eq. 3.6.3 and in determining configurations in which singular behavior occurs is the Jacobian

$$\mathbf{\Phi}_{\mathbf{q}}(\mathbf{q}, t) = \left[\frac{\partial \Phi_i(\mathbf{q}, t)}{\partial q_j} \right]_{nc \times nc} \tag{3.6.4}$$

where matrix calculus notation of Section 2.5 is employed. An important result from advanced calculus [25, 26] is the following:

Implicit Function Theorem: Let $\mathbf{q}^0$ be a solution of Eq. 3.6.3 at $t = t_0$, and let the function $\mathbf{\Phi}(\mathbf{q}, t)$ be twice continuously differentiable with respect to its arguments. Then, if the Jacobian of Eq. 3.6.4 is nonsingular at $(\mathbf{q}^0, t_0)$, there exists a unique solution

$$\mathbf{q} = \mathbf{f}(t) \tag{3.6.5}$$

of Eq. 3.6.3, in some interval of time about t_0, such that $\mathbf{f}(t_0) = \mathbf{q}^0$. That is, for some $\delta > 0$,

$$\mathbf{\Phi}(\mathbf{f}(t), t) = \mathbf{0}, \qquad \text{for } |t - t_0| \leq \delta \tag{3.6.6}$$

Furthermore, the solution of Eq. 3.6.5 is twice continuously differentiable with respect to time; that is, velocity $\dot{\mathbf{q}} = \dot{\mathbf{f}}(t)$ and acceleration $\ddot{\mathbf{q}} = \ddot{\mathbf{f}}(t)$ are continuous.

While the implicit function theorem provides concrete conditions under which a solution of the kinematic equations exists, it does not provide a method for analytically constructing such a solution. The condition that the Jacobian of Eq. 3.6.4 be nonsingular as a sufficient condition for existence of a solution of the kinematic equations can be used to test for the onset of singular configurations that are associated with lock-up of a mechanism, which may be mathematically interpreted as loss of the physical existence of a solution.

In addition to being a valuable theoretical tool, the constraint Jacobian of Eq. 3.6.4 plays a key role in the numerical solution of the kinematic equations. The most common method used in solving nonlinear equations of the form of Eq. 3.6.3 is the *Newton–Raphson method,* which is discussed in detail in Chapter 4. The Newton–Raphson method is an iterative technique that begins with an estimate $\mathbf{q}^{(0)}$ of a configuration that satisfies Eq. 3.6.3 at time t. At a typical iteration k, the following equation is solved for a correction $\Delta\mathbf{q}^{(k)}$:

$$\mathbf{\Phi}_{\mathbf{q}}(\mathbf{q}^{(k)}, t)\Delta\mathbf{q}^{(k)} = -\mathbf{\Phi}(\mathbf{q}^{(k)}, t) \tag{3.6.7}$$

which is then added to the estimate $\mathbf{q}^{(k)}$ to obtain an improved estimate; that is,

$$\mathbf{q}^{(k+1)} = \mathbf{q}^{(k)} + \Delta\mathbf{q}^{(k)}, \qquad k = 0, 1, \ldots \tag{3.6.8}$$

Iteration is continued until an error tolerance in satisfying Eq. 3.6.3 is met.

The Newton–Raphson method has the attractive property that it is *quadratically convergent*; that is, the solution error in a given iteration is proportional to the square of the error in the preceding iteration. The method, however, may diverge if poor initial estimates of the position of all bodies in the system are given or if no solution of the kinematic equations exists. There is a close relationship between the implicit function theorem, which indicates the

need for the Jacobian to be nonsingular, and the requirement that the Jacobian be nonsingular in solving Newton–Raphson equations in Eq. 3.6.7.

Failure of the Newton–Raphson method to converge may indicate that a mechanism has been specified that cannot be physically assembled. However, since the method can also diverge due to poor initial estimates, some other more robust method of solving nonlinear equations is desired to provide a reliable indication that an infeasible mechanism has been specified. One such technique is to seek a vector $\mathbf{q}$ of generalized coordinates at t_0 that minimizes error in satisfying the constraint equations and is as close as possible to the initial estimate $\mathbf{q}(0)$ given. One such technique is to successively minimize

$$\Psi_0(\mathbf{q}, t_0, r) \equiv (\mathbf{q} - \mathbf{q}^{(0)})^T(\mathbf{q} - \mathbf{q}^{(0)}) + r\boldsymbol{\Phi}^T(\mathbf{q}, t_0)\boldsymbol{\Phi}(q, t_0) \qquad \textbf{(3.6.9)}$$

with increasing values of the parameter $r > 0$ to more heavily weight satisfying the constraint equations. Numerical methods of minimizing such functions are discussed in Chapter 4. Such a minimization technique provides a valuable tool to *assemble* a mechanism or to discover that a design has been specified that cannot be assembled. If this optimization method converges as r becomes large to a value of $\mathbf{q}$ for which Eq. 3.6.3 is not satisfied, then the engineer should be concerned that the mechanism cannot be assembled.

3.6.2 Velocity Analysis

Presuming that the Jacobian matrix of Eq. 3.6.4 is nonsingular and that a solution of the kinematic equations has been obtained numerically, the implicit function theorem guarantees that velocity and acceleration of the system exist. The challenge is to calculate these quantities numerically.

Since Eq. 3.6.3 must hold for all time, both sides may be differentiated with respect to time and rearranged to obtain the *velocity equation*

$$\boldsymbol{\Phi}_\mathbf{q}\dot{\mathbf{q}} = -\boldsymbol{\Phi}_t \equiv \boldsymbol{\nu} \qquad \textbf{(3.6.10)}$$

Since the constraint Jacobian is nonsingular, this equation uniquely determines the velocity $\dot{\mathbf{q}}$. This computation is efficient, as well as direct, since the Jacobian must already have been formed and factored (see Chapter 4) to solve the position equations using the Newton–Raphson method in Eq. 3.6.7.

The right side $\boldsymbol{\nu}$ of the velocity equation of Eq. 3.6.10 may be assembled using the right sides of velocity equations for individual kinematic and driving constraints in Sections 3.2 through 3.5. Methods for computer generation of $\boldsymbol{\nu}$ and the Jacobian $\boldsymbol{\Phi}_\mathbf{q}$ are discussed in Chapter 4.

3.6.3 Acceleration Analysis

Just as the velocity equations of Eq. 3.6.10 were obtained by differentiating the kinematic equations of Eq. 3.6.3, differentiating both sides of Eq. 3.6.10 yields

the *acceleration equation*

$$\boldsymbol{\Phi}_{\mathbf{q}}\ddot{\mathbf{q}} = -(\boldsymbol{\Phi}_{\mathbf{q}}\dot{\mathbf{q}})_{\mathbf{q}}\dot{\mathbf{q}} - 2\boldsymbol{\Phi}_{\mathbf{q}t}\dot{\mathbf{q}} - \boldsymbol{\Phi}_{tt} \equiv \boldsymbol{\gamma} \tag{3.6.11}$$

that determines the acceleration $\ddot{\mathbf{q}}$. Just as in the case of the velocity equation, the right side of the acceleration equation of Eq. 3.6.11 can be assembled using the right sides of acceleration equations for the constraints of Sections 3.2 through 3.5. For details, see Chapter 4.

Note that, as in the velocity equation, the constraint Jacobian plays a dominant role in acceleration analysis. The right side of Eq. 3.6.11 can be evaluated after the solution for velocities is obtained, leading to direct and efficient computation of acceleration.

Example 3.6.2: Consider the one degree of freedom double pendulum shown in Fig. 3.6.2. Body 1 is driven by an absolute angle driver

$$\phi_1 = \frac{5\pi}{3} + \frac{\pi}{6}t, \qquad 0 \leq t \leq \tfrac{3}{2}$$

With a maximal set of Cartesian generalized coordinates, $\mathbf{q} = [x_1, y_1, \phi_1, x_2, y_2, \phi_2]^T$, the system of kinematic and driving constraint equations, using Eq. 3.6.3, is

$$\boldsymbol{\Phi}(\mathbf{q}, t) \equiv \begin{bmatrix} x_1 - \cos\phi_1 \\ y_1 - \sin\phi_1 \\ x_2 - \cos\phi_1 - \cos\phi_2 \\ y_2 - \sin\phi_1 - \sin\phi_2 \\ y_2 + 1 \\ \phi_1 - \dfrac{\pi}{6}t - \dfrac{5\pi}{3} \end{bmatrix} = \mathbf{0}$$

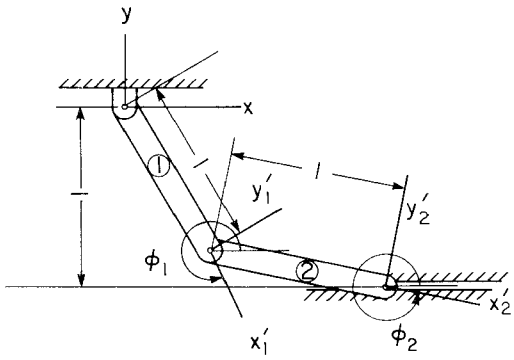

Figure 3.6.2 One degree of freedom double pendulum.

The constraint Jacobian is

$$\mathbf{\Phi}_{\mathbf{q}}(\mathbf{q}, t) \equiv \begin{bmatrix} 1 & 0 & \sin\phi_1 & 0 & 0 & 0 \\ 0 & 1 & -\cos\phi_1 & 0 & 0 & 0 \\ 0 & 0 & \sin\phi_1 & 1 & 0 & \sin\phi_2 \\ 0 & 0 & -\cos\phi_1 & 0 & 1 & -\cos\phi_2 \\ 0 & 0 & 0 & 0 & 1 & 0 \\ 0 & 0 & 1 & 0 & 0 & 0 \end{bmatrix}$$

The determinant of this Jacobian is $|\mathbf{\Phi}_{\mathbf{q}}| = -\cos\phi_2$. Unless body 2 is in an upright position, that is, $\phi_2 = \pi/2 + k\pi$, where k is an integer, the determinant is never zero. When $\cos\phi_2 = 0$, the system is in a singular configuration, which is discussed in Section 3.7.

When $t = 0$, $\phi_1 = 5\pi/3$. Let the error tolerance for the Newton–Raphson method be $\varepsilon = 1.0 \times 10^{-4}$ and estimate $\mathbf{q}^{(0)} = [0.5, -0.8660, 5\pi/3, 1.5, -1.0, 6.14]^T$. Equation 3.6.7 becomes

$$\begin{bmatrix} 1 & 0 & -0.8660 & 0 & 0 & 0 \\ 0 & 1 & -0.5 & 0 & 0 & 0 \\ 0 & 0 & -0.8660 & 1 & 0 & -0.1427 \\ 0 & 0 & -0.5 & 0 & 1 & -0.9898 \\ 0 & 0 & 0 & 0 & 1 & 0 \\ 0 & 0 & 1 & 0 & 0 & 0 \end{bmatrix} \begin{bmatrix} \Delta x_1 \\ \Delta y_1 \\ \Delta\phi_1 \\ \Delta x_2 \\ \Delta y_2 \\ \Delta\phi_2 \end{bmatrix} = \begin{bmatrix} 0 \\ 0 \\ -0.0102 \\ -0.0087 \\ 0 \\ 0 \end{bmatrix}$$

The solution of this matrix equation is

$$\Delta\mathbf{q}^{(1)} = [0, 0, 0, -0.0089, 0, 0.0088]^T$$

From Eq. 3.6.8,

$$\mathbf{q}^{(2)} = [0.5, -0.8660, 5\pi/3, 1.4911, -1.0, 6.1488]^T$$

Substituting $\mathbf{q}^{(2)}$ into Eq. 3.6.7 and solving for $\Delta\mathbf{q}^{(2)}$,

$$\Delta\mathbf{q}^{(2)} = [0, 0, 0, -0.0001, 0, 0]^T$$

Hence

$$\mathbf{q}^{(3)} = [0.5, -0.8660, 5\pi/3, 1.4910, -1.0, 6.1488]^T$$

Substituting $\mathbf{q}^{(2)}$ into Eq. 3.6.7 and solving for $\Delta\mathbf{q}^{(2)}$,

$$\Delta\mathbf{q}^{(2)} = [0, 0, 0, -0.0001, 0, 0]^T$$

After only two iterations, the constraint violation is smaller than the prescribed error tolerance.

Equation 3.6.10 for velocity is

$$\begin{bmatrix} 1 & 0 & -0.8660 & 0 & 0 & 0 \\ 0 & 1 & -0.5 & 0 & 0 & 0 \\ 0 & 0 & -0.8660 & 1 & 0 & -0.1340 \\ 0 & 0 & -0.5 & 0 & 1 & -0.9910 \\ 0 & 0 & 0 & 0 & 1 & 0 \\ 0 & 0 & 1 & 0 & 0 & 0 \end{bmatrix} \begin{bmatrix} \dot{x}_1 \\ \dot{y}_1 \\ \dot{\phi}_1 \\ \dot{x}_2 \\ \dot{y}_2 \\ \dot{\phi}_2 \end{bmatrix} = \begin{bmatrix} 0 \\ 0 \\ 0 \\ 0 \\ 0 \\ 0.5236 \end{bmatrix}$$

and the solution is

$$\dot{\mathbf{q}} = [0.4534, 0.2618, 0.5236, 0.4180, 0, -0.2642]^T$$

Since $\boldsymbol{\Phi}_{\mathbf{q}t} = \mathbf{0}$ and $\boldsymbol{\Phi}_{tt} = \mathbf{0}$, the acceleration equation of Eq. 3.6.11 is

$$\begin{bmatrix} 1 & 0 & -0.8660 & 0 & 0 & 0 \\ 0 & 1 & -0.5 & 0 & 0 & 0 \\ 0 & 0 & -0.8660 & 1 & 0 & -0.1340 \\ 0 & 0 & -0.5 & 0 & 1 & -0.9910 \\ 0 & 0 & 0 & 0 & 1 & 0 \\ 0 & 0 & 1 & 0 & 0 & 0 \end{bmatrix} \begin{bmatrix} \ddot{x}_1 \\ \ddot{y}_1 \\ \ddot{\phi}_1 \\ \ddot{x}_2 \\ \ddot{y}_2 \\ \ddot{\phi}_2 \end{bmatrix} = \begin{bmatrix} -0.1371 \\ 0.2374 \\ -0.2063 \\ -0.2468 \\ 0 \\ 0 \end{bmatrix}$$

and the solution is

$$\ddot{\mathbf{q}} = [-0.1371, 0.2374, 0, -0.2397, 0, -0.2490]^T$$

3.6.4 Kinematic Analysis on a Time Grid

Rather than calculating position, velocity, and acceleration at isolated times, it is often desired to solve for these variables at a grid of time points t_i, $i = 1, \ldots, m$, that is, to calculate

$$\left.\begin{aligned} \mathbf{q}_i &= \mathbf{q}(t_i) \\ \dot{\mathbf{q}}_i &= \dot{\mathbf{q}}(t_i) \\ \ddot{\mathbf{q}}_i &= \ddot{\mathbf{q}}(t_i) \end{aligned}\right\}, \qquad i = 1, \ldots, m \tag{3.6.12}$$

Use of the Newton–Raphson method of Eqs. 3.6.7 and 3.6.8 to solve for position is enhanced by starting the iterative computation at a good estimate of $\mathbf{q}$. Presuming that position, velocity, and acceleration are known at time t_i, $\mathbf{q}$ at time t_{i+1} may be approximated using the second-order Taylor expansion [25, 26]

$$\mathbf{q}_{i+1} \approx \mathbf{q}_i + (t_{i+1} - t_i)\dot{\mathbf{q}}_i + \tfrac{1}{2}(t_{i+1} - t_i)^2\ddot{\mathbf{q}}_i \tag{3.6.13}$$

This estimate can be used to begin Newton–Raphson iteration and, if the increment in time points is not large, rapid convergence may be expected.

3.7 SINGULAR CONFIGURATIONS

The preceding sections are devoted to formulating and solving constraint equations for the kinematic analysis of mechanical systems in which motion proceeds smoothly with time. For trial designs, however, singular configurations may be encountered, beyond which motion cannot continue or more than one possible motion can occur. To see that such pathological behavior is not restricted to peculiar cases invented by a mathematician, consider the following elementary slider–crank example.

Example 3.7.1: Consider first the elementary model of a slider–crank mechanism in Example 3.1.2, with $\ell < 1$, which is driven in the positive ϕ_1 direction. As motion continues from the position shown in Fig. 3.1.3, the system reaches a configuration in which $\sin \phi_1 = \ell$, as shown in Fig. 3.7.1. It is physically clear that in this configuration the crank can no longer be driven in the positive ϕ_1 direction. This is called a *lock-up configuration.*

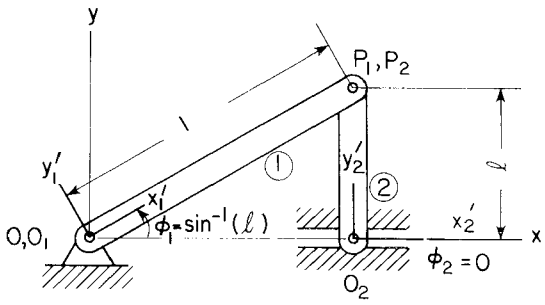

Figure 3.7.1 Slider–crank at lock-up configuration.

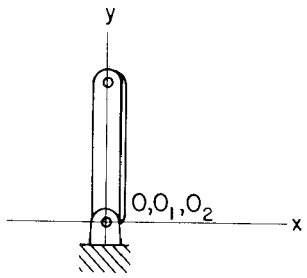

Figure 3.7.2 Slider–crank at bifurcation configuration.

An interesting observation can be made when the system is driven in the negative ϕ_1 direction from the configuration shown in Fig. 3.7.1. Two possible motions can occur: point O_2 could move either to the left or to the right. This branching of motion to two possible paths is called *bifurcation.*

Consider next the slider–crank of Example 3.1.2, but with $\ell = 1$. When $\phi_1 = \pi/2$, $\phi_2 = 0$, as illustrated in Fig. 3.7.2. As ϕ_1 is driven in the positive sense, O_2 may either stay at O, and hence bodies 1 and 2 are locked together and move as a pendulum pivoted at O [Fig. 3.7.3(a)], or O_2 passes point O and moves along the negative x axis [Fig. 3.7.3(b)]. This is another example of bifurcation.

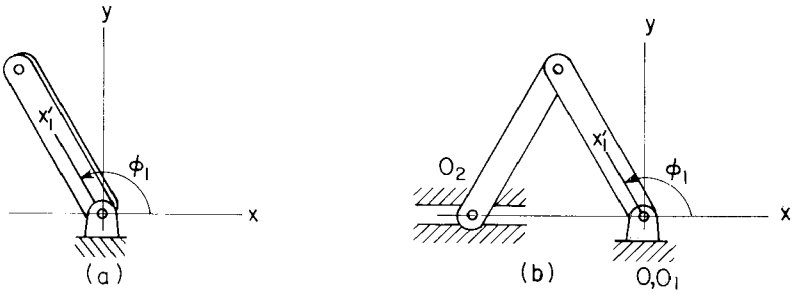

Figure 3.7.3 Bifurcation of slider–crank.

Example 3.7.2: A second example of bifurcation can be illustrated with a parallelogram four-bar linkage with two pairs of equal-length members, shown in Fig. 3.7.4. If body 1 is driven in the positive ϕ_1 direction from the flat configuration, that is, $\phi_1 = \phi_3 = 0$, two types of motion are possible, as illustrated in Fig. 3.7.5.

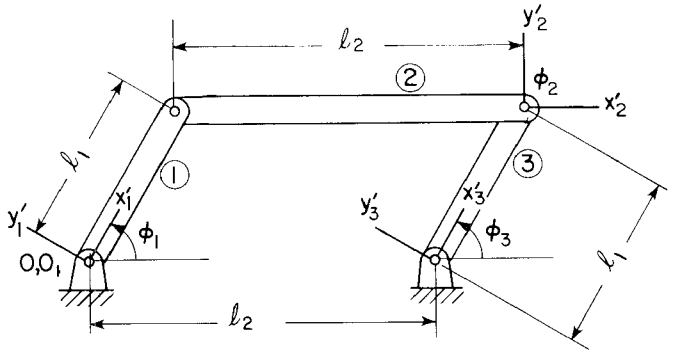

Figure 3.7.4 Parallelogram four-bar linkage.

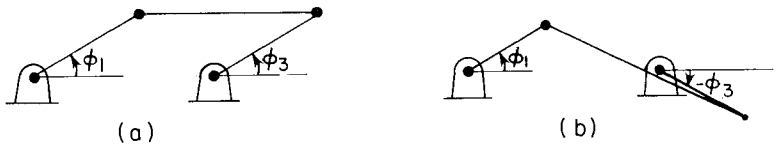

Figure 3.7.5 Bifurcation motion of four-bar linkage.

Example 3.7.3: As a first step in developing analytical methods for finding and analyzing singular configurations, consider the alternative two-body model of the slider–crank mechanism shown in Fig. 3.7.6, which was studied with the aid

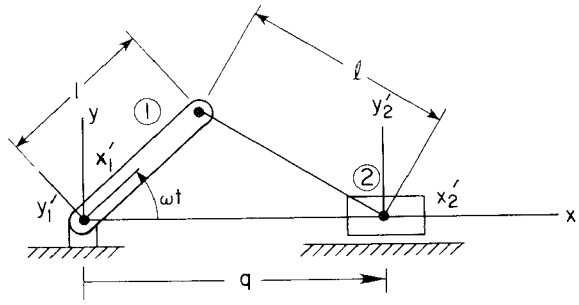

Figure 3.7.6 Two-body slider–crank model.

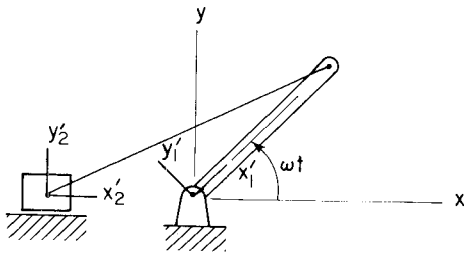

Figure 3.7.7 Alternative assembly of two-body slider–crank.

of physical arguments in Example 3.7.1. The crank is driven at constant angular velocity ω; that is, $\phi_1 = \omega t$. If absolute constraints are used to define coupling between bodies 1 and 2 and ground, $x_1 = y_1 = y_2 = \phi_2 = 0$. Thus, only $x_2 \equiv q$ remains as a generalized coordinate. The distance constraint imposed by the coupler of length ℓ may be written in terms of q as

$$\Phi(q, t) = (q - \cos \omega t)^2 + \sin^2 \omega t - \ell^2 = 0 \tag{3.7.1}$$

Expanding Eq. 3.7.1 as a quadratic equation in q and solving it,

$$q = \cos \omega t \mp \sqrt{\cos^2 \omega t + (\ell^2 - 1)} \tag{3.7.2}$$

where the plus sign corresponds to the assembled configuration shown in Fig. 3.7.6 and the minus sign corresponds to the configuration shown in Fig. 3.7.7. Note, from Example 3.7.1, that if $\ell > 1$ then the mechanism will stay in only one of the distinct configurations for all values of ϕ_1. If $\ell < 1$, on the other hand, then at singular points $\sin \phi_1 = \ell$ the configuration can change.

From Eq. 3.7.2, it is clear that if $\ell > 1$ there is a valid solution for all time. If $\ell < 1$, however, then when $\cos^2 \omega t = 1 - \ell^2$ (equivalently when $\sin \omega t = \ell$) loss of existence (lock-up) is encountered. Finally, if $\ell = 1$, a solution exists, but when $\cos \omega t = 0$ (equivalently when $\sin \omega t = \ell$), two solution branches (bifurcation) are possible.

Direct differentiation of Eq. 3.7.2 shows that if $\ell < 1$ then $\dot{\mathbf{q}}$ and $\ddot{\mathbf{q}}$ approach infinity as $\sin \omega t$ approaches ℓ. This behavior is typical at lock-up points and can serve as a warning that a lock-up configuration is being approached.

It is comforting to see that the properties of the analytical solution of kinematic equations agree with reality at lock-up and bifurcation points in Example 3.7.3. However, since analytical (closed-form) solutions are seldom possible, it is important to develop criteria for singular points that can be applied to large-scale systems and evaluated numerically. Prior to presenting a general method, the elementary model of Example 3.7.3 is investigated from a different point of view.

Example 3.7.4: Taking the time derivative of the constraint equation of Example 3.7.3 (Eq. 3.7.1),

$$\begin{aligned}\Phi_q\dot{q} &\equiv 2(q-\cos\omega t)\dot{q}\\ &= -2\omega q\sin\omega t \equiv -\Phi_t\end{aligned} \tag{3.7.3}$$

If $\ell > 1$, $q > \cos\omega t$ for all t and no difficulties arise. If $\ell < 1$, then $q = \cos\omega t \neq 0$ when $\sin\omega t = \ell$. Thus, Eq. 3.7.3 shows that $\dot{q}$ approaches infinity as the lock-up point is approached, since there $\Phi_q = 0$ and $\Phi_t \neq 0$. This is, in fact, a general criteria.

The approach illustrated in Example 3.7.4 is typical of analysis that can be carried out using the constraint Jacobian and the implicit function theorem. In general, if $\mathbf{q}$ is an n vector of generalized coordinates and if the combination of kinematic and driving constraints is n equations, then $\mathbf{\Phi}(\mathbf{q}, t) = \mathbf{0}$ is to determine $\mathbf{q}(t)$. Presume an assembled configuration $\mathbf{q}^*$ is known at time t^*. Then, if the Jacobian $\mathbf{\Phi}_\mathbf{q}(\mathbf{q}^*, t^*)$ were nonsingular, the implicit function theorem would guarantee a smooth unique solution $\mathbf{q}(t)$ near $\mathbf{q}^*$ in the time interval $|t - t^*| < \delta$, for some $\delta > 0$. If lock-up or bifurcation occurs at t^*, however, then arbitrarily close to t^* either existence or uniqueness is lost. Thus, $\mathbf{\Phi}_\mathbf{q}(\mathbf{q}^*, t^*)$ must be singular at lock-up and bifurcation configurations. This property and the associated behavior of velocities and accelerations permit systematic detection and interpretation of singular points.

Example 3.7.5: Suppressing absolute constraints and the associated variables in Eq. 3.1.11 and adding the driving constraint of Eq. 3.1.12, constraint equations for the slider–crank in Example 3.1.2 reduce to

$$\mathbf{\Phi}(\mathbf{q}, t) = \begin{bmatrix} -x_2 + \cos\phi_1 + \ell\sin\phi_2 \\ \sin\phi_1 - \ell\cos\phi_2 \\ \phi_1 - \omega t \end{bmatrix} = \mathbf{0} \tag{3.7.4}$$

where $\mathbf{q} = [\phi_1, x_2, \phi_2]^T$. The determinant of the Jacobian is

$$|\mathbf{\Phi}_\mathbf{q}| = \begin{vmatrix} -\sin\phi_1 & -1 & \ell\cos\phi_2 \\ \cos\phi_1 & 0 & \ell\sin\phi_2 \\ 1 & 0 & 0 \end{vmatrix} = -\ell\sin\phi_2 \tag{3.7.5}$$

which is zero when $\phi_2 = 0$.

Two possible situations can be considered for the singular point $\phi_2 = 0$, as in Examples 3.1.2 and 3.7.1.

1. With $\ell < 1$, the singular configuration $\phi_1 = \sin^{-1}(\ell)$ and $x_2 = \sqrt{1 - \ell^2}$ satisfies the constraint equation of Eq. 3.7.4 and represents the lock-up configuration shown in Fig. 3.7.1.
2. With $\ell = 1$, the singular configuration $\phi_1 = \pi/2$ and $x_2 = 0$ satisfies Eq. 3.7.1 and represents the bifurcation configuration shown in Fig. 3.7.3.

Some physical insights into singular behavior can be gained by studying the velocity equation of Eq. 3.6.10:

$$\boldsymbol{\Phi}_{\mathbf{q}}\dot{\mathbf{q}} = -\boldsymbol{\Phi}_t \tag{3.7.6}$$

If $\boldsymbol{\Phi}_{\mathbf{q}}$ is singular at a time t^*, Eq. 3.7.6 has a solution if and only if, by the *theorem of the alternative* [22],

$$\boldsymbol{\beta}^T\boldsymbol{\Phi}_t = 0 \tag{3.7.7}$$

for all solutions $\boldsymbol{\beta}$ of

$$\boldsymbol{\Phi}_{\mathbf{q}}^T\boldsymbol{\beta} = \mathbf{0} \tag{3.7.8}$$

This result clearly shows that Eq. 3.7.6 has a finite solution for velocity only if $\boldsymbol{\Phi}_{\mathbf{q}}$ and $\boldsymbol{\Phi}_t$ are properly related.

Consider next a small *virtual displacement* $\delta\mathbf{q}$ that satisfies constraints to "first order" (a concept that is developed more thoroughly in Chapter 6), with time held fixed. Expanding the constraint equations to first order, $\delta\mathbf{q}$ satisfies

$$\boldsymbol{\Phi}_{\mathbf{q}}\delta\mathbf{q} = \mathbf{0} \tag{3.7.9}$$

Since $\boldsymbol{\Phi}_{\mathbf{q}}$ is singular at t^*, there exists a solution $\delta\mathbf{q} \neq \mathbf{0}$ that may be viewed as tangent to solution trajectories that emanate from $\mathbf{q}(t^*)$. Note that, if a finite $\dot{\mathbf{q}}$ satisfies Eq. 3.7.6 and $\delta\mathbf{q}$ satisfies Eq. 3.7.9, then

$$\boldsymbol{\Phi}_{\mathbf{q}}(\dot{\mathbf{q}} \pm \delta\mathbf{q}) = \boldsymbol{\Phi}_{\mathbf{q}}\dot{\mathbf{q}} \pm \boldsymbol{\Phi}_{\mathbf{q}}\delta\mathbf{q} = -\boldsymbol{\Phi}_t \tag{3.7.10}$$

Thus, two distinct velocities may occur after t^*, which characterizes a bifurcation point. Since the determinant $|\boldsymbol{\Phi}_{\mathbf{q}}|$ is zero at t^*, except in cases for which the rank deficiency of $\boldsymbol{\Phi}_{\mathbf{q}}$ is greater than 1, its sign must change as a bifurcation is passed. This can serve as a computational test for a bifurcation configuration. Only if no solution of Eq. 3.7.6 exists beyond t^*, that is, only if $\dot{\mathbf{q}}$ approaches infinity as t approaches t^*, is there no possibility of continuing a solution. This characterizes a lock-up configuration. Thus, $\dot{\mathbf{q}}$ and/or $\ddot{\mathbf{q}}$ approaching infinity serves as a criteria for lock-up.

A final note on the effect of a design change on performance of a mechanism near a singular point may help in evaluating the engineering feasibility of a design. Let $\mathbf{b} = [b_1, \ldots, b_k]^T$ be a vector of design parameters, such as dimensions. Since these parameters arise in kinematic constraint equations, consider the constraints

$$\boldsymbol{\Phi}(\mathbf{q}, t; \mathbf{b}) = \mathbf{0} \tag{3.7.11}$$

There is a relationship between admissible virtual displacements $\delta\mathbf{q}$ and small variations $\delta\mathbf{b}$ in design. To first order, Eq. 3.7.11 may be expanded (linearized) as

$$\boldsymbol{\Phi}_{\mathbf{q}}\delta\mathbf{q} = -\boldsymbol{\Phi}_{\mathbf{b}}\delta\mathbf{b} \tag{3.7.12}$$

At a singular point t^*, $\boldsymbol{\Phi}_{\mathbf{q}}$ is singular. Thus, for some $\delta\mathbf{b}$ Eq. 3.7.12 may

have multiple solutions for $\delta\mathbf{q}$, and for other $\delta\mathbf{b}$ it may have no solutions. Physically, this may be interpreted as indicating that, for some design variations, multiple changes in configuration are possible, somewhat as in bifurcation, and for other design variations, the mechanism cannot be assembled. This observation will be of value in evaluating the engineering realism of models in Chapter 5.

Example 3.7.6: Consider the slider–crank model of Example 3.7.1 in the lock-up configuration shown in Fig. 3.7.1. If ℓ is a design parameter, a positive $\delta\ell$ leads to two values of δx_2, as shown in Fig. 3.7.8(a). A negative $\delta\ell$, however, leads to a design that cannot be assembled with $\phi_1 = \sin^{-1}\ell$, as shown in Fig. 3.7.8(b).

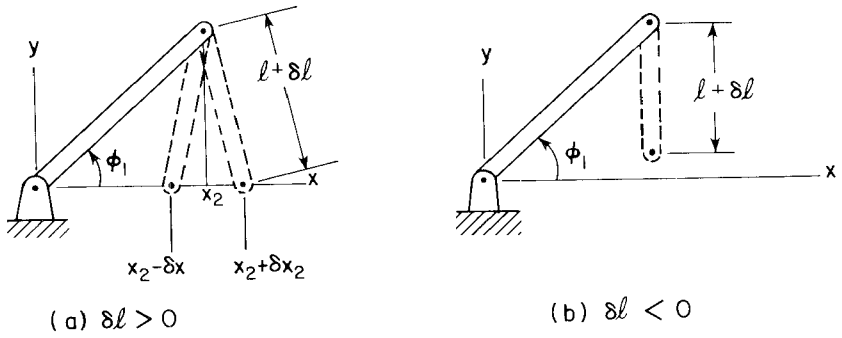

Figure 3.7.8 Effect of design change on slider–crank.

Singular points that define lock-up or bifurcation are *isolated singular points,* that is, intervals of time in which a unique solution of the equations of kinematics occurs on one or both sides of an isolated singular point t^*. Thus, except at t^*, if the mechanism can be assembled, then it is well behaved. Another form of singularity that is commonly encountered is a *redundant constraint.* If a mechanism is modeled using the standard joints of Sections 3.2 through 3.4, it is possible that one or more of the kinematic constraint equations are automatically satisfied if the remaining constraints are satisfied, in which case the automatically satisfied constraints are redundant and consistent.

Example 3.7.7: The five-body parallelogram mechanism of Fig. 3.7.9 is modeled as a single bar, with three absolute distance constraints that represent three bars of unit length that are pivoted in ground. With $\mathbf{q} = [x_1, y_1, \phi_1]^T \equiv [x, y, \phi]^T$, the kinematic constraint equations are

$$\mathbf{\Phi}^K(\mathbf{q}) = \begin{bmatrix} x^2 + y^2 - 1 \\ (x + \cos\phi - 1)^2 + (y + \sin\phi)^2 - 1 \\ (x + 2\cos\phi - 2)^2 + (y + 2\sin\phi)^2 - 1 \end{bmatrix} = \mathbf{0} \qquad (3.7.13)$$

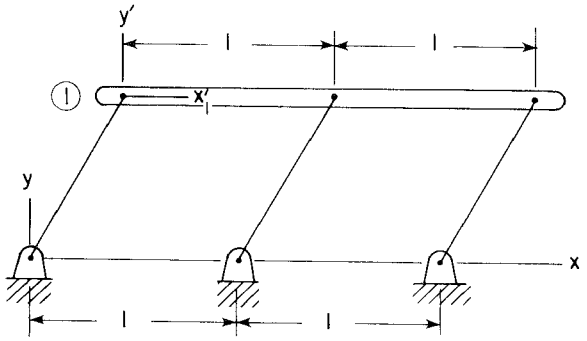

Figure 3.7.9 Five-bar parallelogram mechanism model.

The constraint Jacobian of Eq. 3.7.13 is

$$\Phi_{\mathbf{q}}^{K} = \begin{bmatrix} 2x & 2y & 0 \\ 2(x+\cos\phi-1) & 2(y+\sin\phi) & -2(x-1)\sin\phi+2y\cos\phi \\ 2(x+2\cos\phi-2) & 2(y+2\sin\phi) & -4(x-2)\sin\phi+4y\cos\phi \end{bmatrix} \tag{3.7.14}$$

Subtracting the first row from two times the second row and subtracting the result from the third row leads to a matrix with a zero third row for all values of $\mathbf{q}$. Thus, the rank of the constraint Jacobian is only two, and the third of the constraint equations of Eq. 3.7.13 is dependent. This is clearly true from Fig. 3.7.9, since the third distance constraint is automatically satisfied by the parallelogram that is defined by the first two distance constraints.

A numerical method is presented in Section 4.6 for the identification and elimination of redundant constraints.

PROBLEMS

Section 3.1

3.1.1. Let $f(t) = \sin 10t$ in Example 3.1.1. At instants $t_i = i/10$, $i = 0, 1, \ldots, 10$, in time.

(a) Solve Eq. 3.1.7 for $\mathbf{q}(t_i)$.

(b) Use the result of part a in Eq. 3.1.9 to determine $\dot{\mathbf{q}}(t_i)$.

(c) Use the results of parts a and b in Eq. 3.1.10 to determine $\ddot{\mathbf{q}}(t_i)$.

Report the results in the form of the following table:

i	0	1	2	3	4	5	6	7	8	9	10
$x_1(t_i)$											
$y_1(t_i)$											
$\phi_1(t_i)$											
$\dot{x}_1(t_i)$											
$\dot{y}_1(t_i)$											
$\dot{\phi}_1(t_i)$											
$\ddot{x}_1(t_i)$											
$\ddot{y}_1(t_i)$											
$\ddot{\phi}_1(t_i)$											

3.1.2. Flowchart a digital computer program that could be used to calculate and report the results for Prob. 3.1.1.

3.1.3. Verify that $|\mathbf{\Phi}_\mathbf{q}| = -\ell \sin \phi_2$ for the matrix of Eq. 3.1.14. If $\ell < 1$, then for some angle $\phi_1 < \pi/2$, $\phi_2 = 0$ and $\mathbf{\Phi}_\mathbf{q}$ is singular, leading to infinite velocities and accelerations from Eqs. 3.1.14 and 3.1.15, respectively. Explain this pathological behavior from a physical point of view.

3.1.4. Verify that Eqs. 3.1.14 and 3.1.15 are correct. Can the same flowchart of Prob. 3.1.2 be used to construct a digital computer program to solve the equations of Example 3.1.2?

Section 3.2

3.2.1. Model the system of Prob. 2.4.4 using absolute position constraints. Write velocity and acceleration equations using the approach of Examples 3.1.1 and 3.1.2.

3.2.2 Model the slider–crank mechanism of Example 3.1.2, with body 2 as the only body, using absolute position and distance constraints. Write velocity and acceleration equations using the approach of Examples 3.1.1 and 3.1.2.

3.2.3. Replace the constraint equation of Eq. 3.1.17 in Example 3.1.3 with $\Phi_2 \equiv \phi_1 - \pi/4 = 0$ and show that this equation and Eqs. 3.1.16 and 3.1.18 uniquely define the motion of the system.

Section 3.3

3.3.1. Write out the constraint equations of Example 3.3.1 and show that they are identical to those derived in Example 3.1.2.

3.3.2. Use absolute and relative constraints to create three different but equivalent models of the three-body slider–crank mechanism shown in Fig. P3.3.2.

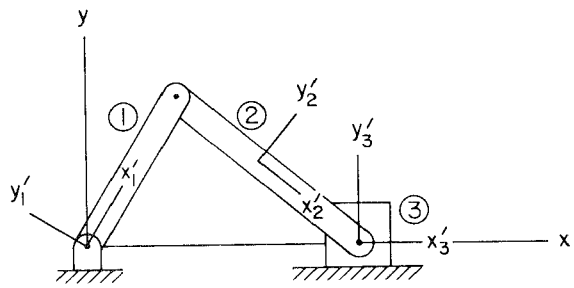

Figure P3.3.2

3.3.3. Identify the specific constraint equations that implement the four alternative models of Example 3.3.2 and define values of $x_i'^P$, $y_i'^P$, and C_k that are used for each.

3.3.4. Verify that the manipulations carried out in deriving the final form of Eq. 3.3.13 are correct.

3.3.5. Derive Eq. 3.3.14.

Section 3.4

3.4.1. Consider the gear set in Fig. 3.4.2. Let the centers P_i and P_j be fixed to ground; hence θ is constant. Show that the rotation on the rates of the gears are inversely proportional to their radii (*Hint:* Use Eq. 3.4.1).

3.4.2. The small rail trolley shown in Fig. P3.4.2 is driven by a 0.3-m diameter gear that has a constant angular acceleration of 5 revs/s^2. Find the vehicle's translational acceleration when the angular velocity of the driving gear is 600 rpm (*Hint:* Use Eqs. 3.4.1 and 3.4.8).

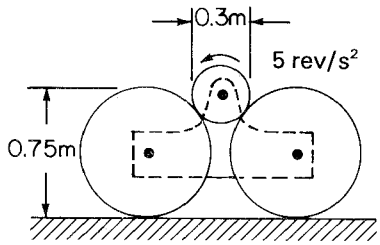

Figure P3.4.2

3.4.3. Consider the oil pumping rig shown in Fig. P3.4.3. The flexible pump rod, body 2, is fastened to a curved sector on body 1 at point Q_1 and is always vertical as it enters the well. This connection between the sector and flexible pump rod can be modeled as a rack and pinion constraint. Choose proper coordinate systems and write out the constraint equation of Eq. 3.4.13.

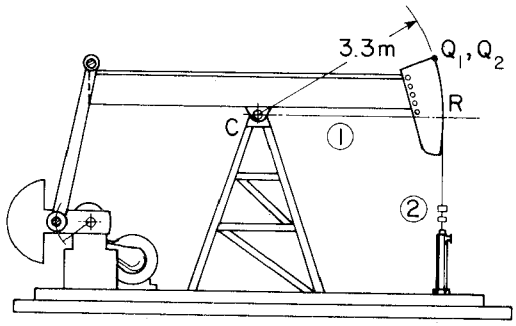

Figure P3.4.3

3.4.4. Derive the Jacobians ν and γ for the rack and pinion constraint equation of Eq. 3.4.13.

3.4.5. Show that the gear and follower in Example 3.4.3 are always in contact at one point (*Hint:* Calculate the radius of curvature of the follower).

3.4.6. Are the first two constraint equations of Eq. 3.4.20 equivalent to the revolute joint constraint equation of Eq. 3.3.11? If not, give an explanation.

3.4.7. Repeat the analysis of Example 3.4.3 with the follower curve

$$\rho_1(\alpha_1) = \begin{cases} 1 + 2\alpha_1^2 - 2\alpha_1^3 + \frac{1}{2}\alpha_1^4, & 0 \le \alpha_1 \le 2 \\ 1, & 2 < \alpha_1 < 2\pi \end{cases}$$

3.4.8. Derive the Jacobian for the cam–follower constraint equation of Eq. 3.4.20.

3.4.9. Derive the Jacobian for the cam–flat-faced follower constraint equation of Eq. 3.4.29.

3.4.10. The slider–crank in Example 3.1.2 can be modeled as the three-body mechanism shown in Fig. P3.4.10. Body 2 and ground (body 3) are connected by a point–follower joint. Write the point–follower constraint equations of Eq. 3.4.31 using explicit expressions for $x_3'^P(\alpha_3)$ and $y_3'^P(\alpha_3)$.

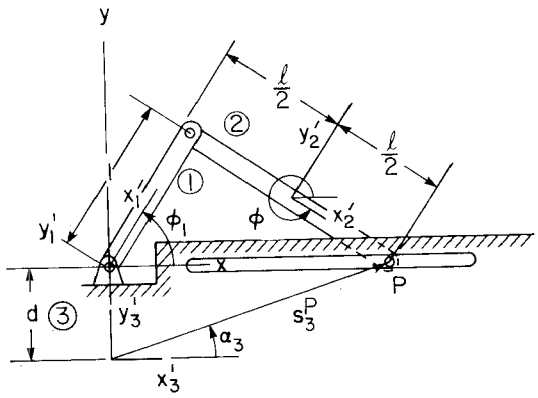

Figure P3.4.10

3.4.11. Derive the Jacobian for the point–follower constraint equation of Eq. 3.4.31.

Section 3.5

3.5.1. By taking the time derivative of the velocity equation in Example 3.5.1, find the angular acceleration $\ddot{\phi}_1$.

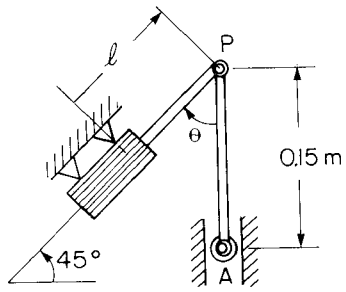

Figure P3.5.3

3.5.2. By taking the time derivative of the velocity equation in Example 3.5.2, find the acceleration vector $\ddot{\mathbf{q}} = [\ddot{\phi}_1, \ddot{x}_2, \ddot{y}_2, \ddot{\phi}_2, \ddot{\phi}_3]^T$.

3.5.3. The piston of the hydraulic cylinder shown in Fig. P3.5.3 moves point P with $\ell = \ell_0 + 0.08t$. Find the acceleration of point A when $\theta = 45°$.

3.5.4. Rod AB shown in Fig. P3.5.4 slides through a collar that is pivoted at point C as A moves along the slot. Rotation of the collar is driven so that $\phi_1 = \pi/3 + t + t^2$. Find the velocity and the acceleration of point A when $t = 0.25\,s$.

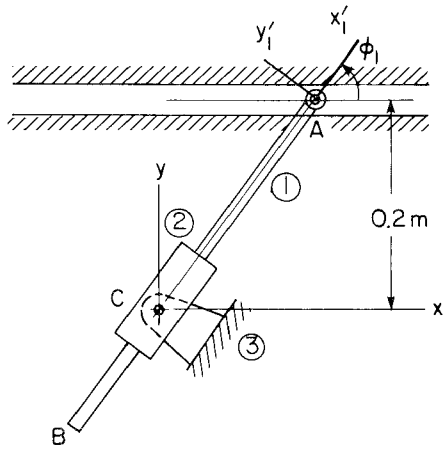

Figure P3.5.4

3.5.5. Consider the two-body mechanism shown in Fig. P3.5.5. The relative angle between bodies 1 and 2 is driven as $\phi_1 - \phi_2 = (\pi/18)t$, $0 \leq t \leq 8$. Find the velocity and acceleration of point O_2 when $\phi_1 - \phi_2 = \pi/3$.

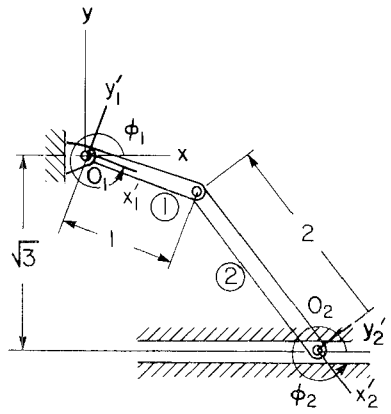

Figure P3.5.5

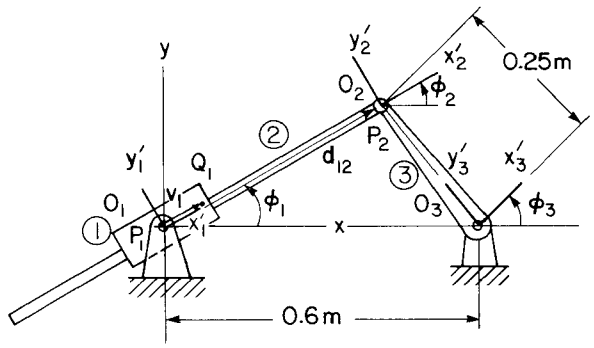

Figure P3.5.6

3.5.6. Consider the mechanism shown in Fig. P3.5.6, which is driven by

$$\frac{\mathbf{v}_1^T\mathbf{d}_{12}}{v_1} + 0.4 - \tfrac{1}{10}t = 0, \qquad 0 \leq t \leq 10$$

Find $\dot{\phi}_3$ and $\ddot{\phi}_3$ when $\phi_3 = 0$.

Section 3.6

3.6.1. Carry out position, velocity, and acceleration analysis for the simple mechanism in Fig. P3.6.1, with rotation of body 1 driven as

$$\phi_1 - \frac{5\pi}{3} - \frac{\pi}{15}t = 0, \qquad 0 \leq t \leq 4$$

Let $\mathbf{q} = [x_1, y_1, \phi_1]^T$ and estimate $\mathbf{q}^{(0)} = [1.05, 1.73, 5\pi/3]^T$.

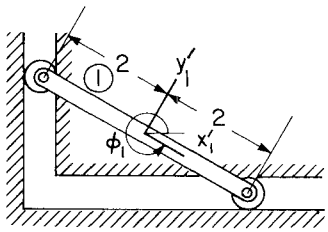

Figure P3.6.1

3.6.2. The pendulum of length 2 is suspended from a slider as shown in Fig. P3.6.2. The slider and pendulum are driven by the following absolute and revolute–rotational drivers:

$$x_1 - 0.2t = 0$$

$$\phi_1 - \phi_2 + \frac{\pi}{6} + \tfrac{1}{10}t = 0$$

Carry out position, velocity, and acceleration analysis for $\mathbf{q} = [x_1, \phi_1, x_2, y_2, \phi_2]^T$, with $\mathbf{q}^{(0)} = [0, 0.001, 0.45, -1.73, \pi/6]^T$, in the interval $0 \leq t \leq 5$.

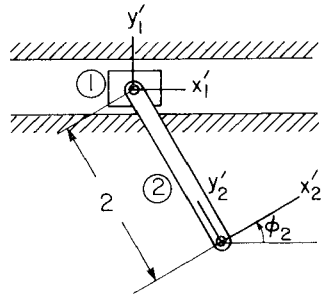

Figure P3.6.2

Section 3.7

3.7.1. Consider the slider–crank mechanism of Fig. 3.3.6. Since the connecting rod (body 2) is longer than the crank (body 1), no singularity occurs when the crank is driven by ϕ_1. A singularity may occur, however, when the slider (body 3) is driven. Use physical arguments to analyze singular configurations of the system when the slider is driven.

3.7.2. Write out the constraint equations, with a driver for the slider, for the slider–crank of Prob. 3.7.1. Calculate the Jacobian and use the implicit function theorem to confirm the singular configurations identified in Prob. 3.7.1.

3.7.3. Let $\ell = \frac{1}{2}$ and $\omega = 1$ for the slider–crank of Example 3.7.3. Write the velocity equation of Eq. 3.6.10 and the acceleration equation of Eq. 3.6.11, and verify that $\dot{q}$ and $\ddot{q}$ approach ∞ as the system approaches the lock-up configuration by filling in the following table:

t	q	Φ_q	$-\Phi_t$	$\dot{q}$	γ	$\ddot{q}$
0.4						
0.45						
0.5						
0.52						
0.523						
0.5235						

3.7.4. Write the constraint equation for the slider–crank of Example 3.7.1, with $\ell = 1$. Construct the composite constraint equation, including a driving constraint $\phi_1 - \omega t = 0$. Evaluate the Jacobian at $\phi_1 = 1.4835$ (85°) and at $\phi_1 = 1.6581$ (95°), and verify that the sign of the determinant of the Jacobian changes when the system passes the bifurcation point.